Chimeric Antigen Receptor T Cell Research For Clinical Applications

Dissertation

der Mathematisch-Naturwissenschaftlichen Fakultät

der Eberhard Karls Universität Tübingen

zur Erlangung des Grades eines

Doktors der Naturwissenschaften

(Dr. rer. nat.)

vorgelegt von

M.Sc. Dominik Peter Lock

aus Biberach

Tübingen

2017

Gedruckt mit Genehmigung der Mathematisch-Naturwissenschaftlichen Fakultät der Eberhard Karls Universität Tübingen.

Tag der mündlichen Qualifikation:	23.04.2018
Dekan:	Prof. Dr. Wolfgang Rosenstiel
1. Berichterstatter:	apl. Prof. Dr. Peter Lang
2. Berichterstatter:	Prof. Dr. Hans-Georg Rammensee

Eidesstattliche Erklärung

Diese Arbeit wurde von mir selbstständig angefertigt und verfasst. Es sind keine anderen als die angegebenen Quellen und Hilfsmittel benutzt worden. Von anderen Personen übernommene Daten oder durchgeführte Arbeiten wurden als solche gekennzeichnet.

Köln, den   _____

_____

Dominik Peter Lock

Publikationen und Patente

Nowak A, **Lock D**, Bacher P, Hohnstein T, Vogt K, Gottfreund J, Giehr P, Polansky JK, Sawitzki B, Kaiser A, Walter J, Scheffold A. *CD137+CD154- Expression As a Regulatory T Cell (Treg)-Specific Activation Signature for Identification and Sorting of Stable Human Tregs from In Vitro Expansion Cultures.* Front Immunol. 2018 Feb 7

EP18152631.0 "Regulatory T cell expressing a chimeric antigen receptor." 2018 Jan

Lock D, Mockel-Tenbrinck N, Drechsel K, Barth C, Mauer D, Schaser T, Kolbe C, Al Rawashdeh W, Brauner J, Hardt O, Pflug N, Holtick U, Borchmann P, Assenmacher M, Kaiser A. *Automated manufacturing of potent CD20-directed CAR T cells for clinical use.* Hum Gene Ther. 2017 Aug 28

EP16204414.3 "Immune cells expressing an antigen binding receptor and a chimeric costimulatory receptor." 2016 Dec 15

Warlich E, Schambach A, **Lock D**, Wedekind D, Glage S, Eckardt D, Bosio A, Knöbel S. *FAS-based cell depletion facilitates the selective isolation of mouse induced pluripotent stem cells.* PLoS One. 2014 Jul 16

- für Davina -

Abbreviations

aa	amino acid
ACT	adoptive cellular therapy
AICD	activation induced cell death
ALL	acute lymphocytic leukemia
APC	allophycocyanin
ATMP	advanced therapy medicinal product
B	B cells
BC	buffy coat
CAR	chimeric antigen receptor
CCR	chimeric co-stimulatory receptor
CD	cluster of differentiation
cGMP	current good manufacturing practice
CIK	cytokine-induced killer cell
CLL	chronic lymphocytic leukemia
CPS	counts per second
CRISPR	clustered regularly interspaced short palindromic repeats
CSPG4	chondroitin sulfate proteoglycan 4
cTCR	chimeric T cell receptor
DLBCL	diffuse large B cell lymphoma
DNA	deoxyribonucleic acid
EF-1α	elongation factor-1 alpha
eGFP	enhanced green fluorescence protein
EGFR	epidermal growth factor receptor
E:T	effector to target ratio
FcγR	fragment crystallizable gamma receptor
FFluc	firefly luciferase
FITC	fluorescein isothiocyanate
G	granulocytes
GFP	green fluorescent protein
GM-CSF	granulocyte macrophage colony-stimulating factor
gRNA	guide ribonucleic acid
h	hour(s)
HAMA	human-anti-mouse antibody
HCL	hairy cell leukemia
HD	healthy donor
HMW-MAA	high molecular weight-melanoma-associated antigen
HIV	human immunodeficiency virus
HLA	human leukocyte antigen
IFN-γ	interferon gamma

IgG	immunoglobulin G isotype
IL	interleukin
i.p.	intraperitoneal
ITAM	immunoreceptor tyrosine-based activation motif
i.v.	intravenous
IVIS	*In vivo* Imaging System
ko	knock-out
lacZ	β-galactosidase encoding gene
LDLR	low density lipoprotein receptor
LNGFR	low-affinity nerve growth factor receptor
LP	leukapheresis
LTR	long terminal repeat
LV	lentiviral
M	monocytes
MACS	magnetic-activated cell sorting
MB	microbead
MCL	mantle cell lymphoma
MDSC	myeloid-derived suppressor cells
MHC	major histocompatibility complex
min	minutes
MOI	multiplicity of infection
MV	Measles virus
NHL	non-Hodgkin lymphoma
NK	natural killer cells
NKT	natural killer T cells
n.s.	not significant
NSG	non-obese diabetic severe combined immunodeficiency gamma
nt	nucleotides
RSV	Rous sarcoma virus
RT	room temperature
RV	retroviral
P	promoter
PBMC	peripheral blood mononuclear cells
PE	phycoerythrin
PGK	phosphoglycerate kinase
PI	propidium iodide
PM	patient material
s.c.	subcutaneous
scFv	single-chain variable fragment
SEM	standard error of the mean
SIN	self-inactivating

SSC$_{hi}$	sideward scatter high
SLAM	signaling lymphocyte-activation molecule
T	T cells
T$_{CM}$	central memory T cells
TCT	T Cell Transduction
TCR	T cell receptor
T$_{eff}$	effector T cells
T$_{EM}$	effector memory T cells
T$_{EMRA}$	end-differentiated effector memory T cells
TIL	tumor-infiltrating lymphocytes
TK	thymidine kinase
TM	transmembrane domain
T$_N$	naïve T cells
TNC	total nucleated cells
T$_{reg}$	regulatory T cell
TRUCKs	T cells redirected for universal cytokine killing
T$_{SCM}$	stem cell memory T cells
TNF-α	tumor necrosis factor alpha
VB	vioblue
VG	viogreen
vh	variable heavy
vl	variable light
VSV-G	vesicular stomatitis virus glycoprotein
WB	whole blood
WPRE	woodchuck posttranscriptional regulatory element

Abstract

Genetically engineered T cells are a promising therapeutic tool for the treatment of cancer or infectious diseases. The generation of potent chimeric antigen receptor (CAR) T cells for clinical use, however, is associated with a plurality of challenges covering medical, economical as well as scientific aspects. Therefore, the present study focusses on specific medical and technical difficulties limiting the dissemination of adoptive cellular therapies (ACT). Furthermore, strategies aiming to improve the potential of CAR modified T cells, especially in a solid tumor setting, were investigated.

To this effect, our work initially focused on the generation of a novel CD20-directed CAR which we evaluated in newly established *in vitro* and *in vivo* assays. After confirming the potency of the anti-CD20 CAR T cells, we focused on the manufacturing and consequently demonstrated that a current good manufacturing practice (cGMP)-compliant, automated T cell Transduction (TCT) Process is both reliable and applicable to manufacture CAR T cells in a clinically relevant scale and quality. Despite varying starting material, different operators or the use of other devices, the developed manufacturing process yielded a robust formulated product with regard to cellular composition, T cell phenotype or anti-tumor potency. Overall, the high reproducibility of the TCT Process proved the suitability to manufacture CD20-directed CAR T cells which are intended to be used in two clinical trials.

In addition, this work focused on strategies to enhance the CAR-based immune response in a melanoma model by co-expressing a CAR and a chimeric co-stimulatory receptor (CCR) in the same T cell. This two-receptor approach includes a second generation CAR specific for chondroitin sulfate proteoglycan 4 (CSPG4) and a CCR that recognizes CD20. Here we show that, dependent on intracellular CCR design, only a simultaneous activation of both co-expressed chimeric receptors CAR as well as CCR resulted in a significantly enhanced immune response. Altogether, this data supports the idea of using an anti-CD20 CCR as a tool to increase the potential of CAR T cells.

Zusammenfassung

Genetisch modifizierte T-Zellen repräsentieren einen vielversprechenden klinischen Ansatz zur Behandlung von Krebs oder Infektionskrankheiten. Die Herstellung von chimären Antigen-Rezeptor (CAR) T-Zellen für eine therapeutische Verwendung ist jedoch mit einer Vielzahl an medizinischen, wirtschaftlichen als auch wissenschaftlichen Herausforderungen assoziiert, die in der vorliegenden Arbeit gezielt adressiert wurden, um eine Ausweitung adoptiver zellulärer Therapien zu ermöglichen. Zudem wurden Strategien zur Steigerung des Potentials von CAR T-Zellen erforscht.

Zunächst wurde ein neuer CD20-spezifischer CAR hergestellt und dessen Funktionalität mittels neu etablierter Verfahren evaluiert und sowohl *in vitro* als auch *in vivo* bestätigt. Anschließend fokussierten wir uns auf die Herstellung von genmodifizierten T-Zellen und zeigten, dass der hier etablierte und automatisierte *T cell Transduction* (TCT) Prozess dazu geeignet ist, um CAR T-Zellen *good manufacturing practice* (GMP)-gerecht und zuverlässig in einem klinisch relevanten Maßstab und entsprechend hoher Qualität zu generieren. Trotz variierendem Ausgangsmaterial, das von unterschiedlichen Experimentatoren an verschiedenen Geräten verwendet wurde, resultierte der TCT Prozess in einem stabil formulierten und einheitlichen Produkt bezüglich Zellzusammensetzung, T-Zell Phänotyp und Zytotoxizität. Aufgrund dieser Reproduzierbarkeit und Zuverlässigkeit qualifizierte sich der TCT Prozess zur Herstellung von CD20-gerichteten CAR T-Zellen, die in zwei klinischen Studien verwendet werden.

Darüber hinaus wurde das Potential von chimären co-stimulatorischen Rezeptoren (CCR) zur Steigerung einer CAR-assoziierten Immunantwort in einem Melanom-Modell untersucht. Hierfür wurden T-Zellen generiert, die einen *chondroitin sulfate proteoglycan 4* (CSPG4)-spezifischen CAR und einen CD20-gerichteten CCR co-exprimieren. Wir zeigten, dass abhängig vom intrazellulärem CCR Aufbau nur eine simultane Aktivierung von CAR und CCR in einer signifikant gesteigerten Immunantwort resultieren. Insgesamt belegen die Daten die Möglichkeit zur Steigerung der Potentials von CARs durch die Verwendung entsprechender CCRs.

Content

List of figures

List of tables

1   Introduction

Cancer designates a malignant neoplasm of endogenous cells or tissue with the potential to invade adjacent tissues or to induce a metastatic growth in distant organs. As one of the main causes of death in developed countries, cancer still represents a fundamental medical challenge [1]. According to the Robert Koch-Institute, approximately 480.000 cases are diagnosed every year in Germany with an increasing trend [2]. Thus, the development of novel and innovative therapies are of utmost importance.

1.1   Conventional cancer treatment and novel strategies

Traditional strategies for the treatment of cancer including surgery, radiation- or chemotherapy correspond to a "one size fits all approach" [3] which does not sufficiently consider the complexity of some cancer diseases. Hence, the chances of a cure using surgical treatments, the most effective option so far, requires an early tumor detection and decreases with disease progression. An adequate alternative was for a long time only the use of radiation- or chemotherapeutic therapies, however, although sometimes efficacious, the systemic approach is generally associated with severe toxicities for the patients [4]. Scientific progress and new findings in molecular oncology, though, led to the development of targeted therapies which considerably improved the treatment success for a multitude of cancer [3, 5, 6]. In this context, initial success was achieved with chimeric monoclonal antibodies like rituximab that induces anti-tumor reactions due to a broad versatility of mechanisms such as complement-dependent cytotoxicity, antibody-dependent cytotoxicity or direct apoptosis triggering [7, 8]. Equally important are proteasome inhibitors like Bortezomib, a boron-containing pyridine-carboxamide, used for the treatment of patients with multiple myeloma which impedes the degradation of intracellular ubiquitinated proteins [9, 10]. The next major step towards individualized therapies allowed, amongst others, in-depth genomic investigation of tumors using next generation sequencing approaches and advanced bioinformatic tools. In this way, *BRAF*, a main protein of the *RAS/RAF* signaling pathway, or rather its mutation V600E, which is

present in approximately 60% of melanoma patients [11, 12], was detected and clinically approved as promising therapy approach for melanoma using the protein kinase inhibitor vemurafenib [13, 14].

In 2013, *Science* selected immunotherapy as "Breakthrough of the Year" [15]. They drew this decision based on the promising results of different therapeutic approaches exploiting the potency of the immunotherapy and acknowledged innovative and personalized medicine. Thus, immune checkpoint inhibitors like ipilimumab (anti-CTLA4) or nivolumab (anti-PD-1) prove the significance of modulating immunosuppression mechanisms in a clinical context [16-18] but also patient-derived and *ex vivo* expanded tumor-infiltrating lymphocytes (TILs) demonstrated their efficacy for the treatment of metastatic melanoma [19, 20]. Overall, "harnessing the immune system to battle tumors" [15] opens up a vast potential and particularly engineered T cells come to the forefront of adoptive cellular therapies (ACT). Basically, CAR T cell therapy is taking advantage of deep knowledge on targets and efficacy of T cell effector mechanisms.

Almost three decades ago, Gross *et al.* [21] reported for the first time on genetically modified T cells expressing an artificial receptor used to specifically bind an antigen which resulted in a non-major histocompatibility complex (MHC)-restricted T cell response. These findings and following improvements paved the way from "basic immunology to paradigm-shifting clinical immunotherapy" [22]. In principle, the structure of this first chimeric receptor in contrast to the well-known first generation chimeric antigen receptors (CAR) did not greatly change. Hence, both generally comprise a specific binding domain (mostly a single-chain variable fragment (scFv) derived from an antibody), an extracellular spacer, a transmembrane domain and an intracellular domain containing an immunoreceptor tyrosine-based activation motif (ITAM) like CD3ζ [23] (Fig. 1).
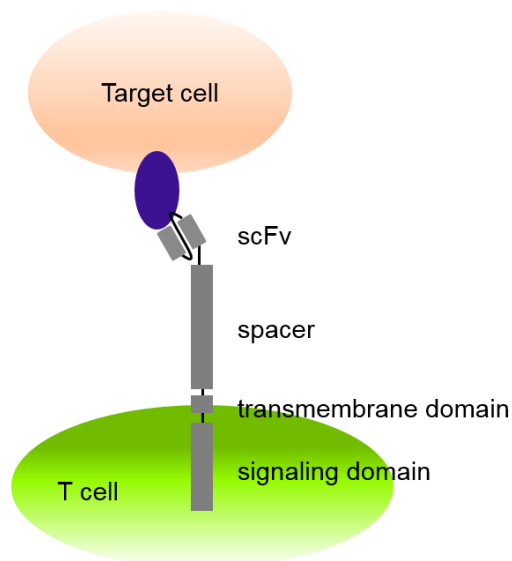
Fig. 1 **First generation CAR T cell.** CARs combine an extracellular binding moiety (mostly a scFv) with an intracellular T cell-derived signaling domain. T cells expressing such an artificial receptor are able to specifically bind an antigen and transmit an activation signal which mediates a MHC-independent target cell lysis.

However, T cells endowed with such a first generation CAR, even though functional *in vitro*, hardly proliferated or persisted *in vivo* and thus showed only modest clinical response [24, 25]. These findings demonstrated the need for further modifications to improve the potential of CAR T cells. Consequently, analogue to conventional T cell activation requiring not only `signal 1´ but also `signal 2´, a co-stimulatory domain such as CD28 or 4-1BB was added to the CD3ζ intracellular signaling domain. Those second generation CAR T cells outperformed the first generation and demonstrated remarkable clinical responses [26-31]. The incorporation of additional co-stimulatory domains in third generation CAR T cells were reported to further ameliorate CAR T cell potential [32-34], however, their clinical use might be also associated with risks, due to a very low activation threshold [35, 36]. Several clinical trials are currently assessing both safety and efficacy of third generation CAR T cells (e.g. ClinicalTrials.gov Identifier NCT02186860, NCT02132624 or NCT01853631). Fig. 2 summarizes essential characteristics of the different CAR generations.
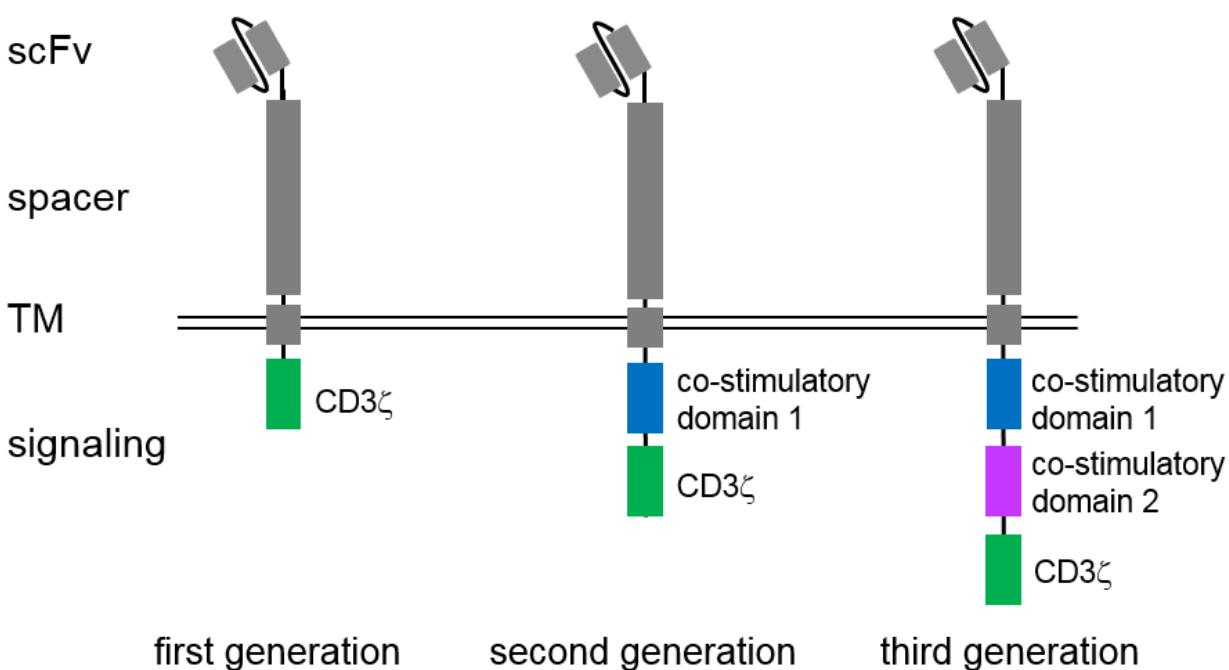
Fig. 2 **Different CAR generations.** CARs have a modular design comprising an extracellular binding portion (scFv), a spacer as well as a transmembrane (TM) domain linked to intracellular signaling domain(s). While first generation CAR T cells only contain a CD3ζ signaling domain, second and third generation CARs additionally incorporate one or two co-stimulatory domains.

The clinically approved second generation anti-CD19 CAR comprises the intracellular motif derived from CD28, however, latest findings showed that especially this co-stimulatory domain, although functional *in vivo*, is associated with a poor persistency of CAR engineered T cells due to an early exhaustion [37]. In contrast to this, 4-1BB signaling in CAR T cells prevents this exhaustion effect resulting in both persistency and functionality [38]. In addition, for the generation of functional CARs, it has been shown that the design of extracellular motifs are of utmost importance as well. Thus, spatial biological correlations between effector cell and target have to be considered in the CAR design and by varying the spacer length, empirically adjusted [39]. Furthermore, activation induced cell death (AICD), caused by FcγR binding to the spacer, has to be avoided [39, 40]. Therefore, an appropriate extracellular stalk or modified spacer domains should be considered in the CAR design.

The binding moiety, mostly an antibody-derived scFv, redirects the genetically engineered T cells to a defined target. However, an optimal binding depends on several factors

4

including antigen expression pattern, antigen expression level, actual affinity of an scFv for an antigen as well as the CAR expression on the T cells. Hence, especially in a solid tumor setting, high affinity CAR T cells have a great inherent potential to cause severe side effects by binding and destroying cells that express an antigen at a low level [41]. Indeed, low affinity scFvs allow a greater flexibility with regard to antigen choice, on the other hand might only induce a reduced T cell response [42].

One common risk which originates from all extracellular CAR domains is their potential immunogenicity. Accordingly, nearly all CAR constructs incorporate a human-derived stalk. But many scFvs, including FCM63 [43] in the anti-CD19 CAR and Leu-16 used in the anti-CD20 CAR [44], were derived from murine monoclonal antibodies and therefore might cause severe human-anti-mouse antibody (HAMA) responses; allergic-like reactions against the mouse peptides that aggravate with increasing treatment duration and repeating injections [45, 46]. Consequently, CAR T cells with scFv derived from chimeric or non-human antibodies might not only induce an anaphylactic reaction but also negatively affect the therapeutic outcome.

1.2   CAR T cells therapies: *Status quo* and challenges

The success of CAR T cell therapies strongly depends on the availability of a suitable target antigen. Ideally, such an antigen is exclusively and homogenously expressed on tumor cells or at least shows a restricted expression on a defined cell population which can be considered as tolerable side effect during the treatment. Amongst others, α-folate receptor for the treatment of ovarian cancer [47], mesothelin for the treatment of lung cancer (ClinicalTrials.gov Identifier NCT02414269), disialoganglioside GD2 for the treatment of neuroblastoma [48], epidermal growth factor receptor vIII for the treatment of malignant gliomas (ClinicalTrials.gov Identifier NCT01454596), epidermal growth factor receptor II for the treatment of colon cancer [41], prostate specific membrane antigen for the treatment of prostate cancer (ClinicalTrials.gov Identifier NCT00664196), carcio embryonic antigen for the treatment of adenocarcinoma (ClinicalTrials.gov Identifier 01723306) and metastatic breast cancer (ClinicalTrials.gov Identifier 00673829) or CD30 for the treatment of Hodgkin´s lymphoma (ClinicalTrials.gov Identifier NCT01316146) are already used as targets for CAR T cells as reviewed by Zhang *et al.* [49]. However, the current "poster child" is CD19 [50] which expression is limited to B cells and some B cell diseases [51]. Complete remission rates over 88% in patients suffering from relapsed or refractory acute lymphocytic leukemia (ALL) [52-54] and other success for chronic lymphocytic leukemia (CLL) [30, 31] and non-Hodgkin lymphoma (NHL) [28] have already been reported for CD19-directed CAR T cell therapies. But despite these remarkable achievements, there are also published setbacks for using CD19 as target. Thus, 60% of patient relapses during the treatment are caused by a loss of CD19 expression [55] as a result of genomic alterations and post-transcriptional modifications [56]. Such a loss is generally associated with a bad prognosis for the patients [57].

In contrast to CD19, CD20 is a non-internalizing epitope [58, 59], widely expressed on B cells and B cell malignancies including diffuse large B-cell lymphoma (DLBCL), hairy cell leukemia (HCL) and to a lesser extend in CLL as well as in ALL. In addition, CD20 was reported to be expressed on a minor subset of cancer-initiating melanoma cells [60, 61]. Consequently, rituximab, a clinically approved CD20-directed chimeric monoclonal antibody for the treatment of lymphoma [62, 63], was used in case studies with metastatic

melanoma patients [64, 65] confirming "a potential therapeutic value" [64]. Finally, Till *et al.* [44] combined the potency of CD20-directed therapies with the inherent biological potential of T cells and generated an anti-CD20 CAR. He assessed in a proof-of-concept clinical trial (ClinicalTrials.gov Identifier NCT00012207) safety and feasibility for the treatment of patients suffering from refractory indolent NHL or mantle cell lymphoma (MCL) and concluded that "adoptive immunotherapy with anti-CD20 cTCR bearing T cells is safe, feasible, and well-tolerated".

The clinical potential of engineered T cells and particularly their dissemination to large patient numbers is limited regarding the complexity of the manufacturing process. In this context, not only technical demands but also statutory regulations are defining very high barriers [66]. Thus, the production of CAR T cells comprises a multitude of laborious, individual work steps including T cell isolation (optional), activation, modification, expansion and formulation. To prevent "contamination, cross contamination and, in general, any adverse effect to the quality of the product" (2003/94/EC of 8 October 2003), this work places extremely strict requirements on operators, facility and infrastructure [66]. In order to meet both Advanced Therapy Medicinal Products (ATMPs) specifications as well as the rising demand of engineered cells, automatization of at least sub-processes is necessary.

While initial semi-automated protocols focused on cell expansion using e.g. G-Rex flasks (Wilson Wolf) or PermaLife bags (OriGen Biomedical) [67-69] and thus still depend on multiple open handling steps, Miltenyi Biotec developed a fully-closed, cGMP-compliant, automated T Cell Transduction (TCT) Process on the CliniMACS Prodigy. In collaboration projects with both Mock *et al.* [70] and Priesner *et al.* [71] the early feasibility to use this device to manufacture CAR engineered T cells was demonstrated. Due to the use of a single-use disposable tubing set which comprises a pump tubing, a separation column and a cultivation chamber (Fig. 3A) the risk of contaminations and particularly cross contaminations is strongly reduced. Defined process steps and parameters are pre-programmed in an `activity matrix´ (Fig. 3B). Overall, the automated TCT Process can be summarized as follows: T cells, enriched from patient-derived peripheral blood mononuclear cells (PBMC) will be activated, lentivirally transduced and expanded. During the latter step media will be regularly exchanged. After twelve days, the cellular product

will be formulated, harvested and if required frozen. The whole manufacture procedure can be closely monitored by analyzing process parameters such as pH and glucose concentration as well as product characteristics including cellular composition, T cell phenotype and transduction efficiency.
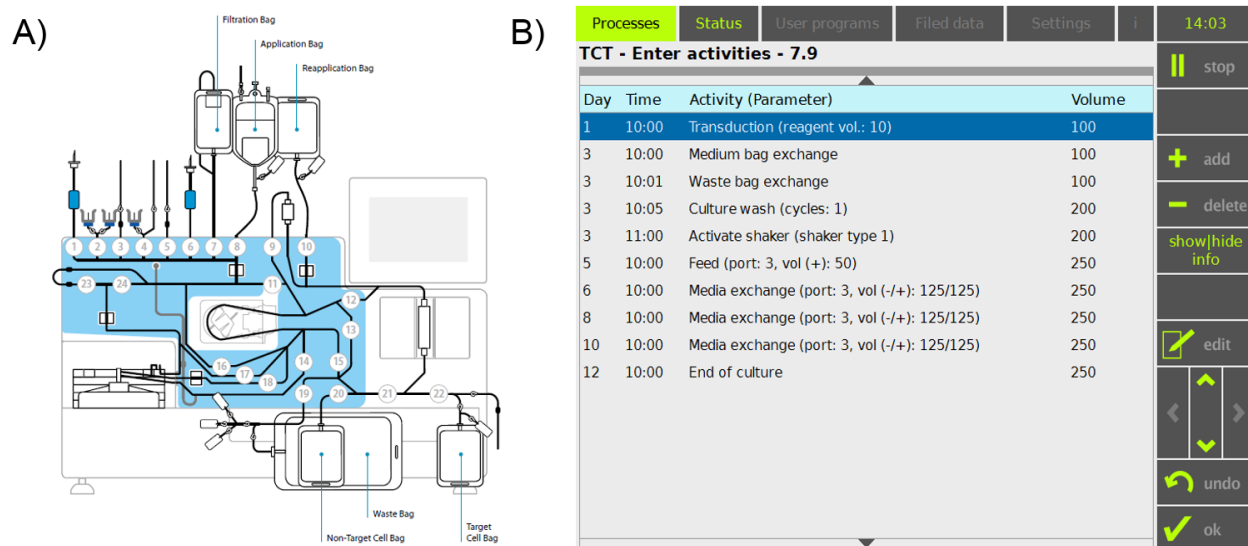
Fig. 3 **Technical description of tubing set and `activity matrix´ of the TCT Process.** (A) The single-use disposable tubing set TS520 comprises a pump tubing, a separation column and a cultivation chamber. (B) Before starting the process, the incoming product as well as later on reagents, lentiviral particle and media was sterile welded onto the closed tubing set. Numbers are indicating valves which are controlled according to the pre-programmed `activity matrix´ which defines the sequence of work steps and respective process parameters. (A) adapted from TS520 user manual; (B) unpublished data Miltenyi Biotec.

A successful process for the manufacturing of ATMPs can be assessed on the basis of following parameters: I) robustness, II) reproducibility, III) scalability, IV) cost efficiency and V) fulfillment of regulatory specifications [66]. A major technical challenge, however, represents the heterogeneity of the starting material. Thus, especially exhausted [72-74] of heavily pre-treated patient material exhibits strong differences regarding cellular composition and phenotypical characteristics. In this context, the use of defined reagents and cytokine combinations are of utmost importance to generate a homogenous cell product for the clinical use. The combination of IL-7 and IL-15 specifically supports the differentiation and maintenance of defined memory T cells [75]. Berger *et al.* [76] in accordance with Wang *et al.* [77] demonstrated that particularly central memory T cells (T_{CM}) persisted long-term after injection and thus maintained a potent T cell effector function. However, not only culture conditions but also initial process parameters might

8

impact both production and safety of the final product. Thus, the enrichment and genetic modification of malignant B cells and the subsequent reinfusion back into the patient must be prevented in all cases.

1.3   Solid tumors: A particular challenge for CAR T cell therapies

The pathophysiological characteristics of solid tumors represent an additional challenge for cellular therapies. Accordingly, T cell activation as well as sustaining an activated level is heavily impeded in a tumor microenvironment not seldom characterized by hypoxia, acidic pH or nutrient deficiency [49, 78]. Furthermore, immune suppressor cells including regulatory T cells (T_{reg}), myeloid-derived suppressor cells (MDSC) or immature dendritic cells are generally overrepresented in the inhospitable environment. Also several inhibitory pathways on solid tumors as well as T cell associated inhibitory mechanisms are upregulated [79, 80].

Currently, in contrast to B cell malignancies, the clinical potential of CAR T cell therapies in a solid tumor setting is disappointing. The issues range from a shortage of known `tumor-only´ antigens, a highly immunosuppressive tumor-microenvironment and an impeded tumor infiltration [49, 81]. While the two latter aspects primarily affect functionality, the lack of available antigens is a serious safety problem. At present all CAR formats target antigens that are highly expressed on tumorigenic cells but also, albeit to a lesser extent, on other tissues [82-84]. Nevertheless, the risk of on-target/off-tumor reactions is omnipresent.

There are several strategies and technologies to circumvent at least defined problems for CAR T cell therapies in a solid tumor setting. Lanitis *et al.* [85], for instance, demonstrated the possibility to physically separate `signal 1´ (CD3ζ) and `signal 2´ (CD28) on two CAR constructs directed against different target antigens. In this case, T cells only persisted and lysed tumor cells when both antigens were simultaneously expressed on the tumor. This AND CAR approach was further refined by Roybal *et al.* [86] who designed a very elegant synNotch receptor-based solution. A constitutively expressed CAR 1 is inducing the expression of CAR 2 upon target binding. The latter kills the tumor cell. Alternative safety approaches could be used, *inter alia*, enzyme-sensitive peptides that block the scFv until the tumor microenvironment-specific protease cleaves the linker [87].

While there are already several technologies focusing on safety, comparatively few approaches were published to improve efficacy of CAR T cells. Nevertheless, pioneer work was done by Melero *et al.* [88, 89]. They proved both that systemically administered anti-4-1BB antibodies and/or 4-1BBL engineered tumor cells can be used to induce a boosted T cell immunity. Stephan *et al.* [90] confirmed the "great value of using effective costimulation to boost anti-tumor T cell activities", however, they also referred to the inherent danger of an undirected T cell activation. To circumvent this issue, they endowed tumor-directed T cells with either CD80 or 4-1BBL and thus systemically enhanced the T cell effector function. Finally, Zhao *et al.* [50] transferred this technique into engineered T cells and demonstrated the superiority of CAR T cells receiving agonistic co-stimulation.

Another promising option to ameliorate the potential of ACT approaches including CAR T cells, T cell receptor (TCR)-modified T cells or TILs, not only in solid tumor settings but also beyond, might be the use of co-expressed chimeric co-stimulatory receptors (CCRs). These artificial receptors comprise an extracellular binding moiety and spacer as well as defined intracellular signaling domains which differ from conventional CAR designs. CCR expressing T cells do not proliferate nor induce any cytolytic activity upon target cell binding, however, are capable of boosting a simultaneously activated CAR T cell response which results in an enhanced release of inflammatory cytokines and increased cytolytic potential. Furthermore, it is conceivable that activated CCRs are able to ensure survival and persistency of engineered T cells. Thus, it is not only possible to enhance the potential of CAR T cells with this tool but also to control the co-stimulatory intensity which offers an option to avert an excessive release of cytokines that might cause a life-threatening cytokine storm [41, 91-93]. In this context, CCRs targeting artificial antigens such as dextran or biotin would provide a valuable tool. Consequently, the boost strength could be fine-tuned by the dose as well as the injection interval of those antigens. In addition, combinatorial approaches of CARs with low affinity scFvs that spare low level target antigen expression in basal tissues and CCRs used to boost their restricted cytolytic potential opens up a wide range of clinical therapies. Therapeutically there are fundamentally two approaches: I) CAR and CCR, co-expressed on T cells, are both directed against different antigens co-expressed on one tumor cell (cis approach) or II) the CAR specifically binds a tumor-associated antigen while the CCR recognizes a non-

tumor-associated antigen and induces the boost (trans approach). The general CCR concept is exemplified in Fig. 4.
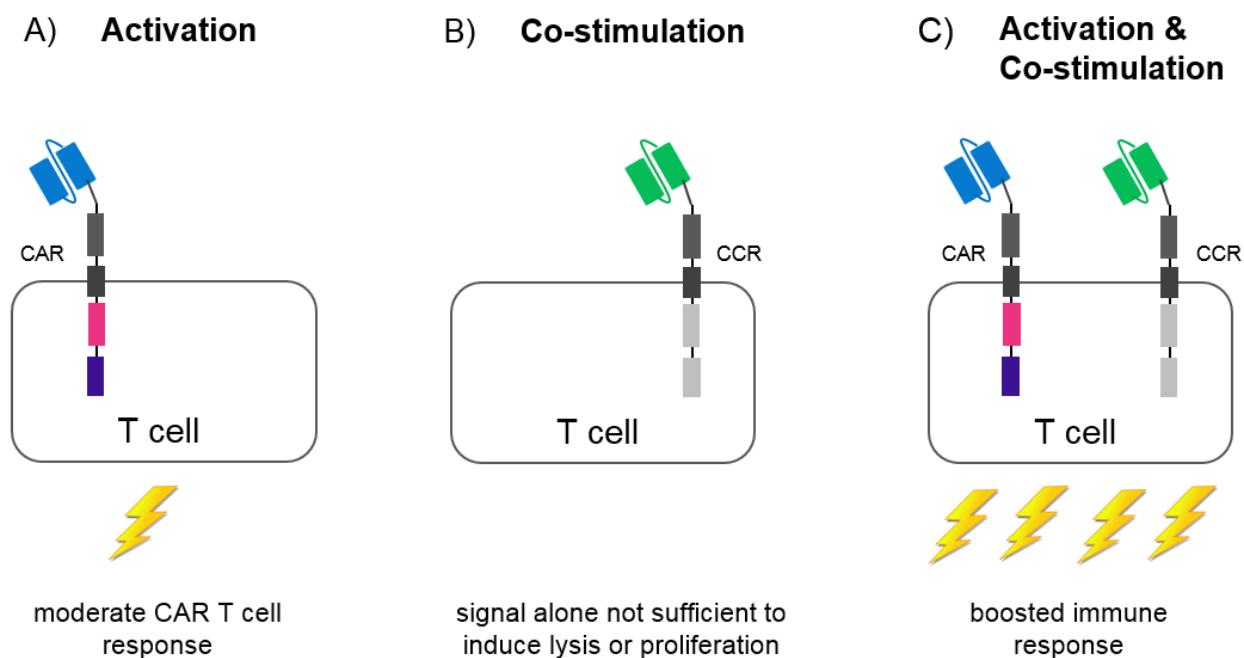
Fig. 4 **CCR concept to ameliorate CAR T cell potency.** T cells expressing a CAR with a low affinity scFv spare low level target antigen expression in basal tissues and thus reduces the risk of on-target/off-tumor reactions. (A) However, CAR T cells show only modest functionality. (B) CCRs on their own do not induce any T cell activation due to the incorporation of defined intracellular domains. (C) A simultaneous activation of both CAR and CCR results in a boosted immune response. This boosting effect can be induced in cis, by activating the CCR via a tumor-associated antigen, or in trans, by redirecting the CCR to a non-tumor-associated antigen.

1.4   Objectives

CAR expressing T cells, re-directed to specifically recognize and eliminate malignant cells, have demonstrated their efficacy in several clinical trials and thus greatly increased the scope and potency of ACT. However, especially in the context of anti-CD19 CAR T cell therapies for the treatment of B cell malignancies, a significant number of patients relapse due to antigen loss. Therefore, this study initially focused on the development of a novel CD20-directed CAR, intended to be used in a clinical setting for the treatment of lymphoma as well as melanoma patients. In addition, we focused on additional requirements facilitating a further dissemination of CAR T cells including a robust manufacturing process and technologies supposed to translate the medical success of CARs into solid tumor settings.

Project 1   Generation and evaluation of CD20-directed CAR T cells

Primary goals included the design of a novel CD20-directed CAR, the production of viral particles and the testing of herewith engineered T cells. For this purpose, molecular biological methods and transgenic cell lines were established. Furthermore, protocols and assays were developed to deeply analyze the potential of CAR T cells *in vitro* as well as *in vivo* and to finally translate our findings from bench to bedside.

Project 2   Automated manufacturing of engineered T cells

In this subproject, a closed cGMP-compliant, automated T Cell Transduction (TCT) Process on the CliniMACS Prodigy platform was established. Both robustness and reproducibility of the manufacturing process was verified with patient material.

Project 3   Assessing a boosting concept

In addition, we developed novel CCRs, tools which are meant to ameliorate the efficacy of CAR T cells especially in a solid tumor setting. Thus, this work provided protocols and tools to generate CAR as well as CCR co-expressing T cells and demonstrated that defined co-stimulatory ligands are required to enhance both killing potential and cytokine release upon a simultaneous activation of CAR and CCR.

2 Material and Methods

2.1 Material

2.1.1 Chemicals

AB Serum, human	Gemini Bio Products (West Sacramento, USA)
Accutase	Merck (Darmstadt, D)
Acetic acid	Sigma-Aldrich (St. Louis, USA)
Agarose	Invitrogen (Carlsbad, USA)
Ampicillin	Roche (Basel, CH)
ATP (10 mM)	Thermo Fisher Scientific (Waltham, USA)
Bovine Serum Albumin (BSA)	Sigma-Aldrich (St. Louis, USA)
CliniMACS CD4 Reagent	Miltenyi Biotec (Bergisch Gladbach, D)
CliniMACS CD8 Reagent	Miltenyi Biotec (Bergisch Gladbach, D)
CliniMACS PBS/EDTA	Miltenyi Biotec (Bergisch Gladbach, D)
Composol	Fresenius (Bad Homburg, D)
Dimethyl sulfoxide (DMSO)	Sigma-Aldrich (St. Louis, USA)
Disodium hydrogenorthophosphate	Merck (Darmstadt, D)
DMEM	Miltenyi Biotec (Bergisch Gladbach, D)
DNA Ladder 1 Kb plus	Thermo Fisher Scientific (Waltham, USA)
Phosphate Buffered Saline (PBS)	Thermo Fisher Scientific (Waltham, USA)
Dithiothreitol (DTT)	Sigma-Aldrich (St. Louis, USA)
Erythrosine B	Sigma-Aldrich (St. Louis, USA)
Ethylenediaminetetraacetate (EDTA)	Carl Roth (Karlsruhe, D)
Ethidium bromide 0,025%	Carl Roth (Karlsruhe, D)
Fetal calf serum (FCS)	Merck (Darmstadt, D)
Human Serum Albumin (HSA)	Grifols (Barcelona, ES)

IL-2, human recombinant	Miltenyi Biotec (Bergisch Gladbach, D)
IL-7, human recombinant	Miltenyi Biotec (Bergisch Gladbach, D)
IL-15, human recombinant	Miltenyi Biotec (Bergisch Gladbach, D)
Ionomycin	Sigma-Aldrich (St. Louis, USA)
Kanamycin sulfate	Sigma-Aldrich (St. Louis, USA)
LB agar (Luria/Miller)	Carl Roth (Karlsruhe, D)
LB growth medium	Invitrogen (Carlsbad, USA)
L-Glutamine	Lonza (Basel, CH)
MACSfectin Reagent	Miltenyi Biotec (Bergisch Gladbach, D)
MACS GMP T Cell TransAct	Miltenyi Biotec (Bergisch Gladbach, D)
Pancoll human	PAN Biotech (Aidenbach, D)
Penicillin-Streptomycin (P/S)	Lonza (Basel, CH)
Phorbol myristate acetate (PMA)	Sigma-Aldrich (St. Louis, USA)
Polyethylenimine, MW 25,000 (PEI)	Polysciences (Warrington, USA)
Potassium chloride	Merck (Darmstadt, D)
Potassium dihydrogen phosphate	Merck (Darmstadt, D)
RetroNectin	Takara (Kusatsu, J)
RPMI 1640	Biowest (Nuaillé, F)
SOC-Medium	NEB (Ipswitch, USA)
Sodium chloride (NaCl)	Merck (Darmstadt, D)
Sodium bicarbonate	Merck (Darmstadt, D)
Sodium butyrate	Sigma-Aldrich (St. Louis, USA)
T Cell TransAct, human	Miltenyi Biotec (Bergisch Gladbach, D)
TexMACS Medium research grade	Miltenyi Biotec (Bergisch Gladbach, D)
TexMACS GMP Medium	Miltenyi Biotec (Bergisch Gladbach, D)
Trypsin-EDTA 0,05%	Thermo Fisher Scientific (Waltham, USA)
Tween-20	Sigma-Aldrich (St. Louis, USA)
Vetflurane 1000 mg/g	Virbac (Fort Worth, USA)
XenoLight D-Luciferin-K$^+$ Salt	PerkinElmer (Waltham, USA)
XenoLight RediJect D-Luciferin Ultra	PerkinElmer (Waltham, USA)
X-Gal	Thermo Fisher Scientific (Waltham, USA)
Xylencyanol	AppliChem (Darmstadt, D)

2.1.2   Buffer, media and supplements

Agarose gel   1% Agarose
                         1x TAE buffer

B16-F10 medium   DMEM
                         10% FCS

CT26.wt medium   RPMI
                         10% FCS

Freezing medium   FCS
                         10% DMSO

HEK 293-T medium   DMEM
                         10% FCS

JeKo-1 medium   RPMI
                         10% FCS
                         2 mM L-Glutamin

Jurkat medium   RPMI
                         10% FCS
                         2 mM L-Glutamin

LB agar plates   40 g LB agar
                         ad 1 l Aqua dest.
                         add either Kanamycin (50 µg/ml) or Ampicillin (100 µg/ml)
                         (optional 40 µg/ml X-Gal) to autoclaved, cooled agar and pour
                         into 10-cm dishes.

LB growth medium   25 g LB growth medium
                         ad 1 l Aqua dest.
                         add either Kanamycin (50 µg/ml) or Ampicillin (100 µg/ml) to
                         autoclaved, cooled medium.

Mel526 medium   RPMI
                         10% FCS
                         2 mM L-Glutamin

NALM6 medium	RPMI
	10% FCS
	2 mM L-Glutamin
PBS 10x pH	80 g NaCl
	14.4 g Na_2HPO_4
	2.0 g KCl
	2.4 g KH_2PO_4
	ad 1 l Aqua dest.
	adjust to pH 7.4
PEB	100 ml PBS 10x
	4 ml 0,5 M EDTA
	5 g BSA
	ad 1 l Aqua dest.
Raji medium	RPMI
	10% FCS
	2 mM L-Glutamin
SupT1 medium	RPMI
	10% FCS
	2 mM L-Glutamin
TAE buffer 50x	57.1 ml acetic acid
	18.6 g EDTA
	ad 1 l with Aqua dest.
T cell medium	TexMACS
	12.5 ng/ml IL-7
	12.5 ng/ml IL-15
	(optional 200 IU IL-2 instead of IL-7 / IL-15)

2.1.3   Restriction endonucleases and buffers

Restriction endonucleases

Avr II	NEB (Ipswitch, USA)
*Bam*H I	NEB (Ipswitch, USA)
Bbs I	NEB (Ipswitch, USA)
Bcl I	NEB (Ipswitch, USA)
Bve I	Thermo Fisher Scientific Waltham, USA)
*Eco*R I	NEB (Ipswitch, USA)
Mlu I	NEB (Ipswitch, USA)
Nco I	NEB (Ipswitch, USA)
Nhe I	NEB (Ipswitch, USA)
Pml I	NEB (Ipswitch, USA)
Pst I	NEB (Ipswitch, USA)
Sal I	NEB (Ipswitch, USA)
Sca I	NEB (Ipswitch, USA)

Buffers

NEBuffer 1.1	NEB (Ipswitch, USA)
NEBuffer 2.1	NEB (Ipswitch, USA)
NEBuffer 3.1	NEB (Ipswitch, USA)
Buffer O	ThermoFisher Scientific Waltham, USA)

2.1.4 Oligonucleotides

All oligonucleotides were synthesized at Metabion (Planegg/Steinkirchen, D) or GATC (Konstanz, D).

gRNA 19.2   5'– CACCCCCCATGGAAGTCAGGCCCG –3´
             3'–   GGGGTACCTTCAGTCCGGGCCAAA –5'

gRNA 20.4   5'– CACCCACGCAAAGCTTCTTCATGA –3´
             3'–   GTGCGTTTCGAAGAAGTACTCAAA –5'

BriD-007	CGATGGGCTGTGGCCAATAG	Sequencing
pDoc-117	TGCGTGAAATCATCAGGGTGTC	Sequencing
pDoc-118	TTTCTTCTTGGCTCGGCGGCAAGG	Sequencing
pDoc-119	ACAGCAGCAGCACGCCACAAGTTC	Sequencing
pDoc-129	GCTTCAGCAGCGAGAAGTTG	Sequencing
pDoc-130	GAACTTGTGGCGTGCTGCTG	Sequencing
pDoc-148	AGTTCCGCTTGGTCTCATGC	Sequencing
pDoc-149	TCCTGCTGTCGCTGGTCATC	Sequencing
pDoc-150	CATGGCCCTTCCAGTAGCTC	Sequencing

2.1.5   Plasmids

Tab. 1   Generated and/or used plasmids

Construct	Description	Reference
#1455	retroviral anti-CD20 CAR	H. Abken (ZMMK Cologne)
Cas9/gRNA	Cas9/guide RNA encoding plasmid	Cong *et al.* 2013 [94]
CD20_1	lentiviral anti-CD20 (vh/vl) CAR derived from #1455	this work
CD20_2	lentiviral anti-CD20 CAR vl/vh IgG1 Spacer, P^{PGK}	Miltenyi Biotec
CD20_3	lentiviral anti-CD20 CAR vl/vh IgG1 Spacer, $P^{EF-1\alpha}$	Miltenyi Biotec
CD20_4	lentiviral anti-CD20 CAR vl/vh CD8 Spacer, $P^{EF-1\alpha}$	Miltenyi Biotec
CD20_5	lentiviral anti-CD20 CAR vh/vl CD8 Spacer, $P^{EF-1\alpha}$	Miltenyi Biotec
CD20_6	lentiviral anti-CD20 CCR 4-1BB_4-1BB IgG1 Hinge_CH2_CD3	this work
CD20_7	lentiviral anti-CD20 CCR 4-1BB_CD3ϵ IgG1 Hinge_CH2_CD3	this work
CD20_8	lentiviral anti-CD20 CCR CD3ϵ_CD3ϵ IgG1 Hinge_CH2_CD3	this work
CD20_9	lentiviral anti-CD20 CCR CD28_4-1BB IgG1 Hinge_CH2_CD3	this work
CD20_10	lentiviral anti-CD20 CCR CD28_CD3ϵ IgG1 Hinge_CH2_CD3	this work
CD20_11	lentiviral anti-CD20 CCR 4-1BB IgG1 Hinge_CH2_CD3	this work
CD20_12	lentiviral anti-CD20 CCR CD28_CD28 IgG1 Hinge_CH2_CD3	this work
CD20_13	lentiviral anti-CD20 CCR CD28 IgG1 Hinge_CH2_CD3	this work
CD20_14	lentiviral anti-CD20 CCR 4-1BB_4-1BB CD8 Spacer	this work
CD20_15	lentiviral anti-CD20 CCR 4-1BB CD8 Spacer	this work
CD20_16	lentiviral anti-CD20 CCR CD28_4-1BB CD8 Spacer	this work
CD20_17	lentiviral anti-CD20 CCR 4-1BB_4-1BB IgG4 Spacer long	this work
CSPG4_1	retroviral aCSPG4 CAR	H. Abken (ZMMK Cologne)
CSPG4_2	lentiviral aCSPG4 CAR 225.28s IgG4 Hinge_CH2_CH3	this work
CSPG4_3	lentiviral aCSPG4 CAR 225.28s IgG4 Hinge_CH3	this work
CSPG4_4	lentiviral aCSPG4 CAR 225.28s IgG4 Hinge	this work
CSPG4_5	lentiviral aCSPG4 CAR TP61.5 IgG4 Hinge_CH2_CH3	this work
CSPG4_6	lentiviral aCSPG4 CAR TP61.5 IgG4 Hinge_CH3	this work
CSPG4_7	lentiviral aCSPG4 CAR TP61.5 IgG4 Hinge	this work
CSPG4_8	lentiviral aCSPG4 CAR 763.74 IgG4 Hinge_CH2_CH3	this work
CSPG4_9	lentiviral aCSPG4 CAR 763.74 IgG4 Hinge_CH3	this work
CSPG4_10	lentiviral aCSPG4 CAR 763.74 IgG4 Hinge	this work
CSPG4_11	lentiviral aCSPG4 CAR 763.74 IgG4 CD8 Spacer	this work
DC_1	lentiviral plasmid, combination of CD20_14 & CSPG_2	this work
DC_2	lentiviral plasmid, combination of CD20_17 & CSPG_2	this work
Doc_1	lentiviral plasmid encoding firefly luciferase_eGFP	this work
Doc_2	lentiviral plasmid encoding hCD20_eGFP	this work
GFP	lentiviral GFP encoding construct	Lentigen
MB_001	lentiviral CAR library scFv IgG4 Hinge_CH2_CH3	this work
MB_002	lentiviral CAR library scFv IgG4 Hinge_CH3	this work

Construct	Description	Reference
MB_003	lentiviral CAR library scFv IgG4 Hinge	this work
MB_004	lentiviral CAR library scFv hCD8	this work
MB_005	lentiviral CAR library endogenous domains (CD20_2 derived)	this work
MB_006	lentiviral CAR library endogenous domains (CD20_4 derived)	this work
pCMVdR8.74	helper plasmid, HIV-1-derived gag pol tat rev	pCMVR8.74 was a gift from Didier Trono (Addgene plasmid # 22036)
pHit60	helper plasmid encoding gag pol	Soneoka *et al.* 1995 [95]
pMDG-2	helper plasmid, VSV-G	pMD2.G was a gift from Didier Trono (Addgene plasmid # 12259)
CG1711	self-inactivating lentiviral vector	Cell Genesis Inc.; South San Francisco (USA)

2.1.6   Kits

Amaxa Cell line Nucleofector Kit V   Lonza (Basel, CH)

Anti-Biotin MultiSort Kit   Miltenyi Biotec (Bergisch Gladbach, D)

B cell isolation Kit II, human   Miltenyi Biotec (Bergisch Gladbach, D)

Cell line Nucleofector Kit V   Lonza (Basel, CH)

CellTrace Violet Cell Proliferation Kit   Thermo Fisher Scientific (Waltham, USA)

EndoFree PlasmidMaxiKit   Qiagen (Hilden, D)

MACSPlex Cytokine 12 Kit, human   Miltenyi Biotec (Bergisch Gladbach, D)

MACS GMP TransAct CD3/CD28 Kit   Miltenyi Biotec (Bergisch Gladbach, D)

NucleoSpin Gel and PCR Clean-Up   Macherey-Nagel (Düren, D)

NucleoSpin Plasmid EasyPure   Macherey-Nagel (Düren, D)

Pan T cell Isolation Kit, human   Miltenyi Biotec (Bergisch Gladbach, D)

Plasmid Maxi Kit   Qiagen (Hilden, D)

Rapid DNA Dephos & Ligation Kit   Sigma-Aldrich (St. Louis, USA)

ZymoPure^{TM} Plasmid Midiprep Kit   Zymo research (Irvine, USA)

2.1.7 Antibodies

Tab. 2   Antibodies and staining reagents

Antibody	clone	conjugate	Producer
7-AAD	---	---	Miltenyi Biotec (Bergisch Gladbach, D)
Biotin	---	MB / APC / VB	Miltenyi Biotec (Bergisch Gladbach, D)
CD20 CAR peptide	---	PE	product in development (Miltenyi Biotec, D)
CD3	BW264/56 & REA613	FITC	Miltenyi Biotec (Bergisch Gladbach, D)
CD4	VIT4	PE / VG	Miltenyi Biotec (Bergisch Gladbach, D)
CD8	BW138/80	VB / APC-Vio770	Miltenyi Biotec (Bergisch Gladbach, D)
CD14	TÜK4	APC	Miltenyi Biotec (Bergisch Gladbach, D)
CD16	REA423	FITC / PE	Miltenyi Biotec (Bergisch Gladbach, D)
CD19	LT19	VB / MB	Miltenyi Biotec (Bergisch Gladbach, D)
CD20	LT20	APC / Biotin	Miltenyi Biotec (Bergisch Gladbach, D)
CD25	4E3	PE	Miltenyi Biotec (Bergisch Gladbach, D)
CD45	REA747	VB	Miltenyi Biotec (Bergisch Gladbach, D)
CD45RO	REA611	PE-Vio770	Miltenyi Biotec (Bergisch Gladbach, D)
CD56	REA196	PE	Miltenyi Biotec (Bergisch Gladbach, D)
CD62L	145/15	VB	Miltenyi Biotec (Bergisch Gladbach, D)
CD69	FN50	APC	Miltenyi Biotec (Bergisch Gladbach, D)
CD95	DX2	APC	Miltenyi Biotec (Bergisch Gladbach, D)
CD271 (∆LNGFR)	ME20.4-1.H4	APC	Miltenyi Biotec (Bergisch Gladbach, D)
CSPG4	EP-1	APC / VB	Miltenyi Biotec (Bergisch Gladbach, D)
EGFR	EGFR.1 (RUO)	PE	BD (Franklin Lakes, USA)
IgG Fc	polyclonal	Biotin	Thermo Fisher Scientific (Waltham, USA)
PE	---	MB	Miltenyi Biotec (Bergisch Gladbach, D)
PI	---	---	Miltenyi Biotec (Bergisch Gladbach, D)

2.1.8 Cell lines

Tab. 3   Generated and/or used cell lines

Cell line	Reference
B16-F10 $^{FFluc\_eGFP}$	this work
CT26.wt $^{FFluc\_eGFP}$	this work
HEK 293-T	ATCC CRL-3216
JeKo-1	ATCC CRL-3006
JeKo-1$^{FFluc\_eGFP}$	this work
JeKo-1$^{FFluc\_eGFP}$ CD19 ko	this work
JeKo-1$^{FFluc\_eGFP}$ CD20 ko	this work
JeKo-1$^{FFluc\_eGFP}$ CD19/CD20 ko	this work
Jurkat	ATCC TIB-152
Mel526	RRID:CVCL_8051
Mel526$^{FFluc\_eGFP}$	this work
Mel526$^{CD20\_FFluc\_eGFP}$	this work
NALM6	ATCC CRL-3273
NALM6$^{FFluc\_eGFP}$	this work
Raji	ATCC CCL-86
Raji$^{FFluc\_eGFP}$	this work
Raji^{FFluc}	Lentigen
SupT1	ATCC CRL-1942

2.1.9 Consumables, devices and software

96/48/24/12-well flat/round bottom cell culture plates (non) tissue culture treated	Corning (New York, USA)
75/175 cm^2 cell culture flasks	Sigma-Aldrich (St. Louis, USA)
96-well black well plates	Miltenyi Biotec (Bergisch Gladbach, D)
10 cm culture dish	Sarstedt (Nümbrecht, D)
ABT 220-4m	Kern+Sohn GmbH (Balingen, D)
ACCU-CHECK Aviva	Roche (Basel, CH)
BD 115	Binder (Tuttlingen, D)

BioRad Power Pac 300 Bio Rad	Bio-Rad (Hercules, USA)
BP 3100S	Sartorius (Göttingen, D)
Cell Strainer 40 µm and 70 µm	BD (Franklin Lakes, USA)
Cell culture hood, Hera Safe KS	Thermo Fischer Scientific (Waltham, USA)
Centrifuge 4515R	Eppendorf (Hamburg, D)
Centrifuge, Multifuge 4KR	Thermo Fischer Scientific (Waltham, USA)
Centrifuge, Eppendorf 5415D	Eppendorf (Hamburg, D)
Centrifuge, Multifuge X3R	Heraeus Instruments (Hanau, D)
Certomat BS-1	Sartorius (Göttingen, D)
CliniMACS Prodigy	Miltenyi Biotec (Bergisch Gladbach, D)
CliniMACS Prodigy TCT application V.1	Miltenyi Biotec (Bergisch Gladbach, D)
Clone Manager 9 Professional Edition	Scientific & Educational Software (Denver, USA)
CO_2 Incubator, Hera Cell	Thermo Fischer Scientific (Waltham, USA)
Conical bottom tubes, 50 ml, 15 ml	BD (Franklin Lakes, USA)
Filter Unit 0,45 µm	Merck (Darmstadt, D)
Gene Pulser II System Bio Rad	Bio-Rad (Hercules, USA)
Graph Pad Prism 7.0	GraphPad Software, Inc. (La Jolla, USA)
Hemocytometer	NanoEntek (Seoul, Korea)
Hera Safe KS	Thermo Fischer Scientific (Waltham, USA)
IncuCyte	Essen Bioscience (Ann Arbor, USA)
IVIS Lumina III	PerkinElmer (Waltham, USA)
Julabo 5	Julabo Labortechnik (Seelbach, D)
Living Image	PerkinElmer (Waltham, USA)
MACSplex Filter plates	Miltenyi Biotec (Bergisch Gladbach, D)

MACSQuant Analyzer 10	Miltenyi Biotec (Bergisch Gladbach, D)
MACSQuantify, version 2.5 – 2.10	Miltenyi Biotec (Bergisch Gladbach, D)
MACS Separator (Octo, Quadro)	Miltenyi Biotec (Bergisch Gladbach, D)
MACS separation columns (MS, LS, LD)	Miltenyi Biotec (Bergisch Gladbach, D)
Microcentrifuge tubes	STARLAB (Hamburg, D)
Microscope, Leica DM IL LED	Leica Microsystems (Wetzlar, D)
Microsoft Office Professional 2010 - 2016	Microsoft Coorporation (Redmond, USA)
Mr. Frosty	Thermo Fischer Scientific (Waltham, USA)
NALGENE Cryogenic vials	Thermo Fischer Scientific (Waltham, USA)
NanoDrop ND-1000 Spectrophotometer	Thermo Fischer Scientific (Waltham, USA)
NEB 5-alpha Competent *E. coli*	NEB (Ipswitch, USA)
Nuaire class II biological safety cabinet	Nuaire (Plymouth, USA)
Nucleofector 2b Device	Lonza (Basel, CH)
Orbital shaker Titramax 100	Heidolph (Schwabach, D)
pH-Meter, pH-Meter 765 Calimatic	Elektronische Messgeräte, (Berlin, D)
pH Test Strips (MColorpHast, pH 6.5-10)	Merck (Darmstadt, D)
Red Blood Cell Lysis Solution (10x)	Miltenyi Biotec (Bergisch Gladbach, D)
Reax top	Heidolph (Schwabach, D)
Surgical Scalpel	Aesculap AG (Tuttlingen D)
Sysmex XP-300	Sysmex Deutschlang, (Norderstedt, D)
Thermomixer comfort	Eppendorf (Hamburg, D)
Transfer bag	Terumo (Tokio, J)
TS520 tubing set	Miltenyi Biotec (Bergisch Gladbach, D)
TSCD II	Terumo (Tokio, J)
VICTOR X4 2030 Multilabel Reader	PerkinElmer (Waltham, USA)

XGI-8 Anesthesia System   PerkinElmer (Waltham, USA)

Additional consumables including pipettes, pipet tips, serological pipets, different reaction tubes or syringes were mainly ordered at Eppendorf (Hamburg, D), PeQlab (Erlangen, D), Greiner bio-one (Kremsmünster, A), Mettler-Toledo (Gießen, D), Sarstedt (Nümbrecht, D) STARLAB (Hamburg, D), BD (Franklin Lakes, USA) and Braun (Bethlehem, USA).

2.2 Molecular biological methods

2.2.1 Standard methods and explanations

All molecular biological methods not described in detail were performed as described by Green and Sambrock [96]. Unless mentioned to the contrary, kits were used according to the manufacturer´s protocol.

2.2.2 Molecular cloning

In silico designed DNA-elements were human codon optimized and synthesized at GenScript (Piscataway, USA) or ATUM (Newark, USA). Enzymatically digested DNA fragments were separated via gel electrophoresis (Cap. 2.2.1) and extracted using the NucleoSpin Gel and PCR Clean-up-Kit. If required, DNA fragments were dephosphorylated using the Rapid DNA Dephos and Ligation Kit and subsequently cloned into the intended plasmid considering the molar ratio of backbone to insert using the Rapid DNA Dephos and Ligation Kit as exemplarily shown in Tab. 4.

Tab. 4   Conventional cloning protocol

ratio backbone : insert	µl		
	x	50 ng backbone	
1:3	x	150 ng/F insert	F = bp backbone / bp insert
1:5	x	250 ng/F insert	
	ad 8	Aqua dest.	
	2	DNA Dilution Buffer	
	10	DNA Ligation Buffer	
		T4 DNA Ligase	

Incubation for 10 min at RT.

Generally, scFv sequences as well as co-stimulatory- and signaling domain-encoding DNA elements were cloned following a high-throughput protocol (Tab. 5) using *Bve* I, a Type IIS restriction enzyme [97].

Tab. 5   High-throughput cloning protocol

	µl
backbone	2
insert 1	2
insert 2 (optional)	2
Buffer O 10x	5
Oligonucleotides 50x	1
Bve I	2
DTT 10 mM	5
ATP 10 mM	2.5
T4 DNA Ligase	2
Aqua dest.	ad 50

Incubation for 5 h at 37°C.

2.2.3   Transformation of chemically competent *E.coli*

1 ng plasmid or rather 5 µl of the ligation preparation (Cap. 2.2.2) were added to freshly thawed NEB 5-alpha competent *E. coli*, carefully mixed and incubated for 30 min on ice. Transformation was achieved via heat shock at 42°C for 30 s. Subsequently, cells were placed on ice for 5 min, before 250 µl SOC-Medium was added into the mixture and incubated for 60 min at 37°C with 250 rpm. The mixture was spread onto LB-Agar selection plates with either 50 µg/ml Kanamycin or 100 µg/ml Ampicillin (optional 40 µg/ml X-Gal, respectively). Plates were incubated at 37°C overnight.

2.2.4   Amplification, isolation and quantification of plasmids

After transformation (Cap. 2.2.3), plasmid DNA was amplified in bacteria due to prokaryotic DNA replication mechanisms and subsequently purified out of the *E. coli*.

Grown colonies were picked from the LB-Agar selection plate and transferred into 2 ml LB growth media containing antibiotics (50 µg/ml Kanamycin or 100 µg/ml Ampicillin). The liquid culture was incubated overnight at 37°C in a shaking incubator (300 rpm). Plasmid DNA was isolated by alkaline hydrolysis using the miniprep kit NucleoSpin Plasmid.

For a higher yield, which was required for plasmids used for lentiviral vector production, a 2 ml pre-culture was used after 6-8 h to inoculate either 50 ml (midiprep) or 200 ml (maxiprep) LB growth media supplemented with either 50 µg/ml Kanamycin or 100 µg/ml Ampicillin. Bacterial culture was incubated overnight at 37°C with 300 rpm. The ZymoPURE Plasmid Midiprep kit was used to purify up to 300 µg endotoxin-free plasmid DNA. Maxipreps were performed with the EndoFree Plasmid Maxi kit enabling the isolation of up to 500 µg plasmid DNA.

Based on the characteristic absorption maximum of DNA at 260 nm, all DNA concentrations and purities (OD_{260}/OD_{280}) were determined using the NanoDrop ND-1000 Spectrophotometer.

2.2.5 Plasmid sequence verification

Successive cloning steps were analyzed via hydrolytic cleavage catalyzed by restriction endonucleases (Tab. 6) followed by gel electrophoresis (Cap. 2.2.1).

Tab. 6   Restriction endonuclease digestion protocol

	µl
plasmid DNA	7
buffer	2
endonuclease 10 U/µl	1
Aqua dest.	ad 20 µl

Incubation for 1 h at 37°C.

All final constructs were sequenced at GATC (Konstanz, D) using appropriate sequencing primers (Cap. 2.1.4). Sequences were analyzed using Clone Manager.

2.3　　　Cell biological methods

Unless mentioned to the contrary, kits were used according to the manufacturer´s protocol.

2.3.1　　　PBMC preparation

Buffy coats and leukapheresis products were obtained from the university hospital in Dortmund and Cologne. Each donor used in this study provided written informed consent before sample collection in accordance with the declaration of Helsinki. PBMC were isolated sterile using Pancoll human and density gradient centrifugation for 35 min at 445 g with moderate break.

2.3.2　　　Isolation, activation and expansion of PAN T cells

PAN T cells were isolated from freshly isolated or frozen PBMC using the human PAN T cell isolation Kit.

T cells were activated in TexMACS supplemented with either 12.5 ng/ml recombinant human IL-7 and 12.5 ng/ml recombinant human IL-15 or 200 IU IL-2 with MACS GMP T Cell TransAct with a titer of 1:17.5 or T Cell TransAct, human with a titer of 1:100. For this purpose, 1E6 T cells per cm^2 were cultured in 1 ml medium for 72 h at 37°C and 5% CO_2 atmosphere before the stimulation reagent was removed. From then onwards T cells were cultured in 24-well plates in 2 ml TexMACS supplemented with either 12.5 ng/ml recombinant human IL-7 and 12.5 ng/ml recombinant human IL-15 or 200 IU IL-2. T cells were splitted 1:2 every other day.

2.3.3　　　Isolation and cultivation of B cells

B cells were isolated from frozen PBMC using the B cell isolation Kit II, human and cultured overnight in TexMACS.

2.3.4   Cultivation of cell lines

All cell lines were cultured in an appropriate media (Cap. 2.1.2) at 37°C and 5% CO_2 atmosphere. Cell lines were splitted twice every week. For this purpose, adherent cell lines were detached using Trypsin-EDTA 0,05% or Accutase (melanoma cell lines) for 5 min at 37°C.

2.3.5   Freezing and thawing of cells

For freezing cells were centrifuged at 300 g, resuspended in freezing medium (Cap. 2.1.2) and subsequently stored at -70°C using a Mr. Frosty freezing container. After 24 h cells were transferred into liquid nitrogen for long term storage.

Cells were thawed at 37°C, immediately washed in their culture medium (Cap. 2.1.2) and appropriately plated.

2.3.6   Production of lentiviral particles

Vesicular stomatitis virus glycoprotein (VSV-G)-pseudotyped lentiviral vectors were produced using HEK 293-T cells. 1.6E7 cells were seeded in 20 ml medium (Cap. 2.1.2) in a T175 flask 20 h prior to transfection. 3.15 µg VSV-G encoding plasmid pMDG-2, 19.37 µg gag/pol/rev encoding plasmid pCMVdR8.74 and 12.59 µg transfer vector plasmid were diluted in 3.5 ml DMEM without additives and mixed with 3.5 ml DMEM supplemented with 280 µl PEI (1 mg/ml). The transfection mixture was incubated for 20 min at RT. HEK 293-T medium was completely removed from the cells and replaced with 16 ml DMEM without additives. Subsequently, the transfection mixture was carefully added to the cells. After 4 - 6 h 2.5 ml FCS were added and cultured for 24 h before 520 µl sodium butyrate (500 mM) was additionally added. 48 h after transfection, supernatant was collected, sterile filtrated and concentrated at 4°C for 24 h at 5350 g. Pelleted lentiviral particles were diluted in PBS and freshly used or stored at -70°C.

If required, titers of the lentiviral particles were determined. For this purpose, either SupT1 or Jurkat cells were transduced with an increasing volume of lentiviral particles. After 72

h the specific transgenic expression was analyzed via flow cytometry (Cap. 2.3.7) and titers were calculated based on the frequency and quantity of transgenic cells.

2.3.7   Cell surface marker staining and detection via flow cytometry

At least 1E4 cells were harvested and resuspended in PEB. Cells were stained in appropriate titers with conjugated antibodies or peptides for 10 min at 4°C. Subsequently, PEB was added to the cells, centrifuged for 5 min at 300 g and resuspended in fresh PEB. If required cells were additionally stained with secondary antibodies, washed and resuspended as described above.

Stained cells were measured using the MACSQuant Analyzer 10.

2.4   Gene-engineering

Unless mentioned to the contrary, kits were used according to the manufacturer´s protocol.

2.4.1   T cell transduction

T cells were transduced 24 - 48 h after activation (Cap. 2.3.2) with fresh or frozen, carefully resuspended VSV-G pseudotyped lentiviral particles.

2.4.2   Automated T Cell Transduction Process

Apel *et al.* [98] briefly summarized all relevant technical characteristics of the TCT Process on the CliniMACS Prodigy.

Initially, a single-use disposable tubing set TS520 was primed with CliniMACS PBS/EDTA supplemented with 0.5% HSA. According to the pre-defined `activity matrix´, samples were stained with CliniMACS CD4 Reagent and CliniMACS CD8 Reagent for 30 min at 4-8°C and subsequently enriched via the integrated separation column for magnetic selection. Up to 1E8 enriched cells, eluted in TexMACS GMP Medium supplemented with 3% heat-inactivated human AB Serum, 12.5 ng/mL recombinant human IL-7 and 12.5 ng/mL recombinant human IL-15, were transferred into the cultivation chamber and activated with 1 vial of the MACS GMP T Cell TransAct. After 24 h T cells were automatically transduced. For this purpose, a 150 ml transfer bag which contains the lentiviral particles (formulated in 10 ml culture medium) was sterile welded onto the TS520 tubing set using the TSCD II. On day three, a culture wash was performed to remove surplus stimulation reagent and lentiviral vector. During the following nine days, the cultivation volume was subsequently increased to 250 ml whereby a maximum of 180 ml medium was exchanged every day. From the sixth day following, cells were cultured without human AB serum. On day twelve, cells were formulated and harvested using either TexMACS medium or Composol supplemented with 2.84% HSA. The TCT Process was closely controlled. Thus, cell numbers and viability were measured frequently using

a hemocytometer and erythrosine B staining. Furthermore, pH and glucose concentration was monitored using pH Test Strips and a handheld blood sugar meter (ACCU-CHECK Aviva). Cellular composition, T cell phenotype as well as transduction efficiency were analyzed on day zero (enriched fraction), on day five or six (in-process control) and on day twelve (final product) using flow cytometry (Cap. 2.3.7).

2.4.3   Enrichment of gene-engineered T cells

If required, CAR-expressing T cells were enriched on day seven after activation (Cap. 2.3.2) via a co-expressed marker gene (either ∆LNGFR or ∆EGFR). For this purpose, gene-modified T cells were harvested, stained with anti-LNGFR-Biotin (titer 1:11) or anti-EGFR-PE (titer 1:5) for 10 min at 4°C, washed and additionally stained with either anti-Biotin MultiSort-MB (titer 1:5) or anti-PE-MB for 15 min at 4°C, respectively. For the enrichment LS columns and a QuadroMACS Separator were used.

Co-transduced T cells expressing both transgenes ∆LNGFR and ∆EGFR were enriched using the anti-Biotin-MultiSort Kit. Initially ∆LNGFR-positive T cells were enriched as described above. After the LS column elution, the anti-Biotin MultiSort-MB was released and EGFR-positive cells were enriched as previously described.

1E6 co-enriched CAR T cells per cm^2 cells were seeded in TexMACS supplemented with 12.5 ng/ml recombinant human IL-7 and 12.5 ng/ml recombinant human IL-15 (or 200 IU IL-2) as well as T Cell TransAct, human with a titer of 1:500 for T cell re-activation. After 48 h at 37°C and 5% CO_2 atmosphere stimulation reagent was removed and transgenic T cells were expanded in TexMACS supplemented with cytokines (Cap. 2.3.2).

2.4.4   Generation of firefly luciferase-expressing cell lines

In this study the following cell lines were genetically modified to express the firefly luciferase (FFluc) gene: JeKo-1, Raji, NALM6, Mel526, CT26.wt and B16-F10. Initially, 1E5 cells were seeded in 1 ml complete growth medium (Cap. 2.1.2) per well in a 48-well plate. After 24 h cells were transduced with LV-Doc_1 (Cap. 2.3.6) (100x, Titer 1,4E7

TU/ml) with multiplicity of infection (MOI) 4. Cells were cultured for 72 h before cells were harvested and seeded (Cap. 2.3.4) at a density of 0.3 cells/well in a 96-well culture plate. Cells were cultured for two weeks and then transferred into 12-well culture plates for further expansion. Marker expression as well as the transgenic GFP-gene expression were analyzed via flow cytometry (Cap. 2.3.7) before several clones of all cell lines were frozen (Cap. 2.3.5).

2.4.5 Generation of CD20-expressing Mel526$^{FFluc\_eGFP}$ cells

Lentiviral particle LV-Doc_2 was generated as previously described (Cap. 2.3.6). Herewith 1E6 Mel526$^{FFluc\_eGFP}$ cells, cultured in complete growth medium in 6-well plates for 24 h, were transduced. After 72 h CD20-positive cells were enriched using anti-CD20-Biotin/anti-Biotin-MB (Cap. 2.3.7), LS columns and a QuadroMACS Separator. Hereafter, 0.3 cells/well in a 96-well culture plate were seeded and CD20 expressing Mel526$^{FFluc\_eGFP}$ single cell clones were expanded for two weeks, analyzed (Cap. 2.3.7) and frozen (Cap. 2.3.5).

2.4.6 Generation of JeKo-1 knock-out cells

GuideRNA 19.2 und 20.4 (Cap. 2.1.4) were cloned (Cap. 2.2.2) into the gRNA plasmid under the control of a T7-promoter using *Bbs* I and subsequently amplified in a Midiprep (Cap. 2.2.4). 2E6 JeKo-1$^{FFluc\_eGFP}$ cells were co-transfected with the 1 µg Cas9 encoding plasmid and either 1 µg gRNA 19.2 or 1 µg gRNA 20.4 using the Nucleofector 2b Device and the Cell line Nucleofector Kit V.

Seven days post transfection CD19-positive as well as CD20-positve cells were depleted using LD-columns after staining with either anti-CD19-MB or anti-CD20-Biotin/anti-Biotin-MB (Cap. 2.3.7). Subsequently, 0.3 cells/well in a 96-well culture plate were seeded and a single cell expansion was performed. After two weeks, JeKo-1$^{FFluc\_eGFP}$ CD19 ko and JeKo-1$^{FFluc\_eGFP}$ CD20 ko single cell clones were analyzed by flow cytometry (Cap. 2.3.7) and frozen (Cap. 2.3.5).

Finally, JeKo-1$^{FFluc\_eGFP}$ CD19/CD20 ko cells were generated. For this purpose, JeKo-1$^{FFluc\_eGFP}$ CD20 ko cells were again co-transfected with 1 µg Cas9 encoding plasmid and 1 µg gRNA 19.2. Single cell clones were generated as described above using LD-columns and a single cell expansion strategy.

2.5   Functionality assays

Unless mentioned to the contrary, kits were used according to the manufacturer´s protocol.

2.5.1   Flow-based killing assay

5E6 target cells were labeled with CellTrace Violet Dye (500 µM) in a 1:500 solution in PBS for 5 min at 37°C and 5% CO_2 atmosphere. Subsequently, 5 ml FCS and 5 ml TexMACS were added and cells were pelleted at 300 g for 10 min. Cells were then resuspended in TexMACS, counted using a hemocytometer and adjusted to 1E5 cells/ml. That followed, 1E4 VioDye-positive target cells were seeded in 100 µl into 96-well round bottom plates before either 100 µl Mock-transduced or 100 µl CAR-positive T cells were added in different effector to target ratios and the plates were centrifuged for 1 min at 100 g. Mock was always adjusted to pipette similar cell numbers. Each sample was measured in duplicates. Blank was defined as 100 µl labeled target cells with 100 µl TexMACS. After 4 - 24 h cultivation at 37°C and 5% CO_2 atmosphere plates were incubated for 20 min at 4°C and then, after adding PI (titer 1:100) to discriminate death cells, 70 µl per well were analyzed via flow cytometry (Cap. 2.3.7). PI-negative, VioDye-positive cells were defined as viable target cells which allowed to calculate the killing frequency using the following equation:

$$\text{Killing } [\%] = \left(1 - \frac{\text{count sample}}{\text{count blank}} \right) \text{x } 100$$

2.5.2   Bioluminescence-based killing assay

For standard killing assays, 2E5 cells/ml FFluc-expressing target cells (Cap. 2.4.4) were resuspended in TexMACS and 100 µl of the cell suspension were seeded in 96-well black well plates before 100 µl effector cells from a serial dilution (e.g. 10:1; 5:1; 2.5:1; 1.25:1) starting with 2E6 Mock transduced or CAR expressing T cells were added. Mock was always adjusted to pipette similar cell numbers. All samples were measured in duplicates. At least six wells were used as `target alone´ and `target lysed´ sample were

no effector cells were added. To the latter, additionally 4 µl/200 µl/well of 50% Tween-20 in TexMACS was pipetted. Plates were then centrifuged for 1 min at 100 g and cultured for 18 h at 37°C and 5% CO_2 atmosphere. The next day, 100 µl of a XenoLight D-Luciferin-K^+ Salt solution (300 µg/ml in TexMACS) was added into every well and CPS was measured after 5 min of incubation using the VICTOR X4 2030 Multilabel Reader. Specific killing was calculated using the following equation:

$$\text{Killing } [\%] = \left(1 - \left(\frac{\text{CPS sample} - \text{CPS target lysed}}{\text{CPS target alone} - \text{CPS target lysed}} \right) \right) \text{x } 100$$

Relative frequency of killed target cells represents the delta between Mock and effector cell killing.

For boosting experiments, 1E5 - 4E5 cells/ml FFluc expressing target cells (Cap. 2.4.4) were resuspended in TexMACS and 50 µl seeded in 96-well black well plates before 50 µl CD20-positve cells from a serial dilution (e.g. 10:1; 5:1; 2.5:1; 1.25:1) starting with 4E6 cells/ml and 100 µl effector cells with the same serial dilution starting with 2E6 cells/ml of Mock or CAR engineered T cells were added. Subsequently, cells were cultured and analyzed as described above.

2.5.3   Cytokine release assay

1E4 – 2E5 target cells were co-cultured with either 5E4 - 1E5 Mock-transduced or CAR-positive T cells in a total volume of 200 µl in a 96-well pate. For trans-boosting experiments 5E4 - 1E5 CD20-positive cells were additionally added. Mock was always adjusted to pipette similar cell numbers. All samples were measured in duplicates. After pipetting, cells were centrifuged for 1 min at 100 g. After 24 h the cytokine secretion was determined in the supernatant using the MACSPlex Cytokine 12 Kit, human.

2.5.4   IncuCyte-based killing assay

2E4 Mel526$^{FFluc\_eGFP}$ or CD20-positive Mel526$^{FFluc\_eGFP}$, resuspended in TexMACS, were co-cultured with either CAR-positive effector or untransduced (Mock) T cells at different effector to target ratios (e.g. 10:1; 5:1; 2.5:1; 1.25:1) in the presence or absence of CD20-positive cells in 96-well flat bottom plates for up to five days in a total volume of 200 µl TexMACS. Mock was always adjusted to pipette similar cell numbers. Killing was measured on the basis of target cell GFP expression every 2 h using the IncuCyte device.

2.5.5   *In vivo* experiments

All experiments were performed in compliance with the "Directive 2010/63/EU of the European Parliament and of the Council of 22 September 2010 on the protection of animals used for scientific purposes".

In vivo performance of anti-CD20 CAR sequence expressing T cells was tested in NOD scid gamma (NSG) (NOD.Cg-Prkdc^{scid}Il2rg^{tm1Wjl}/SzJ) mice. For this purpose, 5E5 FFluc-expressing target cells were injected via tail vain. Tumor cells were engrafted for seven days before either 1E6 Mock-transduced or CD20-directed T cells were injected i.v.. Tumor growth as well as anti-tumor response was monitored frequently using an *In vivo* Imaging System (IVIS Lumina III). For this purpose, 100 µl XenoLight Rediject D-Luciferin Ultra was injected i.p. and subsequently mice were anesthetized using the Isofluran XGI-8 Anesthesia System. Measurement was performed six min after substrate injection.

Bone marrow samples were collected from femur and tibia of both legs. After lysing red blood cells using 1x Red Blood Cell Lysis Solution, cells were subsequently stained with CD45, CD3, CD4, CD8 and CD19 and analyzed by flow cytometry (Cap. 2.3.7).

2.6   Statistics

Statistical significances were calculated with a Student t Test using Graph Pad Prism 7.0. Significance was defined as: $*$ = $p < 0.05$, $**$ = $p < 0.01$ and $***$ = $p \leq 0.001$. Unless mentioned to the contrary, graphs were all shown as mean with standard deviation.

2.7   Ethical concerns

The institutional review board and ethics committee of the university of Cologne approved sample collection for this study. Each patient provided written informed consent before sample collection in accordance with the declaration of Helsinki.

3 Results

3.1 Technologies and tools

Novel technologies and tools are of utmost importance to further contribute to the remarkable potential of CAR expressing T cells for the treatment of cancer and infectious diseases. Thus, during the course of this work, a high-throughput molecular cloning strategy as well as a multitude of reporter cell lines and protocols were initially established.

3.1.1 CAR library generation

Lentiviral constructs encoding a CAR must ensure expression of a modular structure including extracellular binding and spacer domain as well as transmembrane, intracellular co-stimulatory and signaling domain. While the specificity of a CAR is directed by its scFv, its functionality is also dependent on spatial needs, mediated by the spacer domain [39, 99] in order to ensure the most productive interaction between CAR T cell and target cell. Thus, a library of CAR backbones with variable lengths of extracellular spacers was generated. This library was developed to enable the rapid functional testing of different scFvs and therefore a robust method to clone scFvs into the library was also developed (Fig. 5). The library of backbones comprises either a human IgG4 hinge_CH2_CH3 (long spacer; 228 aa), a human IgG4 hinge_CH3 (medium spacer; 119 aa), a human IgG4 hinge (extra short spacer; 12 aa) or a human CD8 spacer (short spacer; 45 aa). All IgG4 spacer domains contained a 4/2 NQ mutation in the CH2 domain [39] as well as a S→P substitution in the hinge region in order to reduce FcγR binding [42].

The design of these new lentiviral CAR encoding constructs along with the high-throughput cloning strategy not only simplified the initial cloning procedure but also reduced the expenditure of time tremendously. Furthermore, the technique used circumvented the need to implement restriction enzyme recognition sites which allowed cloning of unmodified wildtype sequences in frame.
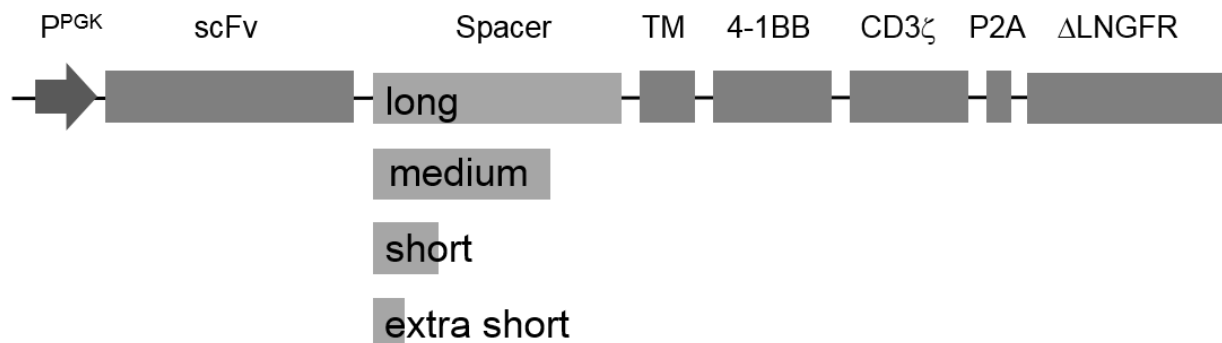
Fig. 5 **Schematic representation of the CAR library.** This library comprises the DNA encoding elements of a phosphoglycerate kinase (PGK) promoter-driven extracellular binding domain (scFv), linked to an extracellular spacer domain with different lengths (long = human IgG4 hinge_CH2_CH3, 228 aa; medium = human IgG4 hinge_CH3, 119 aa; short = human CH8 hinge, 45 aa; extra short = human IgG4 hinge, 12 aa), a human CD8 transmembrane domain, a 4-1BB co-stimulatory and CD3ζ signaling domain as well as a P2A element-linked ∆LNGFR as surface marker.

For this purpose, the scFv domain of the lentiviral backbone was replaced against a selection cassette (Cap. 2.2.2) encoding an inverted, *lacZ* promoter-driven *lacZ* gene with internally located *Bve* I sites that enable the high-throughput cloning (Fig. 6A). New scFv candidates were synthesized with externally located *Bve* I sites (Fig. 6B). The Type IIS restriction enzyme *Bve* I cuts outside the non-palindromic recognition sequence and generates free selectable 4 nt 5´ overhangs. Thus, allowing to perform digestion and ligation within one reaction step, avoiding the need of using pre-digestions with restriction endonucleases and gel electrophoresis with subsequent gel extractions and purification steps. Accordingly, digestion and re-ligation of the plasmids used occurred until the final product was generated as the *Bve* I recognition sites were separated from the compatible sticky end that were ligated and consequently enriched over time. The *lacZ* gene used allowed to visualize the cloning success after transformation (Cap. 2.2.3) on X-Gal containing plates by blue/white selection [100, 101]. Additionally implemented *Bam*H I and *Nhe* I flanking sequences (Fig. 6C) enabled further modifications using conventional cloning techniques.

This cloning system was applicable on the entire CAR library after an initial exchange of the primary scFv sequence against the selection cassette with the flanking, internally located *Bve* I sites resulting in the constructs MB_001 – MB_004.
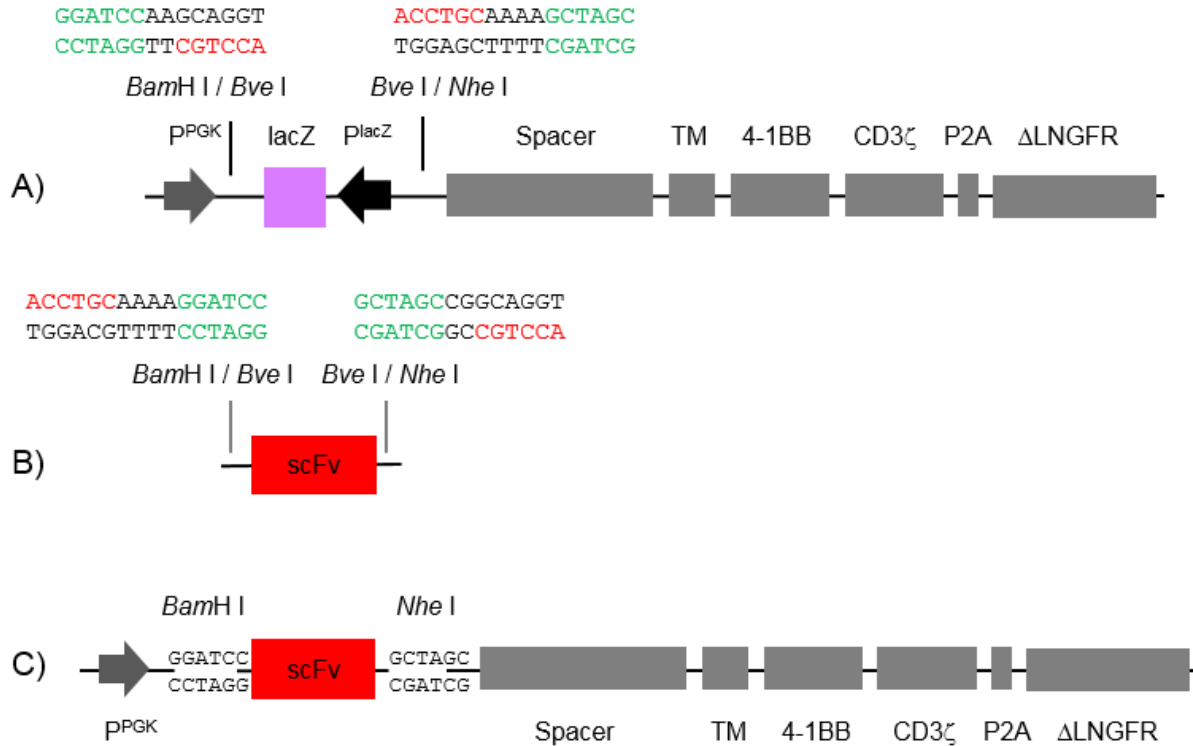

Fig. 6 **Cloning of novel scFvs into the CAR library using a *lacZ* reporter gene.** (A) Initially an inverted orientated *lacZ* promoter-driven *lacZ* gene with internally located *Bve* I sites (red sequences) was cloned into the lentiviral CAR encoding construct. (B) Novel scFv sequences were ordered with externally located *Bve* I sites so that compatible sticky ends are obtained after digestion with the Type IIS restriction enzyme. Additionally implemented restriction endonuclease recognition sites (green sequences) allowed further modifications of the lentiviral CAR encoding construct when necessary. (C) The new scFv was cloned using *Bve* I and ligase within one reaction.

This *Bve* I-based cloning strategy for scFv sequences was further applied to enable the rapid exchange of co-stimulatory and signaling domains. For this purpose, the *lacZ* selection cassette with the associated *Bve* I sites was cloned 3´ of the transmembrane encoding region (Cap. 2.2.2), replacing the conventionally used 4-1BB_CD3ζ sequence (Fig. 7A). Novel co-stimulatory or signaling domain encoding sequences were synthesized with externally located *Bve* I sites (Fig. 7B). The free selectable 4 nt 5´ overhang was designed in a way that a *Pst* I, a *Sca* I and a *Pml* I recognition site were available after ligation in the final construct (Fig. 7C).

The generated constructs MB_005 and MB_006 enabled a high-throughput cloning of alternative co-stimulatory and signaling domain encoding sequences with different spacers either derived from human IgG1 with minor modifications [40] or human CD8.
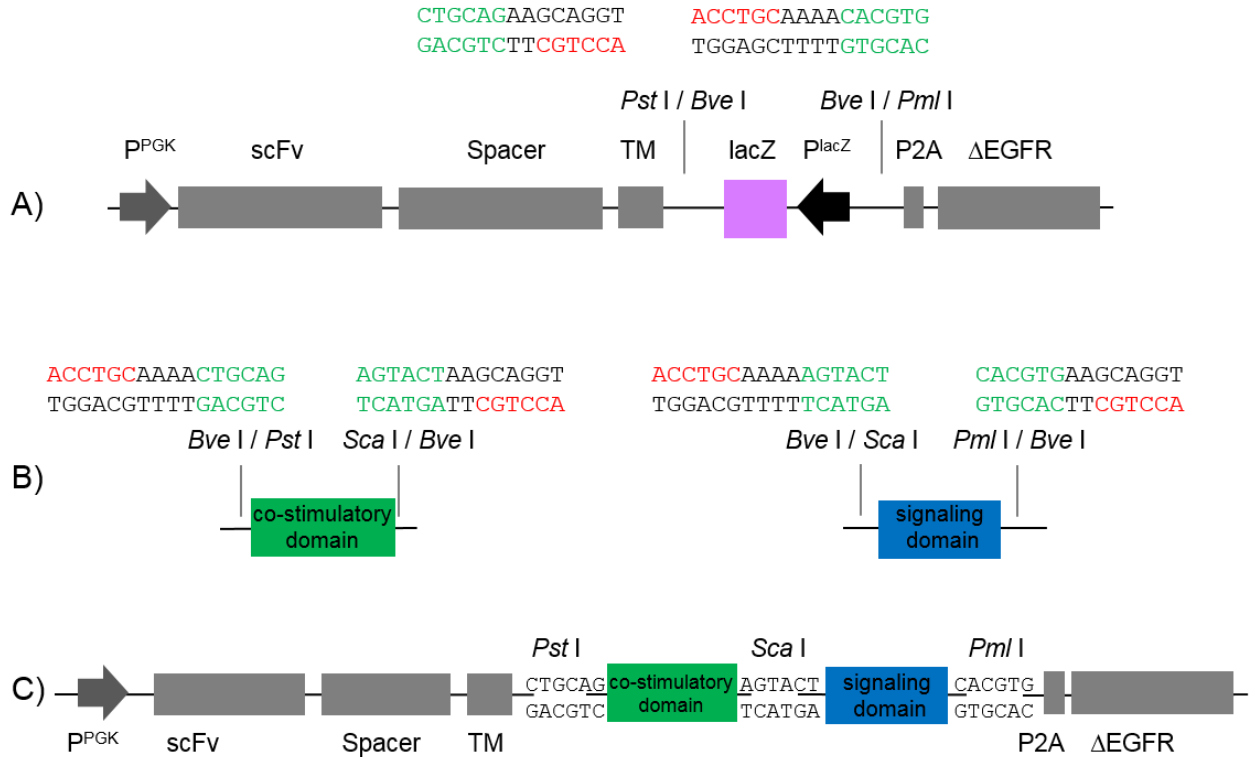

Fig. 7 **Cloning of co-stimulatory and signaling domain encoding sequences**. (A) A *lacZ* encoding gene with internally located, flanking *Bve* I sites was cloned 5´ of the transmembrane sequence enabling a highly efficient exchange of sequences. (B) Novel co-stimulatory and signaling domain encoding sequences were synthesized with externally located *Bve* I sites (red sequences). (C) The final lentiviral CAR encoding construct could be further modified using the implemented restriction endonuclease recognition sites *Pst* I, *Sca* I and *Pml* I (green sequences).

3.1.2   Generation of transgenic cell lines

To evaluate the functionality of the generated CAR expressing T cells different target cell lines were genetically modified to express a firefly luciferase (FFluc) gene and green fluorescent protein (GFP) allowing to perform either bioluminescence-based or flow-based *in vitro* killing assays as well as *in vivo* imaging. For this purpose, the lentiviral construct Doc_1 (Fig. 8) which encodes a phosphoglycerate kinase (PGK) promoter-driven FFluc

gene with a P2A-element linked eGFP gene was cloned (Cap. 2.2.2) and subsequently viral vector was produced (Cap. 2.3.6).
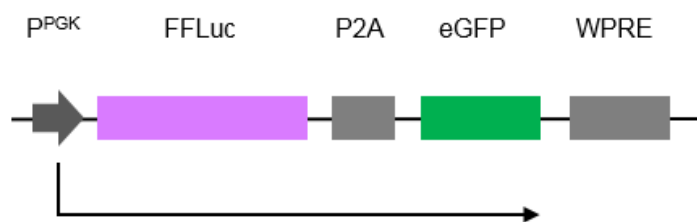
Fig. 8   Schematic representation of Doc_1. A PGK promoter-driven (P^{PGK}) FFluc gene with a P2A-element linked eGFP encoding sequence was used to produce lentiviral particles for the transduction of several cell lines. (WPRE = woodchuck posttranscriptional regulatory element, a posttranscriptional cis-acting stabilization element)

The B cell lines JeKo-1, Raji and NALM6 were transduced with LV-Doc_1 (Cap. 2.4.4). After 72 h bulk cells were analyzed using flow cytometry (Cap. 2.3.7) (Fig. 9A). While > 87% of the transduced JeKo-1 and NALM6 cells were GFP-positive, only 48% Raji cells were successfully transduced. To obtain transgenic single cell clones, cells were diluted (0.3 cells/well in a 96-well culture plate) and single cell clones were expanded for two weeks before GFP gene expression of individual clones was re-analyzed (Fig. 9B). Overall, > 99% of the analyzed cells of the different clones were GFP-positive.
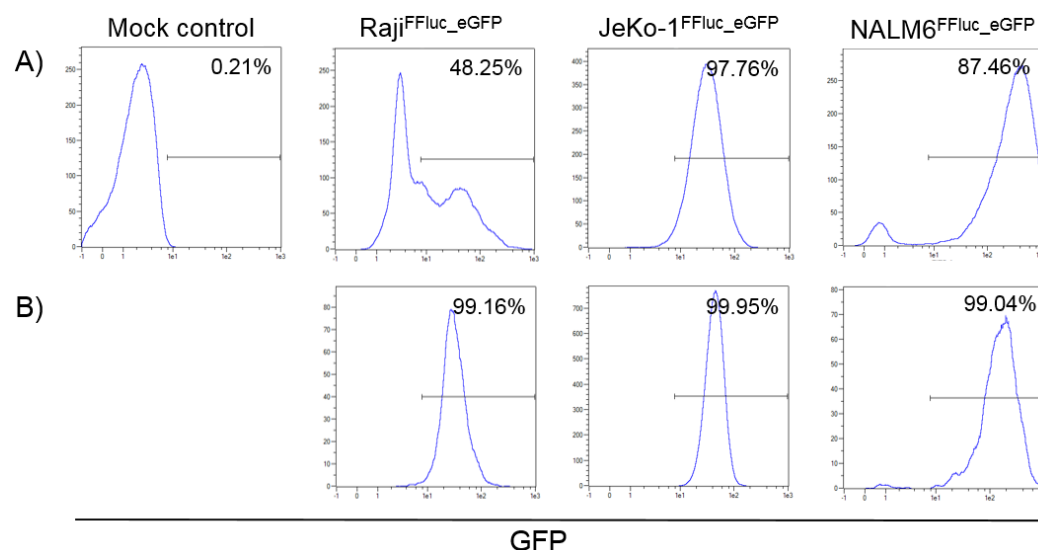
**Fig. 9   Generation of FFluc expressing B cell lines.** JeKo-1, Raji and NALM6 were transduced with a lentiviral construct Doc_1 encoding a FFluc and GFP gene. (A) After 72 h GFP gene expression of the bulk transduced cells was analyzed via flow cytometry. (B) Subsequently, a single clone expansion was performed and after two weeks a uniform GFP expression of individual clones could be detected.

Analogue to the generation of the B cell line derived reporter cell lines, the adherent CSPG4-positive melanoma cell line Mel526 was initially transduced with LV-Doc_1 (Cap. 2.4.4). After expanding the single cell clones for two weeks, flow cytometry analysis revealed two distinct populations when comparing Mock-transduced and LV-Doc_1-modified Mel526 clones regarding their GFP expression (Fig. 10).
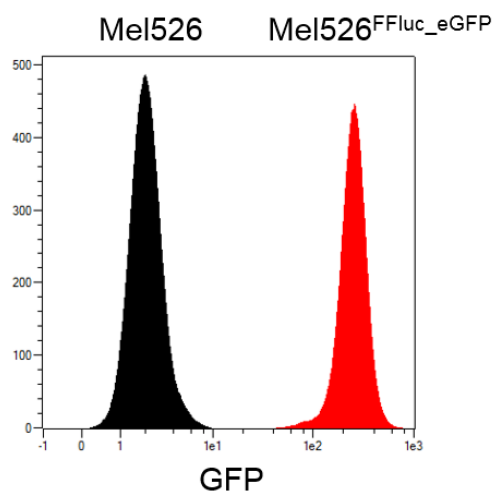

Fig. 10   **Generation of a FFluc expressing melanoma cell line.** Mel526 cells were transduced with Doc_1. After 72 h a single cell expansion was performed and cells were analyzed again after two weeks showing a homogenous GFP expression (red) and two distinct populations compared to the Mock-transduced control (black).

Since this work also required a cell line that co-expresses CSPG4 and human CD20 (will be clarified further), a single cell-derived Mel526$^{FFluc\_eGFP}$ clone was further modified using the lentiviral construct with a PGK promoter-driven human CD20 encoding sequence (Doc_2). For this purpose, FFluc_GFP-positive Mel526 cells were transduced with LV-Doc_2 (Cap. 2.4.5). After 72 h CD20-positive cells were enriched using magnetic activated cell sorting (MACS) technology. Again a limiting dilution strategy was applied to get CD20-positive Mel526$^{FFluc\_eGFP}$ single cell clones.

After two weeks of expansion, CD20 expression was analyzed using flow cytometry (Cap. 2.3.7). While Mel526$^{FFluc\_eGFP}$ were completely negative for CD20, the newly generated Mel526$^{CD20\_FFluc\_eGFP}$ uniformly expressed CD20 in a distinct population (Fig. 11).

Mel526$^{FFluc\_eGFP}$ Mel526$^{CD20\_FFluc\_eGFP}$
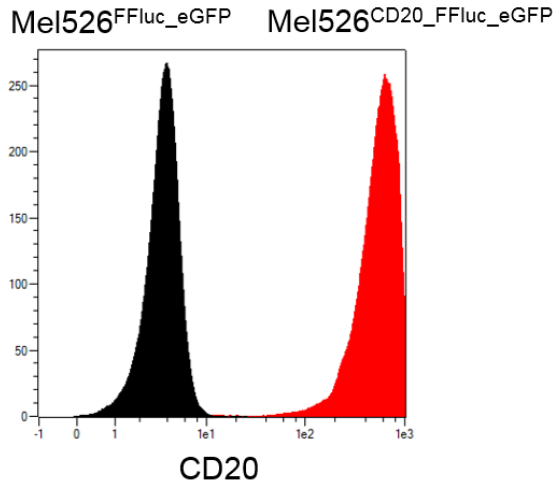
CD20

Fig. 11   Generation of a hCD20-positive Mel526$^{FFluc\_eGFP}$ clone. A FFluc_GFP-positive Mel526 clone was transduced with LV-Doc_2, a PGK promoter-driven human CD20 encoding sequence. Transduced cells were enriched using MACS technology and subsequently expanded as single cell clones. After two weeks CD20 expression (red) could be confirmed by flow cytometry (black was isotype control).

In addition, JeKo-1$^{FFluc\_eGFP}$ knock-out clones were required as control cell lines for the evaluation of CAR modified T cells *in vitro* as well as *in vivo*. In the present work CD19, CD20 and CD19/CD20 ko JeKo-1$^{FFluc\_eGFP}$ were generated using the CRISPR/Cas9 technology [94] (Cap. 2.4.6). For this purpose, the guideRNA 19.2 and 20.4 were designed *in silico*. Both target the first exon of either CD19 or CD20 and affect all splice variants of those genes. Cloning of the guideRNA into the gRNA plasmid as well as co-transfection of JeKo-1$^{FFluc\_eGFP}$ cells with the Cas9 encoding and gRNA plasmid was mainly done within the framework of a Bachelor thesis that I supervised.

Seven days post transfection, CD19- and CD20-positive cells were depleted using the respective microbead reagents and LD depletion columns. Bulk cells were further diluted (0.3 cells/well in a 96-well culture plate) and expanded to obtain single cell clones which were analyzed after a surface staining with CD19 and CD20 by flow cytometry (Cap. 2.3.7). Stained as well as unstained JeKo-1$^{FFluc\_eGFP}$ cells were used as control to detect the ko of either CD19 or CD20 (Fig. 12A). After two weeks both CD19-negative and CD20-negative JeKo-1$^{FFluc\_eGFP}$ clones could be isolated (Fig. 12B & C).

CD19/CD20 ko JeKo-1$^{FFluc\_eGFP}$ were generated by further modifying JeKo-1$^{FFluc\_eGFP}$ CD20 ko with guideRNA 19.2/Cas9 targeting the CD19 gene as described above. The same limiting dilution strategy was used to obtain single cell clones of CD19/CD20 ko

JeKo-1$^{FFluc\_eGFP}$, as confirmed by flow cytometry after staining with CD19-VB and CD20-APC (Cap. 2.3.7) (Fig. 12D).
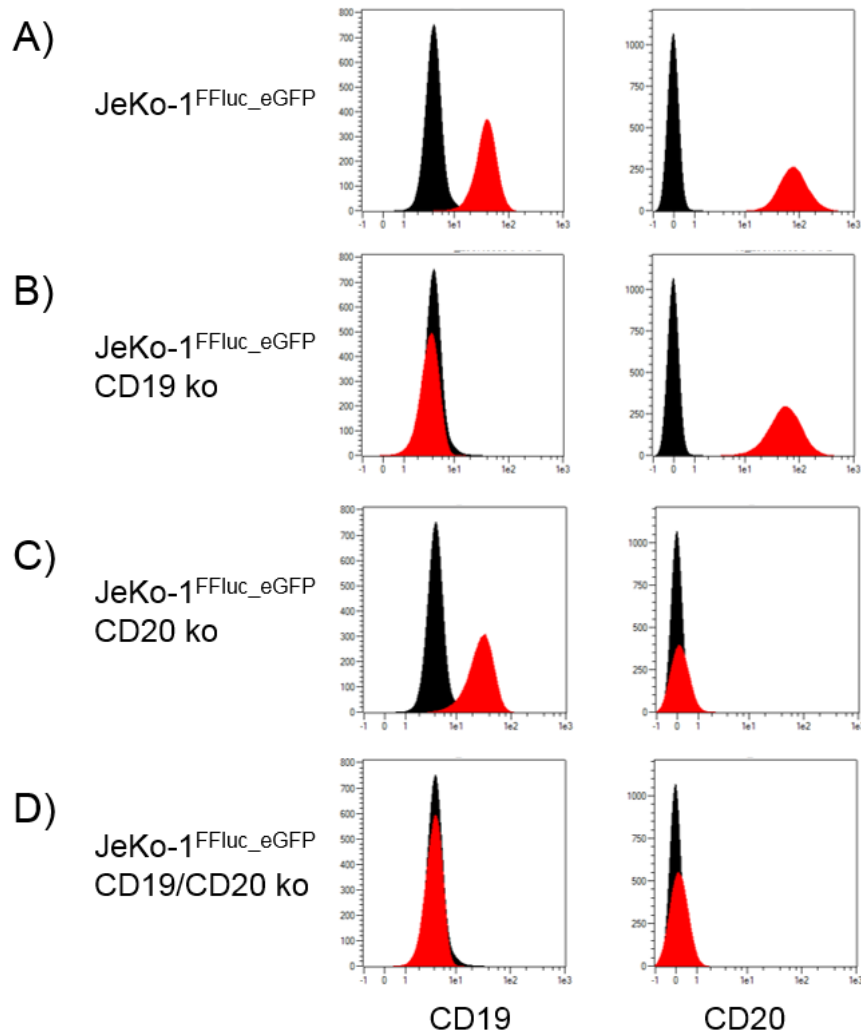
Fig. 12   **Generation of JeKo-1$^{FFluc\_eGFP}$ knock-out clones.** JeKo-1$^{FFluc\_eGFP}$ cells were modified using the CRISPR/Cas9 system. Untransfected cells were depleted and ko cells expanded as single cell clones. (A) After two weeks, cells were stained with CD19-VB and CD20-APC to analyze the ko by flow cytometry. Stained (red) as well as unstained (black) JeKo-1$^{FFluc\_eGFP}$ cells were used as control. (B-D) A complete stable ko of CD19, CD20 and CD19/CD20 of JeKo-1$^{FFluc\_eGFP}$ could be obtained.

Furthermore, based on similar strategies CT26.wt (colon carcinoma) and B16-F10 (melanoma), two mouse cell lines, were modified to express FFluc and GFP (Cap. 2.4.4) (data not shown) to enable first *in vivo* experiments using an *In vivo* Imaging System (IVIS).

3.1.3 Testing of FFluc expressing cell lines and IVIS set-up

As previously reported by Hudecek *et al.* [39] and confirmed by our own findings (Fig. 25) *in vivo* experiments are of utmost importance for the evaluation of CAR modified T cells. Thus, after generating appropriate FFluc expressing cell lines (Cap. 3.1.2), their growth potential and the stability of transgene expression had to be tested *in vitro* as well as *in vivo* by using an IVIS which enables non-invasive monitoring of tumor progression.

Initially, 4E6 CT26.wt^FFluc_eGFP cells (Cap. 2.4.4) were seeded into a 6-well plate. FFluc expression and functionality as well as system settings were assessed by adding D-Luciferin (final concentration 300 µg/ml per well) to three wells (Fig. 13). IVIS measurement revealed a specific signal of the bioluminescent reporter only in the presence of its substrate which confirmed both functionality and suitability of the used FFluc encoding gene to perform IVIS experiments and bioluminescence-based killing assays (Cap. 2.5.2).
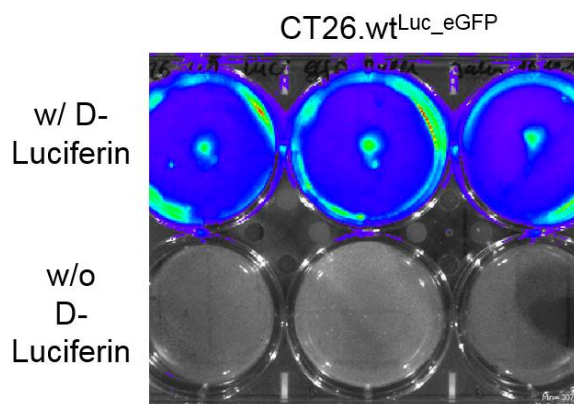
CT26.wt^Luc_eGFP

Fig. 13 ***In vitro* testing of CT26.wt^FFluc_eGFP using an IVIS.** CT26.wt^FFluc_eGFP cells were cultured in a 6-well plate for 48 h before the FFluc substrate was added. IVIS measurement confirmed a specific signal at 560 nm only in the presence of D-Luciferin.

In a next step, representatively 1E6 B16-F10^FFluc_eGFP cells were injected s.c. in the flanks of BALB/c mice to confirm *in vivo* the possibility to detect FFluc modified cells. After 18 d 100 µl XenoLight D-Luciferin - K^+ Salt Bioluminescent Substrate (30 mg/ml) was injected i.p. and mice were anesthetized using isoflurane prior to the IVIS measurement. Six minutes after substrate injection, measurement was initiated revealing an established tumor which was further confirmed by an autopsy of the euthanized mice (Fig. 14).

Consequently, it could be shown that the FFluc gene, used for the modification of diverse cell lines, was allowing to perform both *in vitro* and *in vivo* experiments.
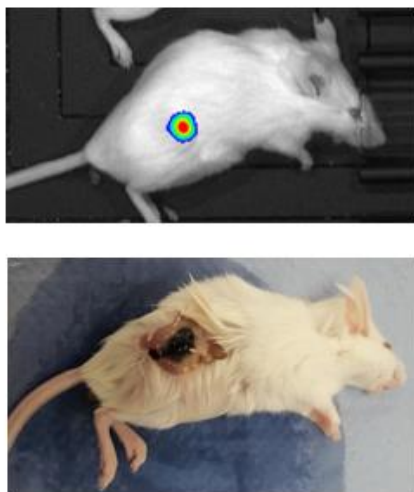
Fig. 14 **Testing of FFluc expressing cells *in vivo* using an IVIS.** 1E6 B16-F10^FFluc_eGFP cells were injected s.c. into BALB/c mice. After 18 d the IVIS measurement revealed a tumor engraftment which was further confirmed by an autopsy.

Finally, tumor growth kinetics of JeKo-1^FFluc_eGFP cells were assessed. For this purpose, 5E6 JeKo-1^FFluc_eGFP were injected i.v. via the tail vein of NOD scid gamma (NSG) (NOD.Cg-Prkdc^scidII2rg^tm1Wjl/SzJ) mice. After four days, 100 µl RediJect D-Luciferin Ultra Bioluminescent Substrate (30 mg/ml) was injected i.p.. Subsequently mice were anesthetized using isoflurane and bioluminescence was measured. The procedure was repeated on day six, 13, 20 und 27 affirming a tumor engraftment in all treated mice as well as an exponential tumor growth which correlated with the loss of weight and a splenomegaly, determined after euthanizing the mice on day 27 (Fig. 15). A mouse which did not receive any tumor cells served as control. Both blood and spleens were further analyzed regarding the GFP expression. The isolated spleens were manually dissociated, red blood cells of both samples lysed using 1x Red Blood Cell Lysis Solution and remaining cells analyzed via flow cytometry (Cap. 2.3.7) to finally verify the functionality of both transgenes FFluc and GFP in the used reporter cell line. Consequently, only in tumor-bearing mice GFP-positive cells could be detected varying from 72% - 77% in the spleen (Fig. 16A) and from 70% - 88% in the blood (Fig. 16B).
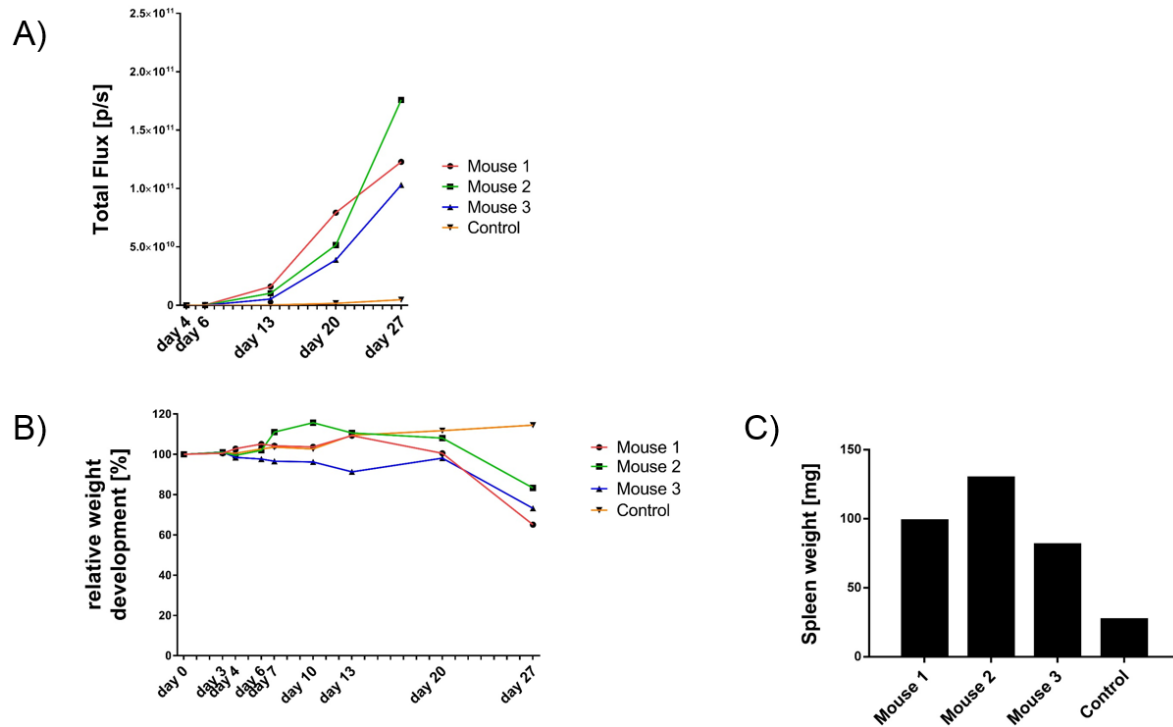
Fig. 15 **Assessing tumor growth kinetics of JeKo-1$^{FFluc\_eGFP}$ in NSG mice.** 5E6 JeKo-1$^{FFluc\_eGFP}$ cells were injected i.v. in NSG mice. (A) Tumor growth and weight was measured frequently showing a tumor engraftment with an exponential tumor growth (B) and an associated loss of weight. (C) Spleen weight of euthanized mice was further analyzed showing an expected splenomegaly.
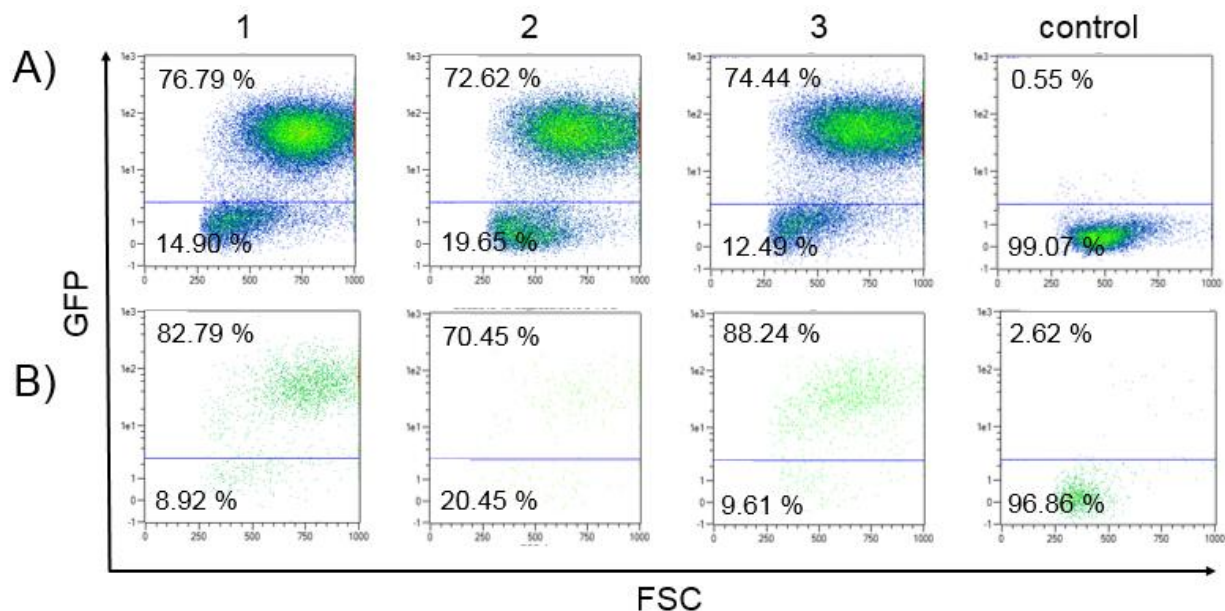
Fig. 16 **Analyzing GFP expression of *in vivo* passaged JeKo-1$^{FFluc\_eGFP}$ cells.** Blood and spleen of euthanized mice was analyzed by flow cytometry. (A) The frequency of GFP-positive cells varied from 72% - 77% in the spleen (B) and from 70% - 88% in the blood. No GFP-expressing cells could be detected in the untreated control mouse.

51

3.2 Anti-CD20 CAR development and testing

Although anti-CD19 CAR expressing T cells have demonstrated a remarkable clinical success in several clinical trials [26-31], there is still a significant number of patients that relapse due to the loss of CD19 gene expression, induced by frameshift and missense mutations as well as alternative splicing of CD19 [55-57]. Those relapses are associated with a very unfavorable prognosis for the patients [57]. CD20, however, is an antigen which is not only highly expressed on more than 90% of B cell lymphomas [44], but also on a minor subset of cancer-initiating melanoma cells [60, 61]. Therefore, CD20 is an alternative, promising target for adoptive CAR T cell therapy.

3.2.1 Anti-CD20 CAR development and lentiviral vector production

In the context of this work, several anti-CD20 CAR constructs with minor differences were generated and compared. For this purpose, #1455, a gamma-retroviral anti-CD20 CAR which was kindly provided by H. Abken (ZMMK Cologne) was modified. For purposes of clinical use, it was re-designed *in silico*, human codon optimized and synthesized at ATUM. The 5842 long nt sequence comprises the flanking chimeric Rous sarcoma virus (RSV)-HIV 5´ long terminal repeat (LTR) [102] and the 3´ LTR with a self-inactivating (SIN) modification [103]. Besides, the elongation factor-1 alpha (EF-1α) promoter was replaced against a human PGK promoter which drives the CAR encoding sequence consisting of a murine kappa chain leader sequence, a murine Leu-16-derived scFv (vh/vl orientation, linked by a $(G_4S)_3$ linker), a human IgG1 spacer with a PELLGG➔PPVAG and ISR➔IAR mutation [40], a human CD8a transmembrane domain as well as the human intracellular co-stimulatory and signaling domains 4-1BB and CD3ζ (Fig. 17). In addition, the construct comprises a woodchuck posttranscriptional regulatory element (WPRE), a woodchuck hepatitis virus-derived cis-acting RNA element, which increases the level of transgene expression [104]. The synthesized element was enzymatically digested with *Mlu* I and *Avr* II and subcloned (Cap. 2.2.2) into the lentiviral backbone pRRL [102]. The resulting lentiviral construct CD20_1 was amplified in a maxiprep (Cap. 2.2.4) and sequence

verified at GATC. Subsequently, lentiviral particles were produced (Cap. 2.3.6) by co-transfecting HEK 293-T cells with the helper plasmids pMDG-2 and pCMVdR8.74 in combination with the transfer plasmid CD20_1 (Fig. 18).
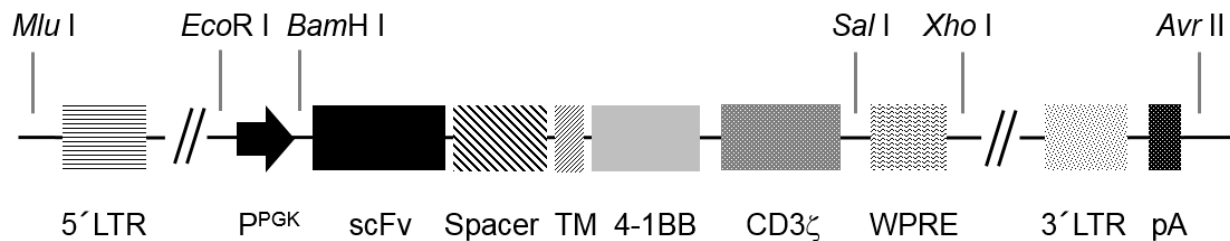
Fig. 17   **Schematic representation of CD20_1.** The anti-CD20 CAR encoding construct comprises the nucleotide sequences of a PGK promoter (P^{PGK}) driven murine Leu-16-derived scFv, a modified human IgG1 spacer, a human CD8a transmembrane domain, a human 4-1BB co-stimulatory domain and a human CD3ζ signaling domain. The cis-acting RNA element WPRE was used to increase the transgene expression. The CAR encoding sequence is flanked with modified LTRs. *Mlu* I and *Avr* II were used to implement the synthesized element into the lentiviral backbone pRRL.
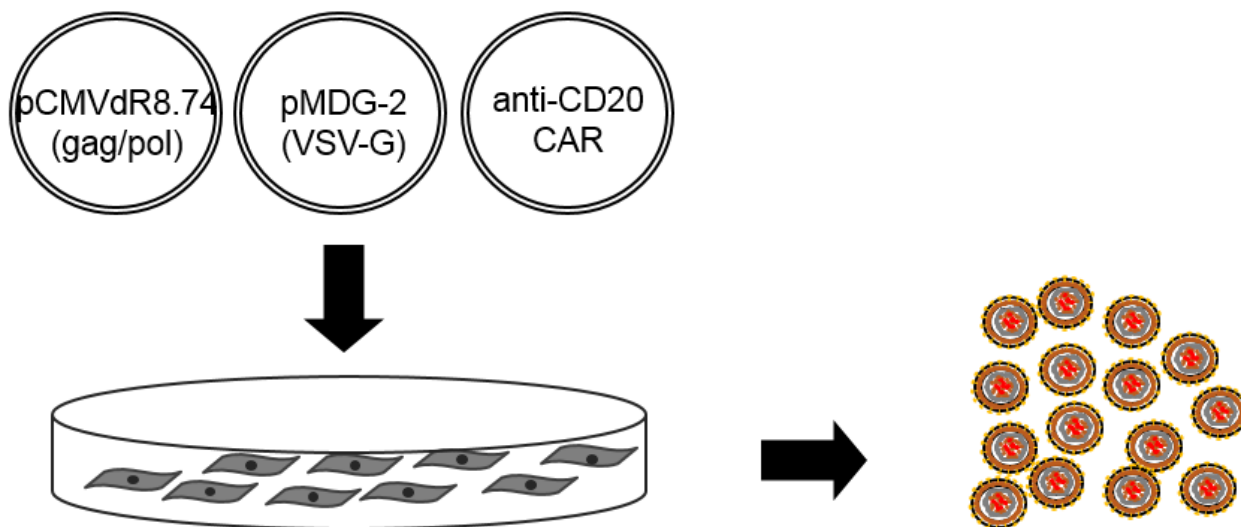
Fig. 18   **Graphical representation for the generation of lentiviral particles.** HEK 293-T cells were co-transfected with pMDG-2, pCMVdR8.74 and an anti-CD20 CAR encoding construct. After 48 h supernatant was harvested, concentrated and either freshly used or stored at -70°C.

To determine the viral titer of LV-CD20_1, 3E5 Jurkat cells were transduced with either 1 µl, 0.1 µl or 0.01 µl (done in triplicates) of the thawed lentiviral particles. After 48 h, cells were stained with anti-IgG1-Fc-Biotin/anti-Biotin-APC and analyzed via flow cytometry

(Cap. 2.3.7) to detect the CAR sequence expression. The frequency of CAR-positive cells varied from 84.5 ± 2.32% for 1 µl over 17.1 ± 0.7% for 0.1 µl to 3.9 ± 0.7% for 0.01 µl (Fig. 19). For the titer calculation, the minimal volume of LV-CD20_1 allowing a clear and distinct CAR-positive population to be detected (as low as 0.01 µl) was used. Thus, for this lentiviral production batch, a titer of 1.1E9 LV-particles/ml was achieved.
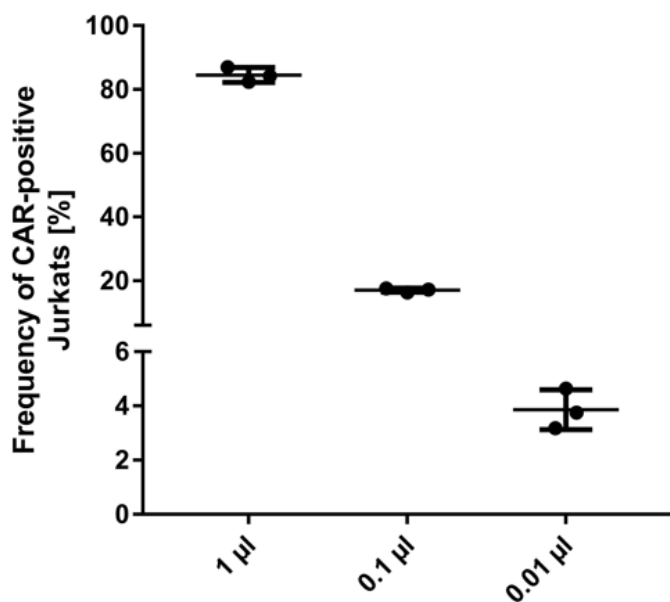
Fig. 19   **LV-CD20_1 titer determination using Jurkat cells.** 3E5 Jurkat cells were transduced with a decreasing amount of LV-CD20_1 (n=3). After 48 h the CAR expression was detected via flow cytometry. Even with the lowest amount of viral vector a distinct CAR-positive population was detectable. Consequently, titer was calculated with a frequency of 3.9 ± 0.7% CAR sequence expressing cells.

3.2.2   Assessing the cytolytic activity of anti-CD20 CAR modified T cells

The cytolytic potential of lentivirally engineered T cells was initially assessed *in vitro* and in addition compared with retrovirally modified T cells expressing the original #1455 anti-CD20 CAR. For this purpose, PBMC was prepared (Cap. 2.3.1). Subsequently T cells were isolated and activated using a nanomatrix-based polyclonal T cell stimulation reagent TransAct (Cap. 2.3.2). Transduction with LV-CD20_1 took place after 48 h with a multiplicity of infection (MOI) of four (Cap. 2.4.1). In advance to the retroviral transduction,

RV #1455 was generated by co-transfecting HEK 293-T cells with 3 µg pMDG-2, 22.5 µg pHit60 and 23.98 µg #1455, analogue to the generation of lentiviral particles (Cap. 2.3.6). A spin-based transduction was applied to retrovirally transduce T cells. Accordingly, a non-tissue culture treated 48-well plate was coated with 250 µl RetroNectin (10 µg/ml) overnight at 4°C. Then, 1 ml PBS/BSA (1%) was added and incubated for 30 min at RT before the PBS/BSA blocking solution was removed and 200 µl unconcentrated RV-#1455 was added and centrifuged with 2000 g for 90 min at 32°C. Subsequently, 0.5 ml T cells (1E6 cells/ml) were added and again centrifuged with 540 g for 10 min at 32°C. After 24 h incubation at 37°C and 5% CO_2 atmosphere T cells were transferred into a 24-well plate and cultivated (Cap. 2.3.2). On day eight, CD4/CD8 ratio as well as the CAR expression was determined by flow cytometry (Cap. 2.3.7) as exemplarily shown for LV-CD20_1 transduced T cells (Fig. 20).

Compared to the Mock control T cells no significant differences regarding the CD4/CD8 ratio was detectable. The frequency of CD4-positive cells varied from 18 - 53% among the three different donors, independently of the transduction. The frequency of CD8-positive cells, which ranged from 43 - 81%, was higher, however, also no significant differences were detectable between Mock, lentivirally or retrovirally transduced T cells. The same applied to the CAR-positive population where the lentivirally transduced donors expressed the CAR sequence at frequencies from 34 to 50% (mean 44.2 ± 8.8%) and retrovirally modified T cells ranged from 31 - 40% (mean 36.2 ± 4.9%) (Fig. 21).
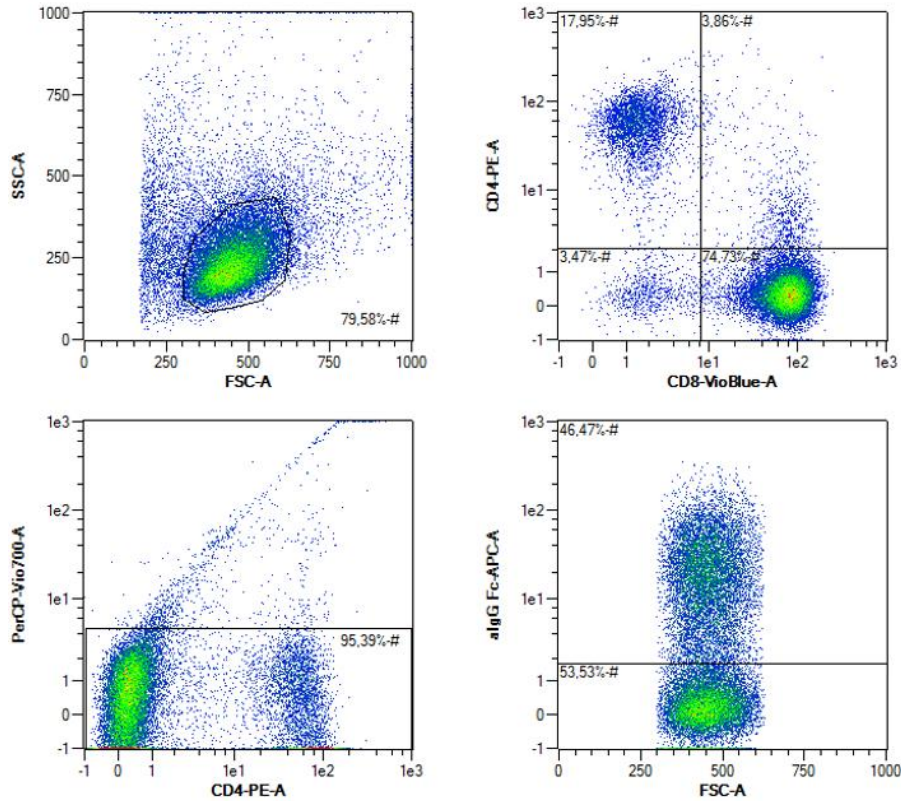
Fig. 20   **Representative example for the detection of CD4/CD8 ratio and CAR expression of LV-CD20_1 transduced T cells.** T cells were stained with anti-CD4-PE, anti-CD8-VB and anti-IgG Fc-Biotin/anti-Biotin-APC. CD4/CD8 ratio as well as CAR-positive cells were determined among viable cells (PerCP-Vio700 negative).
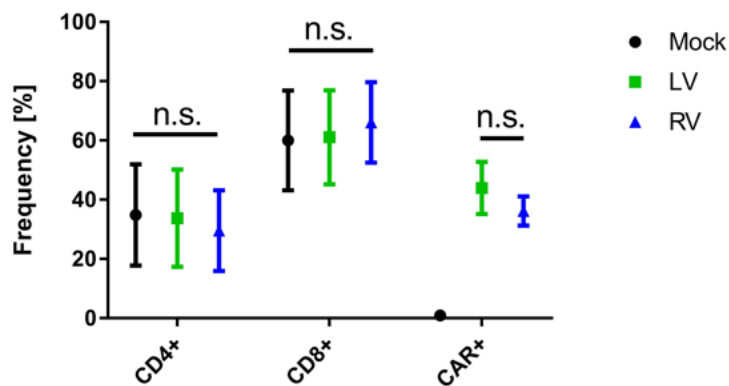
Fig. 21   **Comparison of Mock, lentivirally or retrovirally transduced T cells regarding CD4, CD8 and CAR expression.** T cells derived from three different donors were either transduced with LV-CD20_1 or RV-#1455 and analyzed after 8 days. Significant differences were neither detected for CD4- nor for CD8-positive cells among Mock or modified T cells. In addition, also for the CAR-positive population, no significant differences were detectable among the three donors. Parametric unpaired t-test with 95% confidence level.

After confirming the CAR expression of lentivirally and retrovirally transduced T cells, functionality assays were performed to assess and compare the cytolytic potential of the engineered T cells. For this purpose, autologous B cells were isolated from frozen PBMC (Cap. 2.3.3) and used as target cells for a flow-based killing assay (Cap. 2.5.1) in which 1E4 VioDye-labeled target cells were co-cultured at different effector to target ratios (E:T) with either Mock or CAR-positive T cells, both normalized for the CAR expression to use identical cell numbers. After 4 h at 37°C and 5% CO_2 atmosphere 70 μl resuspended cells were analyzed (Cap. 2.3.7). Dead cells were discriminated and the remaining VioDye-positive B cells as well as a Blank control cultured without effector cells allowed to calculate the killing frequency (Fig. 22). Overall, the killing frequencies at E:T 10:1 for lentivirally modified T cells varied from 22.8 – 45.4% (mean 36.9 ± 8.6%) and for retrovirally engineered T cells from 40 – 57% (mean 47.4 ± 6.4%). Even at the highest E:T ratio Mock T cells did not show a noteworthy cytolytic potential. Although the retrovirally transduced T cells killed slightly better than lentivirally modified T cells at the highest E:T ratio, at the lower 5:1 ratio no significant differences were detectable between the both. However, at the lowest E:T ratio of 1:1 the picture changed and the lentivirally engineered T cells showed a higher killing potential for donor A and B, not for donor D.
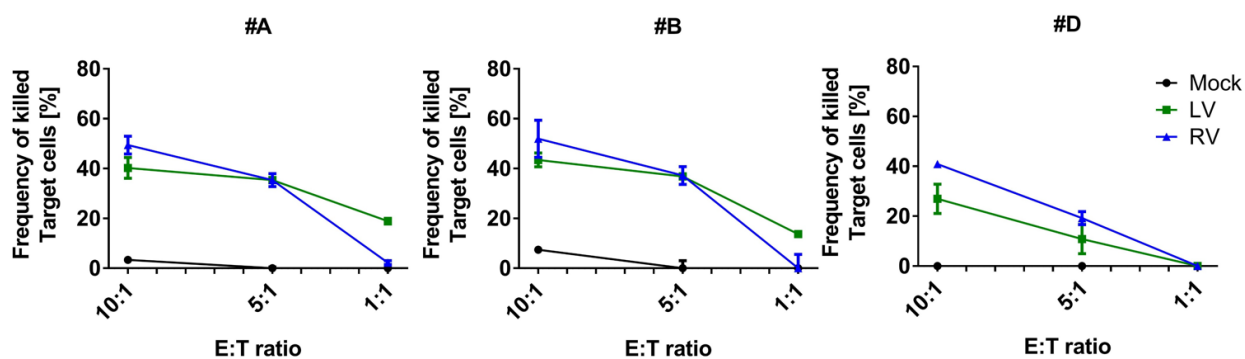
Fig. 22   *In vitro* **functionality of lentivirally and retrovirally modified T cells.** CAR-positive T cells were co-cultured with autologous B cells for 4 h. Subsequently, killing efficiency was measured by flow cytometry. While retrovirally modified T cells killed better than lentivirally transduced T cells at the highest E:T ratio, the picture changed at a 1:1 E:T ratio where lentivirally engineered T cells of donor A and B were better than their counterpart. Mock T cells did not show any cytolytic potential. #A, #B and #D represent different donors.

In addition to the killing experiments, cytokine release assays were performed (Cap. 2.5.3). Again, 2E5 autologous B cells were co-cultured with 1E5 either Mock or CAR-positive T cells for 24 h. The cytokine secretion was subsequently determined using a flow-based detection method which confirmed the functional potential of both lentivirally and retrovirally transduced T cells (Fig. 23A). Retrovirally modified T cells, however, released significantly more type-1 cytokines than the lentivirally engineered T cells (Fig. 23B).
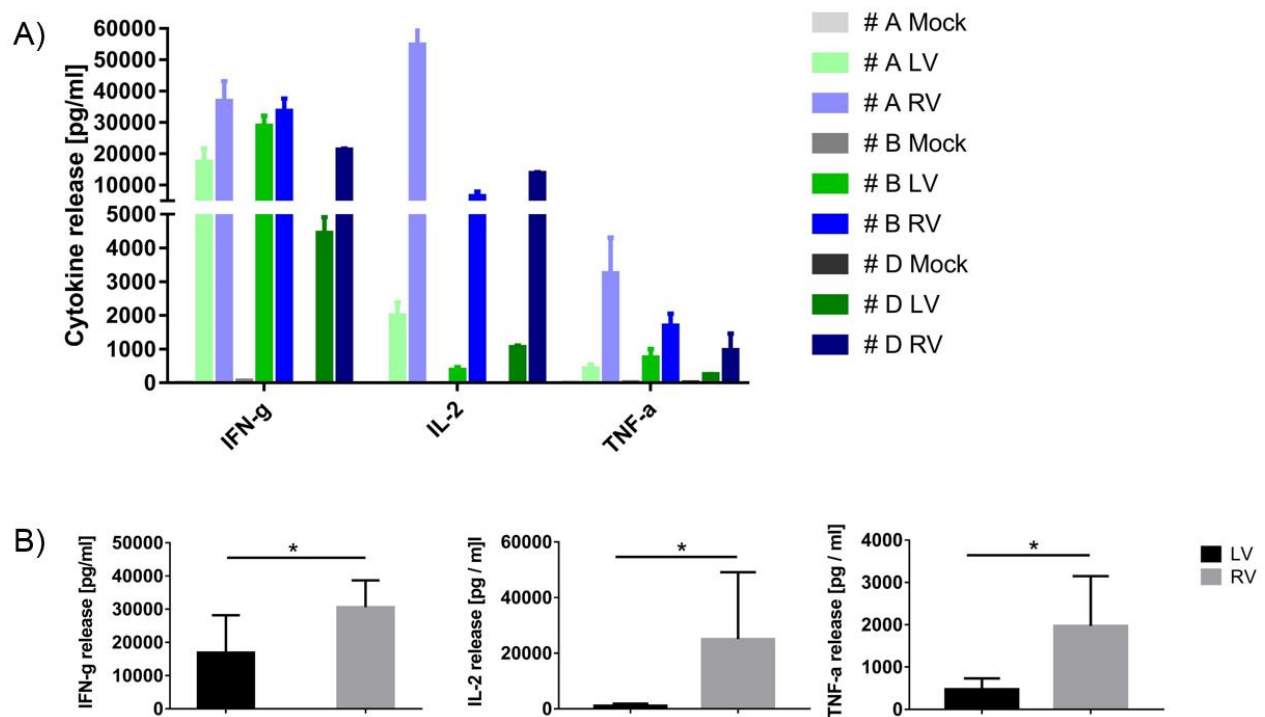
Fig. 23 **Cytokine release of lentivirally and retrovirally engineered T cells.** (A) The supernatant of co-cultured T cells was used to determine the cytokine release of either lentivirally or retrovirally transduced T cells showing that both are inducing the release of type-1 cytokines upon encountering their target while Mock T cells did not release IFN-γ, IL-2 or TNF-α in the presence of CD20-positive B cells. (B) Comparing the detected cytokine amounts among lentivirally and retrovirally modified T cells revealed a significant difference. Parametric unpaired t-test with 95% confidence level. #A, #B and #D represent different donors.

3.2.3 Further anti-CD20 CAR modifications and testing

Note: In the present study, the anti-CD20 CAR encoding lentiviral construct CD20_1 was cloned, lentiviral particles produced and T cells transduced. The cytolytic potential of those engineered T cells was confirmed using established *in vitro* assays. Furthermore, this work led to the development and establishment of protocols used to assess the potential of CAR modified T cells *in vivo*. Further modifications of CD20_1 over a period of 12 month as well as testing was mainly done by colleagues at Miltenyi Biotec using the said established protocols. This chapter briefly summarizes additional modifications of CD20_1 leading to the final CAR construct CD20_5 which is intended to be used in two different clinical trials.

In a proof-of-concept clinical trial (ClinicalTrials.gov Identifier NCT00012207) Till *et al.* [44] confirmed the safety and potential of Leu16-scFv directed engineered T cells for patients with relapsed or refractory indolent B cell lymphoma or mantle cell lymphoma. They used a first generation CAR with a CD4 transmembrane region and implemented the Leu-16 scFv, compared to CD20_1, in a vl/vh orientation. To stay as comparable as possible to this clinically approved construct, the CD20_1 construct was further refined. Thus, not only the scFv orientation was modified according to Till *et al.* [44] but also originally transferred cloning sites were deleted, the murine kappa chain leader sequence was replaced against human CD8 leader sequence and the lentiviral backbone was exchanged against a CG1711-derived backbone, a self-inactivating lentiviral vector packaged by a 3rd generation plasmid (designed and produced under GMP guidelines by Cell Genesis Inc.). The resulting constructs CD20_2 and CD20_3 were further characterized in Tab. 7.

Tab. 7   Overview about the differences in the anti-CD20 CAR constructs

	CD20_1	CD20_2	CD20_3
lentiviral backbone	pRRL	pRRL	CG1711
Generation transfer plasmid	3rd	3rd	3rd
promoter	PGK	PGK	EF-1α
leader peptide	murine kappa chain	human CD8 leader	human CD8 leader
Leu16 scFv orientation	vh/vl	vl/vh	vl/vh
spacer	modified human IgG1	modified human IgG1	modified human IgG1

Finally, lentiviral particles for all constructs were produced (Cap. 2.3.6), T cells transduced (Cap. 2.4.1) and expanded (Cap. 2.3.2) before *in vitro* experiments (Cap. 2.5.1) were

performed allowing to assess the cytolytic potential of the newly generated constructs. The JeKo-1 co-culture assays revealed that the three differently modified T cells were all functional (Fig. 24). Thus, the frequency of killed JeKo-1 cells among the three donors at E:T 1:1 varied for LV-CD20_1 modified T cells from 21.1 – 52.6% (mean 33.7 ± 16.6%), for LV-CD20_2 engineered T cells from 34.2 – 56.4% (mean 43.8 ± 11.4%) and for LV-CD20_3 transduced T cells from 36.0 – 74.9% (mean 56.7 ± 19.5%).
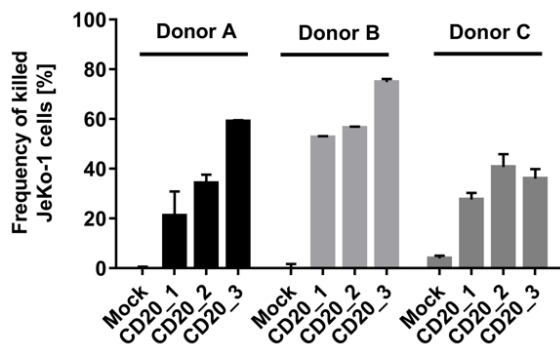
Fig. 24 **Comparison of differently transduced T cells *in vitro*.** JeKo-1 cells were co-cultured with engineered T cells at an 1:1 E:T ratio. The cytolytic potential was measured by flow cytometry after 24 h. (unpublished data by Miltenyi Biotec)

Even though all constructs and especially CD20_3 efficiently killed CD20-positive target cells, the two additional constructs CD20_4 and CD20_5 were generated. Both encode a human CD8 spacer instead of the modified human IgG1 motif. Furthermore, CD20_5 contained the Leu-16 scFv in its original vh/vl orientation. After confirming their functionality *in vitro* (data not shown), the anti-tumor reactivity of LV-CD20_3 and LV-CD20_5 transduced T cells was tested in a xenograft model (Cap. 2.5.5) showing that only the latter was able to control the tumor outgrowth in the NSG mice (Fig. 25). The *in vivo* comparison of LV-CD20_4 and LV-CD20_5 engineered T cells furthermore revealed that the Leu-16-derived vh/vl scFv orientation has a higher cytolytic potential than the counterpart with the opposite vl/vh orientation (data not shown).
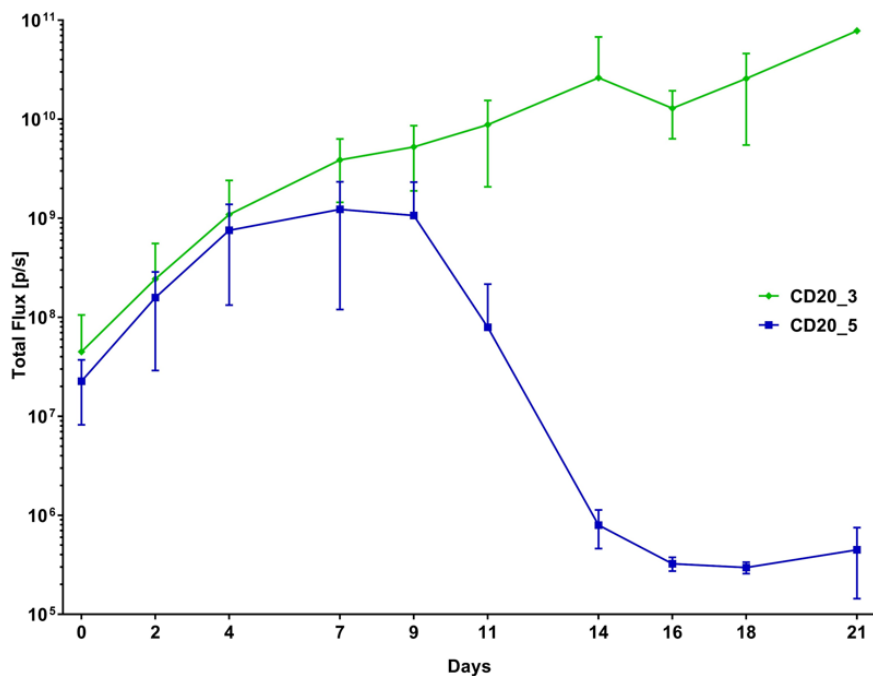
Fig. 25   **Comparison of LV-CD20_3 and LV-CD20_5 transduced T cells *in vivo*.** After establishing a tumor with Raji[FFluc] cells in the NSG mice CAR engineered T cells were injected i.v. and tumor growth was monitored frequently for 21 days using an IVIS. Only LV-CD20_5 engineered T cells with a CD8 spacer instead of the IgG1 spacer were able to control the tumor outgrowth. (n=7) (unpublished data by Miltenyi Biotec)

3.3   Automated manufacturing of CAR T cells

Note: All data, tables and figures presented in this chapter were published by Lock *et al.* as a collective work which is subdivided as follows: Drechsel K. TCT software development; Barth C., Mauer D. and Kolbe C. technical support including flow cytometric analysis and TCT operation; Al Rawashdeh W. and Brauner J. *in vivo* experiment; Lock. D and Schaser T. lentiviral vector development; Lock D. establishment of protocols, cell lines and tools enabling to perform *in vitro* as well as *in vivo* experiments; Lock D. and Mockel-Tenbrinck N. data analysis and leading authors; Assenmacher M., Mockel-Tenbrinck N. and Kaiser A. project managers.

The success of CAR T cell therapies for the treatment of B cell leukemia and lymphomas has been confirmed in several clinical trials [26-31], however, the manufacturing process of such engineered T cells is complex requiring extensively trained operators and a special working environment [66, 70]. Thus, the dissemination of CAR T cells therapies to a wider field of patients is strongly dependent on an improved and simplified cGMP-compliant manufacturing process for engineered T cells.

3.3.1   Robustness of the automated T Cell Transduction Process

Taking advantage of the CliniMACS Prodigy platform, a fully-closed, automated T Cell Transduction (TCT) Process was used to manufacture gene-engineered T cells in a closed tubing set (Cap. 2.4.2) (Fig. 26). Initially, CD4- and CD8-positive T cells were magnetically isolated from either healthy donor (HD)- or patient material (PM)-derived leukapheresis (LP), whole blood (WB) or buffy coat (BC), activated and after 24 h transduced with aseptically conjoined anti-CD20 CAR encoding lentiviral particles. Subsequently, T cells were expanded for additional eleven days and finally harvested on day twelve.

To assess reproducibility and robustness of the TCT Process, 15 runs with different conditions were performed. Thus, the process was challenged by the use of either HD or PM as starting material, by their status which was fresh and frozen or only limited available. Tab. 8 summarizes the characteristics of the donors used for the different runs.
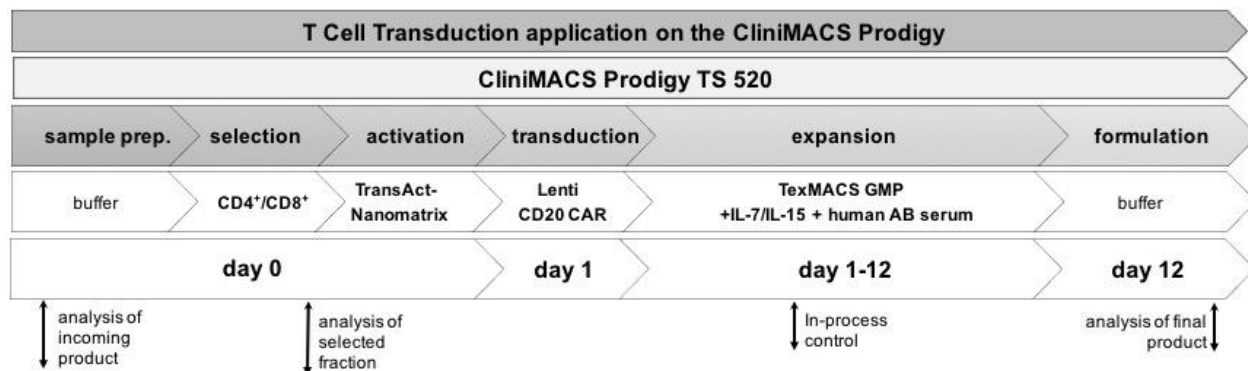
Fig. 26 **The automated TCT Process on the CliniMACS Prodigy platform.** CD4- and CD8-positive T cells, derived from either LP, WB or BC, were magnetically isolated, activated and after 24 h lentivirally transduced. Subsequently, genetically engineered T cells were expanded for additional eleven days and finally formulated in Composol and harvested. QC pouches enabled a consequent in-process control to check cell count, viability, pH value and glucose consumption.

Tab. 8 Characterization of starting material used to evaluate robustness and reproducibility of the TCT Process.

Run ID	starting material	donor description	cryopre-served	transduction performed	% CD3-positive starting material	number TNC start culture with
LP-1	LP	HD	no	yes	81	1E8
BC-2	BC	HD	no	yes	59	1E8
WB-3	WB	melanoma	no	yes	4	0.2E8
LP-4	LP *)	DLBCL	no	yes	19	1E8
LP-5				no		1E8
LP-6	LP *)	HD	no	no	63	1E8
LP-7				yes		1E8
LP-8				yes		1E8
LP-9	LP *)	DLBCL	yes	yes	46	0.6E8
LP-10				yes		0.6E8
LP-11	LP *)	HD	no	yes	83	1E8
LP-12				yes		1E8
LP-13	LP *)	HD	no	yes	75	1E8
LP-14				yes		1E8
LP-15				yes		1E8

*) split pack run: enriched T cell fraction was used for manufacturing runs on different CliniMACS Prodigy devices

Generally, 1E8 CD4/CD8 enriched T cells (less for run WB-3, LP-9 and LP-10; Tab. 8) were polyclonally activated. After 24 h as well as 72 h their activation status was qualitatively assessed without disturbing the initial T cell activation phase or losing cells in the early beginning by using an integrated microscope camera (Fig. 27A). Considering the fact that WB-3 started with just 2E7 cells instead of 1E8, all 15 Prodigy runs yielded

comparable T cell expansion curves (Fig. 27B) that ranged from 2.9E9 – 6.3E9 T cells for HD to 3.2E9 – 4.9E9 lymphocytes for DLBCL patients and 2.4E9 cells for the melanoma patient on day twelve (Fig. 27C). Neither for the final cell count nor for the final cell density (17.2E6 ± 5.5E6 cells/mL for HD and 14.0E6 ± 3.7E6 cells/mL for PM; Fig. 27D) were significant differences observed even though cryopreserved material (LP-9 and LP-10) or lower starting numbers (WB-3, LP-9 and LP-10) were used to run the process. 97.8% of fresh cells (LP-4 and LP-5) were initially viable compared to 82.4% starting with the cryopreserved product (LP-9 and LP-10) (Fig. 27E). However, while this value dropped for the fresh cells to 81.3 ± 2.5% and increased back to 91.8 ± 0.7%, the viability of cryopreserved cells peaked at 93.1 ± 4.2% on day six and then continuously decreased to 80.7 ± 2.4% on day twelve. Overall, no statistically significant differences were detectable when analyzing the viability in the final product which ranged from 90.4 ± 4.3% for HD and 88.4 ± 7.4% for PM (Fig. 27F). The final expansion rates varied from 43 ± 14 fold for HD and from 65 ± 36 fold for PM (Fig. 27G).
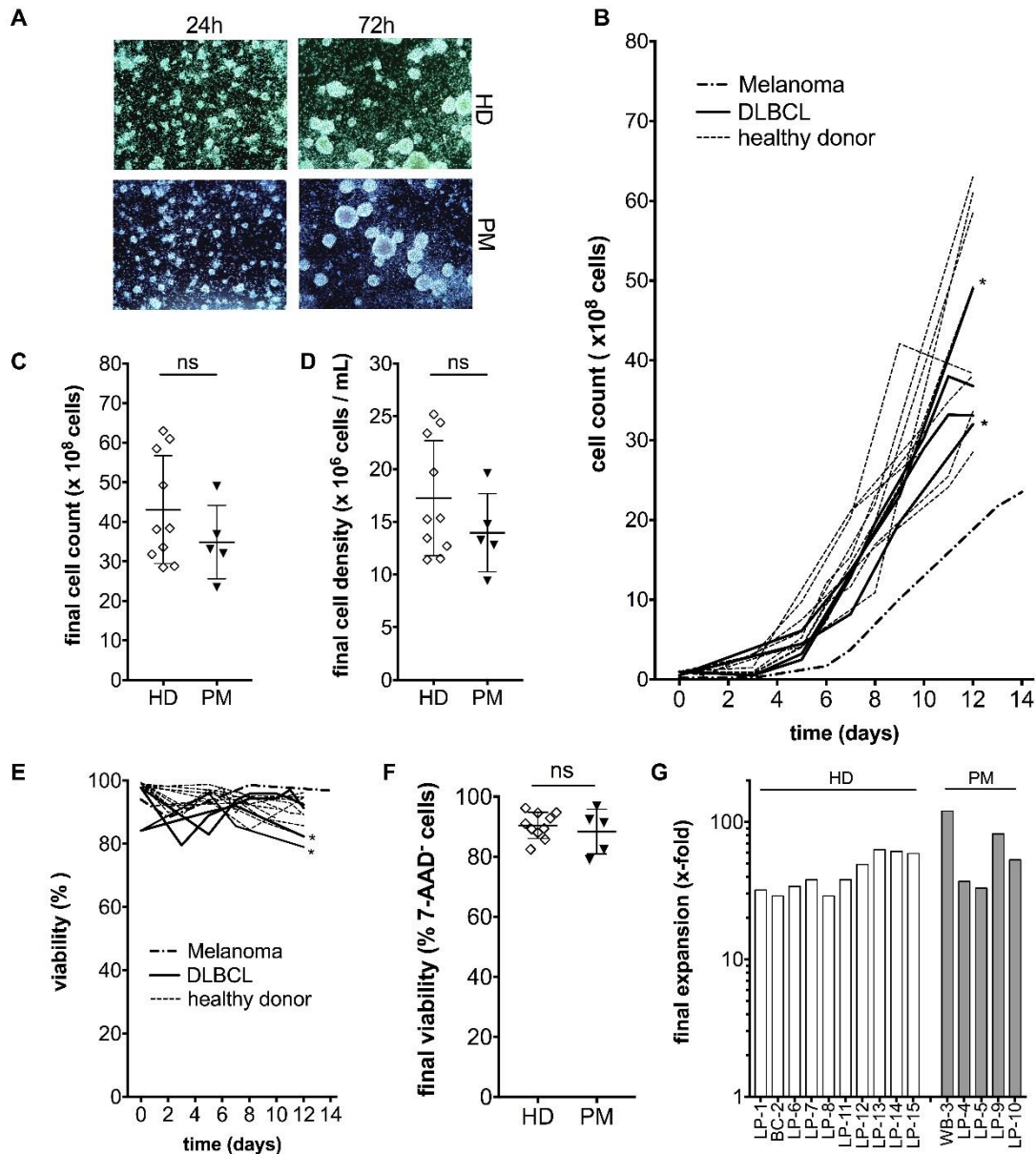
Fig. 27 **The TCT Process allows the manufacturing of T cells in a clinically relevant scale independently of the starting material**. (A) The activation status of polyclonally activated T cells was qualitatively assessed after 24 h and 72 h using the CliniMACS Prodigy integrated camera. (B) Independently of the starting material, comparable T cell expansion curves, (C) final cell counts as well as (D) final cell densities were measured. (E) Generally, the viability was > 80% during the process and ranged from (F) 90.4 ± 4.3% for HD and 88.4 ± 7.4% for PM in the final product. (G) Overall, the final expansion rates were comparable for HD and PM. (* = cryopreserved cells) Parametric unpaired t-test with 95% confidence level.

3.3.2 Phenotypic characteristics of automated manufactured T cells

Analyzing the cellular composition of the enriched fraction (Cap. 2.3.7) revealed that HD-derived samples with 83.4 ± 9.6% were mainly composed of CD3-positive cells in contrast to PM-derived samples (54.8 ± 11.5% T cells) where significantly more B cells (CD19+), monocytes (CD14+), NK cells (CD56+), NKT cells (CD3+/CD56+) and granulocytes (CD16±/CD56±/SSC$_{hi}$) were detected (Fig. 28A). In the final product, however, the frequency of T cells with 91.3 ± 5.0% for HD and 88.3 ± 7.1% for PM was comparable (Fig. 28B). Hence, the established culture conditions favored a T cell outgrowth and only NKT cells were further detectable as `contaminating´ cells with frequencies of 5.1 ± 2.2% for HD and 8.0 ± 4.3% for PM. Analogue to the cellular composition, phenotypical characteristics were analyzed by flow cytometry (Cap. 2.3.7) using CD62L, CD45RO and CD95. It was shown that the enriched HD fraction was equally composed of naïve T cells (T$_N$: CD45RO-CD62L+CD95-; 26.1 ± 16.5%), central memory T cells (T$_{CM}$: CD45RO+CD62L+CD95+; 22.0 ± 13.0%) and effector memory T cells (T$_{EM}$: CD45RO+CD62L-CD95+; 28.5 ± 10.6%) while the enriched PM fraction contained significantly more effector T cells (T$_{EFF}$: CD45RO-CD62L-CD95+; 24.7 ± 11.3%) whereas T$_N$ with 7.3 ± 0.5% were significantly diminished (Fig. 28C). Although the PM-derived T cells contained more differentiated effector cells in the enriched fraction, 64.7 ± 5.8% T cells in the final product showed the phenotypical characteristics of long-term persisting T$_{CM}$. HD-derived T cells were mainly composed of stem cell memory T cells (T$_{SCM}$: CD45RO-CD62L+CD95+; 45.0 ± 11.2%) and T$_{CM}$ (33.99 ± 15.31%) (Fig. 28D). Overall, the frequency of memory T cells in the final product was comparable for HD (79.0 ± 13.5%) and PM (87.1 ± 7.7%). Finally, the frequency of CD4- and CD8-positive T cells in the enriched fraction (Fig. 28E) was analyzed (Cap. 2.3.7) revealing a CD4/CD8 ratio of 3.8 ± 0.8 for HD and 2.3 ± 0.8 for PM (Fig. 28F) that changed during the twelve day culture in the final product to 2.0 ± 1.6 for HD and 1.9 ± 0.9 for PM (Fig. 28G and H).
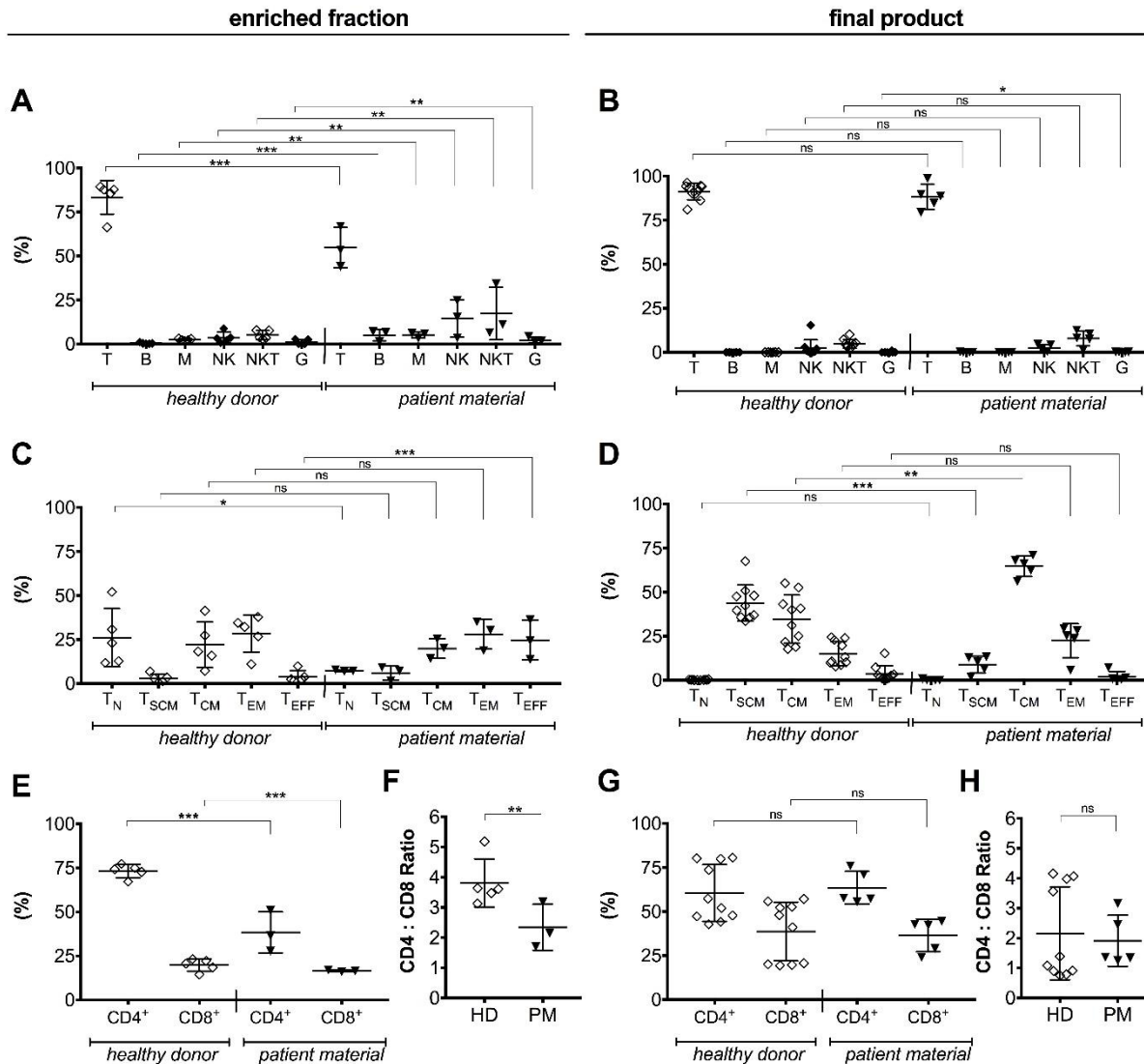
Fig. 28 **Cellular composition, phenotypical characteristics and CD4/CD8 ratio of the final TCT Process product are comparable for HD and PM.** Frequencies of T: T cells, B: B cells, M: monocytes, NK: NK cells, NKT: NK T cells and G: granulocytes (total of eosinophils and basophils) were analyzed (A) before and (B) after the finished TCT Process confirming that the culture conditions favor a T cell outgrowth. T cell phenotype was measured using CD45RO, CD62L and CD95 to define T_N: naïve T cells, T_{SCM}: stem cell memory T cells, T_{CM}: central memory T cells, T_{EM}: effector memory T cells and T_{EFF}: effector T cells. (C) While HD-derived T cells showed less differentiated phenotypical characteristics than PM-derived samples (D) the frequency of long-term persisting memory T cells was comparable. (E-F) The same applies to the frequency and ratio of CD4/CD8 T cells in the enriched fraction (G-H) where significant differences disappeared in the final product. (For the enriched fraction in total n=5 runs with HD and n=3 runs with PM. For the final product in total n=10 runs with HD and n=5 runs with PM.) Parametric unpaired t-test with 95% confidence level.

3.3.3 Anti-tumor reactivity of automated manufactured CAR T cells

Transduction efficiency of lentivirally engineered T cells was measured using a CD20 peptide linked to PE (Cap. 2.3.7). The frequency of CAR expressing T cells ranged for HD samples from 14.0 – 28.0% (mean 25.2 ± 7.8%) on day five to 17.3 – 54.3% (mean 34.5 ± 11.7%) one week later (Fig. 29A). PM-derived samples showed a similar expression profile with 21.4 – 24.0% (mean 22.2 ± 1.2%) for PM in the in-process control on day five and 22.2 – 59.1% (mean 36.4 ± 17.7%) on day twelve (Fig. 29B). Accordingly, not only the final T cell count (HD 4.4 ± 1.4E9 and PM 3.6 ± 1.1E9) but also similar transduction efficiencies as well as the final number of CD20-directed CAR T cells (HD 1.4 ± 0.7E9 and PM 1.0 ± 0.4E9) confirmed both robustness and reproducibility of the automated manufacturing process showing that neither starting material nor cryopreservation seems to negatively influence the final product (Tab. 9).

Tab. 9   Characterization of automatically manufactured T cells

Run ID	final T cell count (x1E9 cells)	% anti-CD20 CAR T cells	final number anti-CD20 CAR T cells (x1E9 cells)	lentiviral vector batch	Operator
Healthy donor					
LP-1	3,01	42.41	1,28	A	A
BC-2	2,64	40.53	1,07	A	A
LP-7	3,08	35.95	1,11	A	B
LP-8	2,61	40.56	1,06	B	C
LP-11	3,42	22.20	0,76	B	B
LP-12	4,21	17.36	0,73	D	D
LP-13	5,80	24.00	1,39	G	D
LP-14	5,61	32.88	1,85	E	B
LP-15	5,61	54.33	3,05	F	D
	4.42 (±1.40)	34.47 (±11.67)	1.36 (±0.71)		
Patient material					
WB-3	2,11	59.10	1,25	A	A
LP-4	3,33	41.90	1,40	A	D
LP-9	4,17	22.21	0,93	C	B
LP-10	2,56	22.53	0,58	D	C
	3.55 (±1.05)	36.44 (±17.69)	1.04 (±0.36)		

After the twelve days of manufacturing, CD20-directed T cells, either derived from HD or PM, were subsequently used in *in vitro* assays to assess their cytolytic potential (Fig. 29C and D). The frequency of killed target cells varied at an E:T ratio of 1:1 from 13.9 - 75.0% (mean 44.2 ± 19.3%) for HD and from 15.4 - 70.7% (mean 39.3 ± 21.3%) for PM (Cap. 2.5.1). Thus, independently of the starting material or starting conditions, potent CAR engineered T cells were manufactured during the TCT Process which was further confirmed in cytokine release assays (Cap. 2.5.3) (Fig. 29E and F).
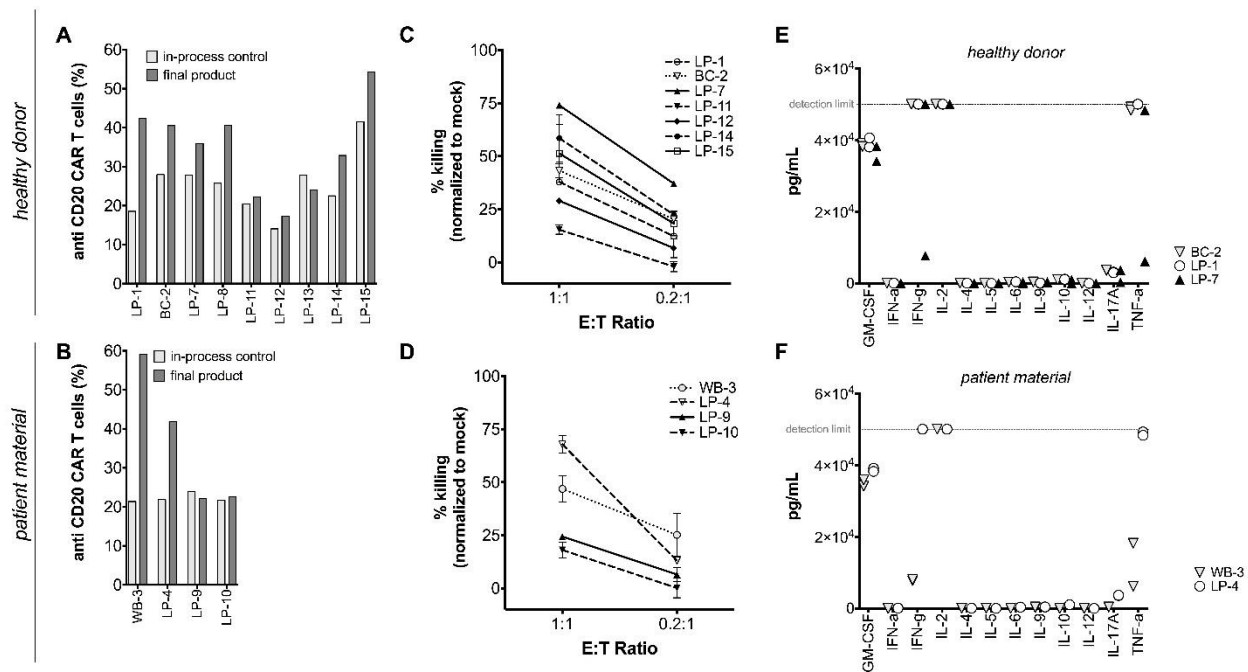
Fig. 29 **Potency of automatically manufactured CAR T cells was confirmed *in vitro*.** CAR expression of (A) HD- and (B) PM-derived T cells was measured during the process on day five as well as in the final product on day twelve. Subsequently, co-culture assays with JeKo-1 cells were performed showing a comparable killing efficiency for (C) HD- (n=7) and (D) PM-derived samples (n=4) (Each sample tested in duplicates, SEM indicated) (E-F) as well as a comparable release of cytokines (HD n=3; PM n=2).

After verifying the cytolytic potential of automatically manufactured T cells *in vitro*, their anti-tumor reactivity was assessed *in vivo* using a lymphoma xenograft model (Cap. 2.5.5). Hence, 5E5 Raji^FFluc cells were injected i.v. into the tail vein of NSG mice. Tumor cells were engrafted for one week before either 1E6 Mock-transduced or anti-CD20 CAR T cells (HD-derived) were injected again i.v. via their tail vein. Tumor growth was monitored frequently for 20 days using an IVIS (Fig. 30A). It could be shown that only mice

that received anti-CD20 CAR sequence expressing T cells were able to eradicate tumor cells and thus control tumor outgrowth (Fig. 30B and C). Those findings were further confirmed *post mortem* by analyzing the frequency of tumor cells in the bone marrow using flow cytometry (Cap. 2.3.7) (Fig. 30D).
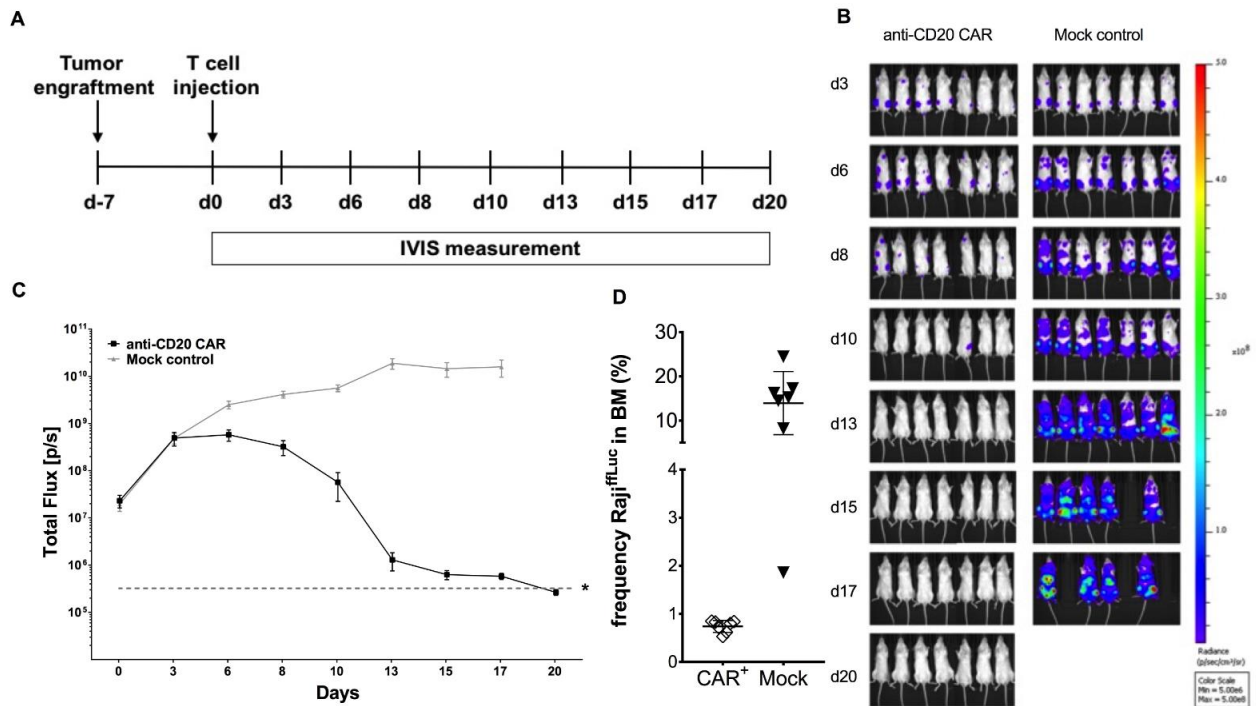
Fig. 30   **Automatically manufactured CD20-directed T cells eradicated tumor cells *in vivo*.** (A) After engrafting a Raji[FFluc*] tumor in NSG mice, either Mock or CD20-directed CAR T cells were injected i.v. as described in the experimental workflow. (B-C) While the treatment with Mock T cells did not have any effect on the tumor outgrowth, anti-CD20 CAR T cells efficiently lysed tumor cells as detected by IVIS as well as (D) flow cytometry. (* = flux on day 0)

3.4 Chimeric co-stimulatory receptor as a novel CAR T cell technology

The treatment of solid tumors with CAR engineered T cells is still more than challenging. Thus, a fundamental problem still represents the scarcity of known specific tumor-associated antigens allowing a defined and safe therapy without causing severe on-target/off-tumor toxicities. In addition, the clinical success of current approaches is limited due to the poor infiltration of gene-engineered lymphocytes into the tumor as well as a highly immunosuppressive tumor microenvironment which heavily impedes the instigation and maintenance of any inevitable T cell response [105]. Novel CAR T cell technologies, however, might have the potential to circumvent those limitations and therefore extend the scope of ACT.

Additionally to the development of an anti-CD20 CAR and the automated manufacturing of gene-modified T cells, this study also focused on a strategy to ameliorate the CAR-based immune response in a solid tumor setting by co-expressing a second generation CAR and a CCR in the same T cell.

3.4.1 Anti-CSPG4 CAR and anti-CD20 CCR development

The present study takes place in a melanoma setting to evaluate the potential of a CCR as a tool to enhance the cytolytic potential of CAR T cells. For this purpose, a CAR directed against chondroitin sulfate proteoglycan 4 (CSPG4) as well as a CCR specific for CD20 were generated and tested.

CSPG4_1, a retroviral construct encoding an anti_CSPG4 CAR, was a kind gift from H. Abken (ZMMK Cologne) which was enzymatically digested with *Bam*H I and *Sal* I and subsequently cloned into MB_001 (Cap. 2.2.2). Furthermore, the scFv sequences derived from either TP 61.5, 225.28s or 763.74 were cloned into the CAR library using *Bve* I (Cap. 2.2.2 and Cap. 3.1.1) (Fig. 31). After sequence amplification in a midiprep (Cap. 2.2.4) and sequence verification (Cap. 2.2.5), lentiviral particles were produced (Cap. 2.3.6) and subsequently T cells transduced (Cap. 2.4.1) to assess the functionality (Cap. 2.5.2 and

2.5.3) of the different lentiviral constructs dependent on the used binding domain and spacer length (data not shown).
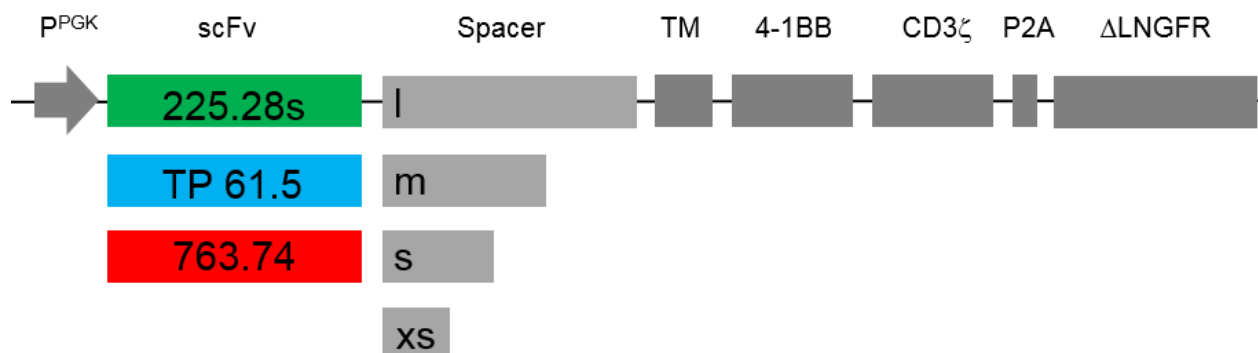
Fig. 31 **Schematic description of *Bve* I generated anti-CSPG4 CAR encoding lentiviral constructs.** 225.28s-, TP 61.5- and 763.74-derived scFv sequences were cloned into the established and described CAR library.

After confirming the functionality of CSPG4_2, a lentiviral construct encoding for the 225.28s-derived binding moiety with a long spacer (IgG4 Hinge_CH2_CH3), different CCR encoding constructs were generated. Therefore, different signaling motif encoding sequences were synthesized with flanking *Bve* I sites and cloned into MB_005 (Leu16 scFv vl/vh with long IgG1 spacer) using the established high-throughput cloning protocol (Cap. 2.2.2 and Cap. 3.1.1). For a first screening experiment, five lentiviral constructs with different combinations of 4-1BB, CD28 and CD3ε as signaling domains were generated (Fig. 32). Again, midipreps were performed (Cap. 2.2.4), sequence was verified (Cap. 2.2.5) and lentiviral particles were produced (Cap. 2.3.6).
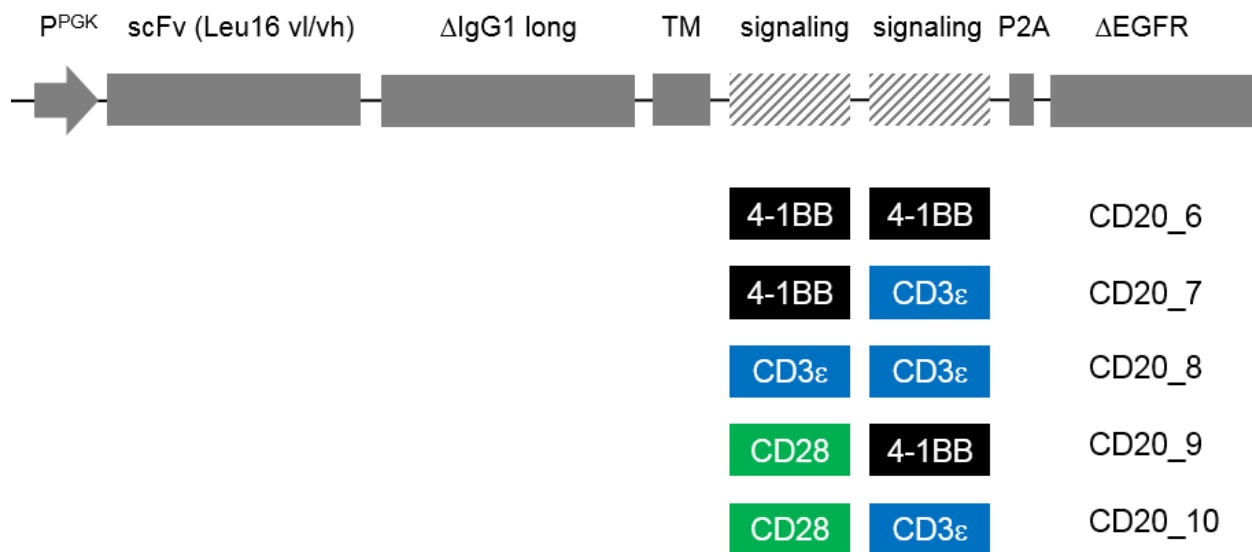
Fig. 32 **Overview of anti-CD20 CCR encoding lentiviral constructs.** Different combinations of 4-1BB, CD28 and CD3ε were cloned into MB_005 using the established high-throughput cloning protocol.

3.4.2 *In vitro* evaluation of the boosting concept

To test the boosting CCR concept, PBMC of two different donors were prepared (Cap. 2.3.1), T cells were isolated and activated (Cap. 2.3.2) and subsequently co-transduced with LV-CSPG4_2 and one CCR encoding lentiviral particle (CD20_6 – CD20_10). Controls were only transduced with one CAR or CCR encoding lentiviral construct, respectively. T cells were then expanded in TexMACS supplemented with 200 IU IL-2 (Cap. 2.3.2) until gene-modified T cells were enriched (Cap. 2.4.3) on day seven. The magnetically selected T cells were further expanded, initially without any re-stimulation, for additional six days (Fig. 33A). On day 13, after confirming the CSPG4 gene expression of Mel526 cells (Fig. 33B), 1E4 melanoma cells were co-cultured with 5E4 either Mock, controls (expressing either CAR or CCR) or T cells expressing both CAR and CCR in the presence or absence of 5E4 CD20-positive autologous B cells which were isolated from frozen PBMC, one day in advance (Cap. 2.3.3). The applied trans-boosting experiment was used to assess the different CCR constructs (Fig. 33C) by analyzing the release of cytokines (Cap. 2.5.3). Alternatively, CCR and CAR co-expressing T cells can be compared in a cis setting using target cells that express both genes CSPG4 and CD20 (Fig. 33D).
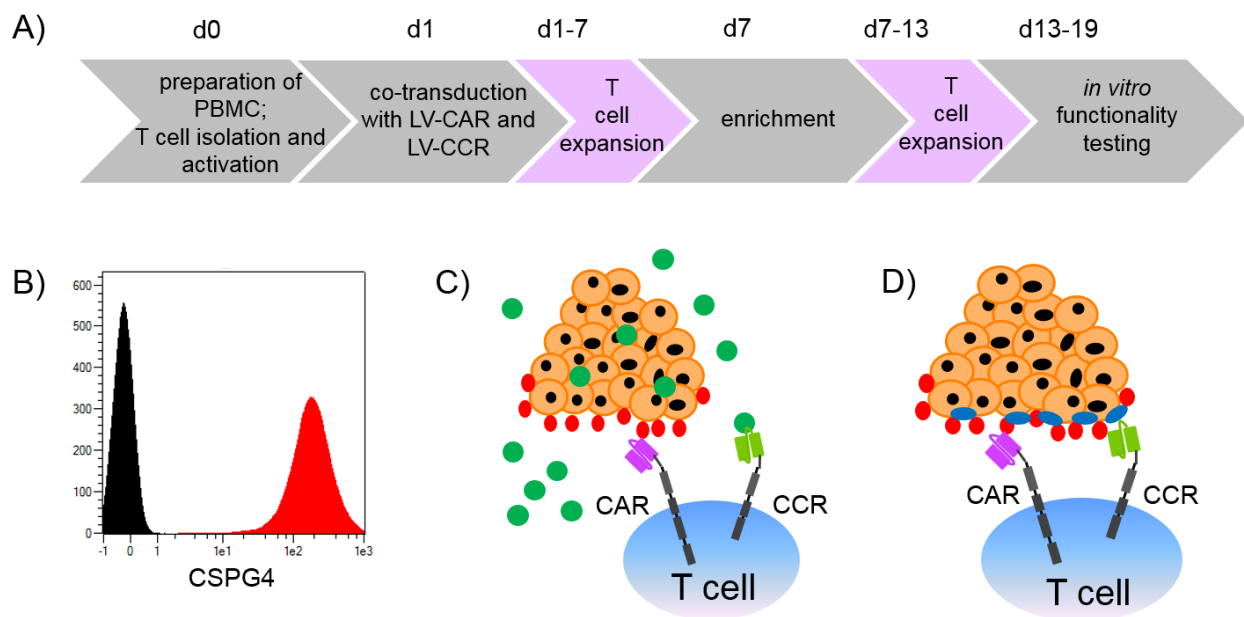
Fig. 33 **Schematic workflow of a trans-boosting approach to assess and compare the potential of different CCRs.** (A) Within 19 days the boosting CCR potential could be tested using co-culture assays. (B) CSPG4 gene expression on Mel526 cells (red) was detected via a specific surface staining and flow cytometry. (C) Graphical representation of a trans-boosting approach. In this setting, a non-tumor-associated target gene was used to activate the CCR on the T cells. (D) Alternatively, CAR and CCR sequence co-expressing T cells were tested in cis. Accordingly, both CAR and CCR get activated via tumor-associated surface proteins.

An enhanced release of TNF-α was detected for the CCRs with either 4-1BB_4-1BB or CD28_4-1BB endodomains while for the other CCR versions no TNF-α was detectable (Fig. 34A). The boosting potential of 4-1BB_4_1BB and CD28_4-1BB equipped CCRs was further confirmed by measuring additional proinflammatory cytokines including GM-CSF, IFN-γ and IL-2 (Fig. 34B). Mock as well as anti-CSPG4 CAR T cells served as control, revealing an expected result. Thus, unmodified Mock T cells did not release any cytokines while CSPG4-directed T cells released only low quantities of the analyzed cytokines.

Those findings were further confirmed in a second experiment. Therefore, double transduced T cells were generated again as described above aside from the culture medium which was supplemented with 12.5 ng/ml IL-7 and IL-15, respectively. Furthermore, after the LNGFR/EGFR co-enrichment (Cap. 2.4.3) cells were re-stimulated with T Cell TransAct, human (1:500) for two days. Functionality assays were performed on day 16 in trans using autologous B cells as well as in cis using CD20-positive Mel526$^{FFluc\_eGFP}$ cells (Cap. 2.5.3). This experiment focused on a further comparison of 4-

1BB_4-1BB and CD28_4-1BB and included additional controls. CCR controls (T cells that just express the CCR sequence) were analyzed as well. In the trans experiment, a boosted release was detected for all the analyzed proinflammatory cytokines (GM-CSF, IFN-γ, IL-6 and TNF-α) only in the presence of both targets CSPG4 and CD20 (Fig. 35A). 4-1BB_4-1BB modified CCRs, however, have a greater potential to increase the release of this cytokines compared to CD28_4-1BB equipped ones. Donor variances were detected with regard to this boosting effect. Nevertheless, CSPG4 as well as CCR controls showed a unique cytokine expression profile, independently of added B cells. Mock T cells co-cultured with Mel526 cells and B cells as well as Mel526 cells on their own did not release any cytokines. The results of the cis experiment were comparable (Fig. 35B). Hence, only T cells that express both transgenes CAR and CCR showed an increased release of cytokines compared to CAR and CCR controls. Again, Mock T cells as well as the target cell line Mel526$^{CD20\_FFluc\_eGFP}$ did not release any cytokines. Interestingly, the unleashed amounts of GM-CSF, IFN-γ and TNF-α either in cis or in trans were virtually similar (Fig. 35C). Only for IL-6 appreciable differences were observed.
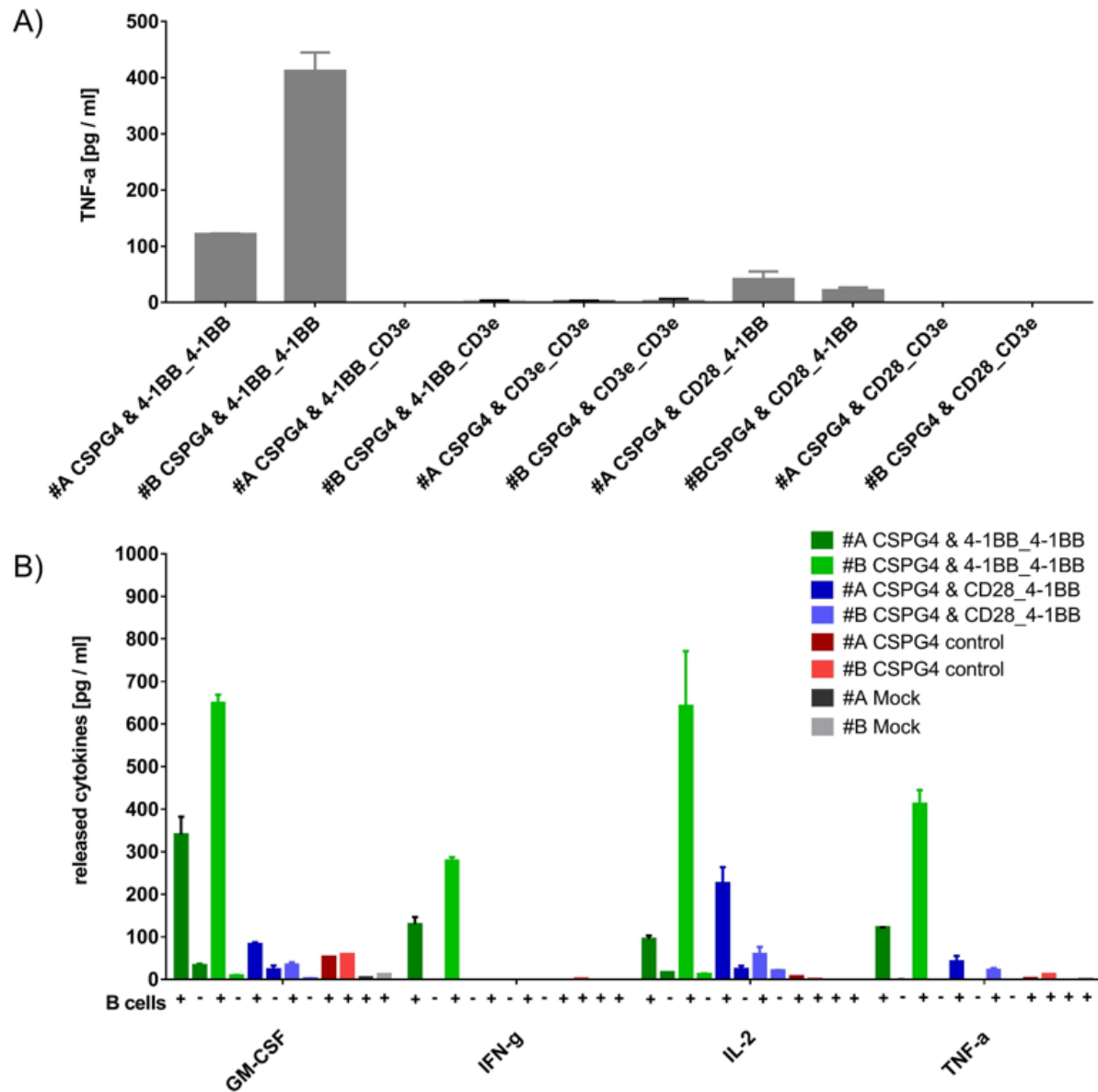
Fig. 34 **CCRs equipped with defined endodomains have the potential to enhance a CAR T cell response.** CAR and CCR co-expressing T cells were co-cultured with CSPG4-positive Mel526 cells in the presence or absence of CD20-positive B cells. (A) Initially, the release of TNF-α was measured showing that CCRs with the combinations of 4-1BB_4-1BB as well as CD28_4-1BB endodomains led to an increased release of this cytokine. (B) This finding was confirmed by analyzing additional cytokines. Thus, only in the presence of B cells a boosted immune response was detected. CSPG4-directed CAR T cells as well as Mock T cells served as control. #A and #B represent different donors. The indication CSPG4 means that the T cells in this group were CAR transduced. The indication after the `&´ (e.g. 4-1BB_4-1BB) stands for the endodomains of the CCR directed against CD20.
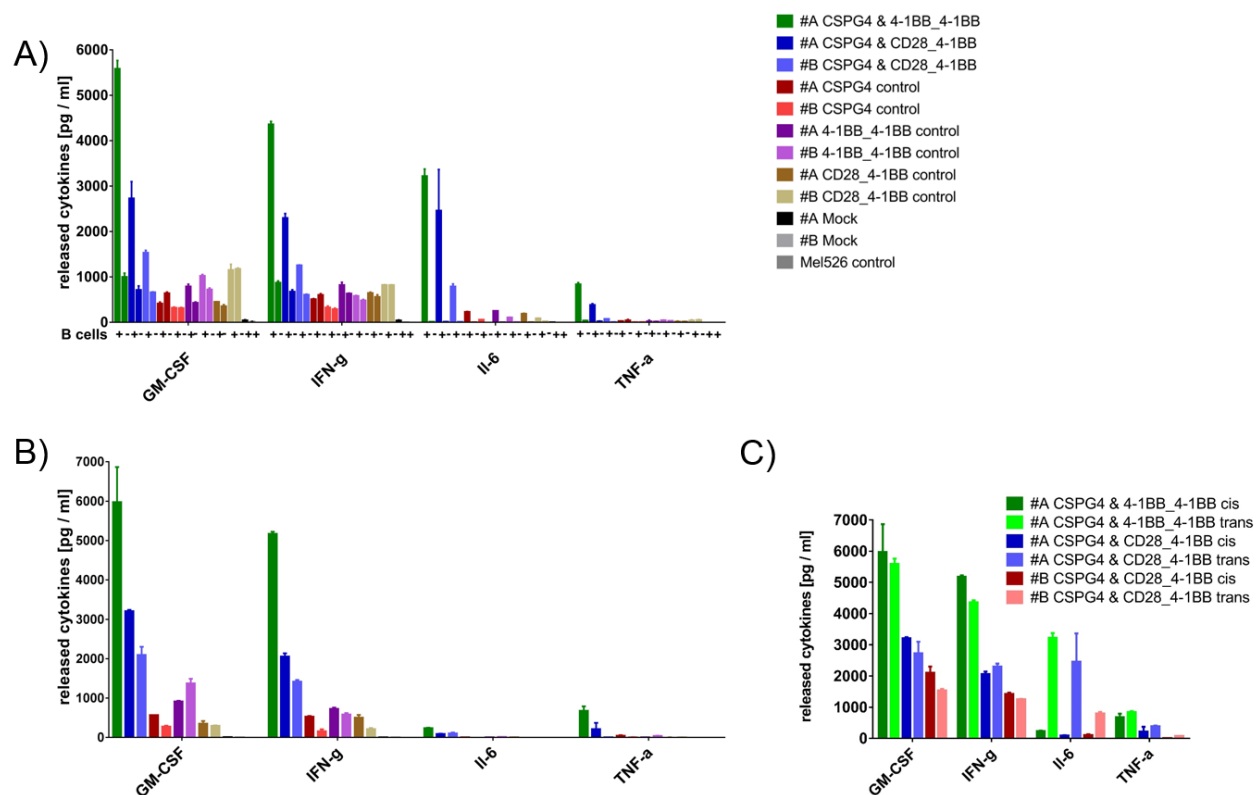
Fig. 35 **CCRs with 4-1BB_4-1BB endodomains have higher boosting potential than CCRs with CD28_4-1BB.** (A) Only in the presence of both surface antigens CSPG4 and CD20 an increased release of the type-1 cytokines GM-CSF, IFN-γ, IL-6 and TNF-α were detected whereby the released amounts were considerably higher for 4-1BB_4-1BB equipped CCRs than for those with CD28_4-1BB endodomains. (B) Those findings were further confirmed in a cis experiment where CD20-positive Mel526 clones were co-cultured with the transgenic T cells. Overall, Mock T cells co-cultured with Mel526 clones in cis or with B cells in trans did not release any cytokines. The same applies to the used Mel526 clones cultured without effector cells. (C) Except for IL-6, the released cytokine amounts were almost similar among the performed cis and trans experiment. #A and #B represent different donors. The indication CSPG4 means that the T cells in this group were CAR transduced. The indication after the `&´ (e.g. 4-1BB_4-1BB) stands for the endodomains of the CCR directed against CD20.

3.4.3 Generation and assessment of additional CCRs

To further investigate the relevance of 4-1BB and CD28, the two endodomains in the CCR that demonstrably enhanced the CAR immune response, the current CCR library was supplemented by additional combinations including 4-1BB alone, CD28_CD28 and CD28 alone (Fig. 36). The lentiviral constructs were generated using *Bve* I (Cap. 2.2.2 and Cap. 3.1.1) and used for the production of lentiviral particles (Cap. 2.3.6). *In vitro* functionality

experiments with two donors were initiated as already described (Cap. 3.4.2). T cells were cultured in TexMACS supplemented with 12.5 ng/ml IL-7 and IL-15.
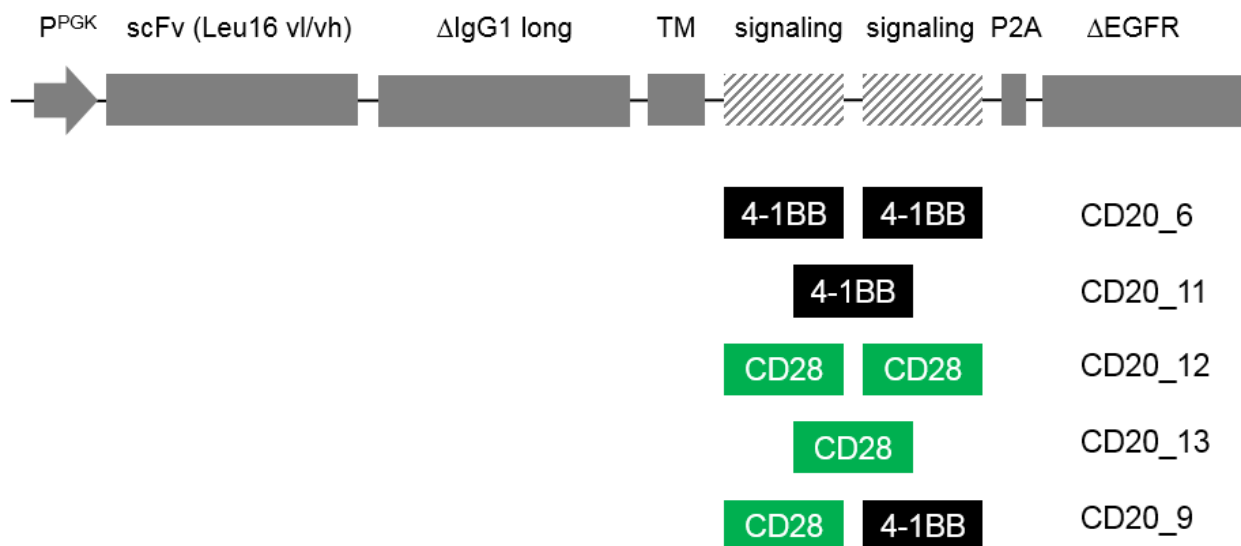
Fig. 36 **Novel CCR encoding lentiviral constructs used to assess the importance of 4-1BB, CD28 as well as a combination thereof in the boosting context.** Additional combinations of 4-1BB- and CD28- derived endodomains were cloned into MB_005 (Leu16 scFv vl/vh with long IgG1 spacer) and further investigated in functionality assays after transducing T cells.

Transgenic ΔLNGFR and ΔEGFR expression was measured by flow cytometry (Cap. 2.3.7) on day six exemplified for one donor (Fig. 37A). Overall, the frequency of co-transduced T cells that co-expressed both transgenes varied from 9 – 19%. The next day, gene-modified cells were magnetically enriched (Cap. 2.4.3) and two days later re-analyzed via flow cytometry as exemplified for the same donor (Fig. 37B). The frequency of T cells that co-expressed ΔLNGFR as well as ΔEGFR raised to a range of 31 – 69%.

On day 16, functionality assays were performed including a cytokine release assay (Cap. 2.5.3) as well as bioluminescence based killing assays (Cap. 2.5.2). In those experiments, due to a limited availability of B cells for some donors, CD20-positive JeKo-1 cells were used to activate the CCR in trans. Thus, for the trans cytokine detection assay 2E4 Mel526 cells were co-cultured with 1E5 effector cells including Mock, controls and T cells expressing both sequences CAR and CCR in the presence or absence of 1E5 JeKo-1 cells. After 24 h the cytokine secretion was determined in the supernatant. At first, TNF-α release of differently co-transduced T cells was compared revealing that all of them have

the potential to boost the cytokine release varying from 37 – 380 fold, however, only when the CAR and CCR was activated simultaneously (Fig. 38). T cells that only express the transgenic CCR, even though co-cultured on Mel526 in the presence of JeKo-1, did not release noticeable amounts of TNF-α.
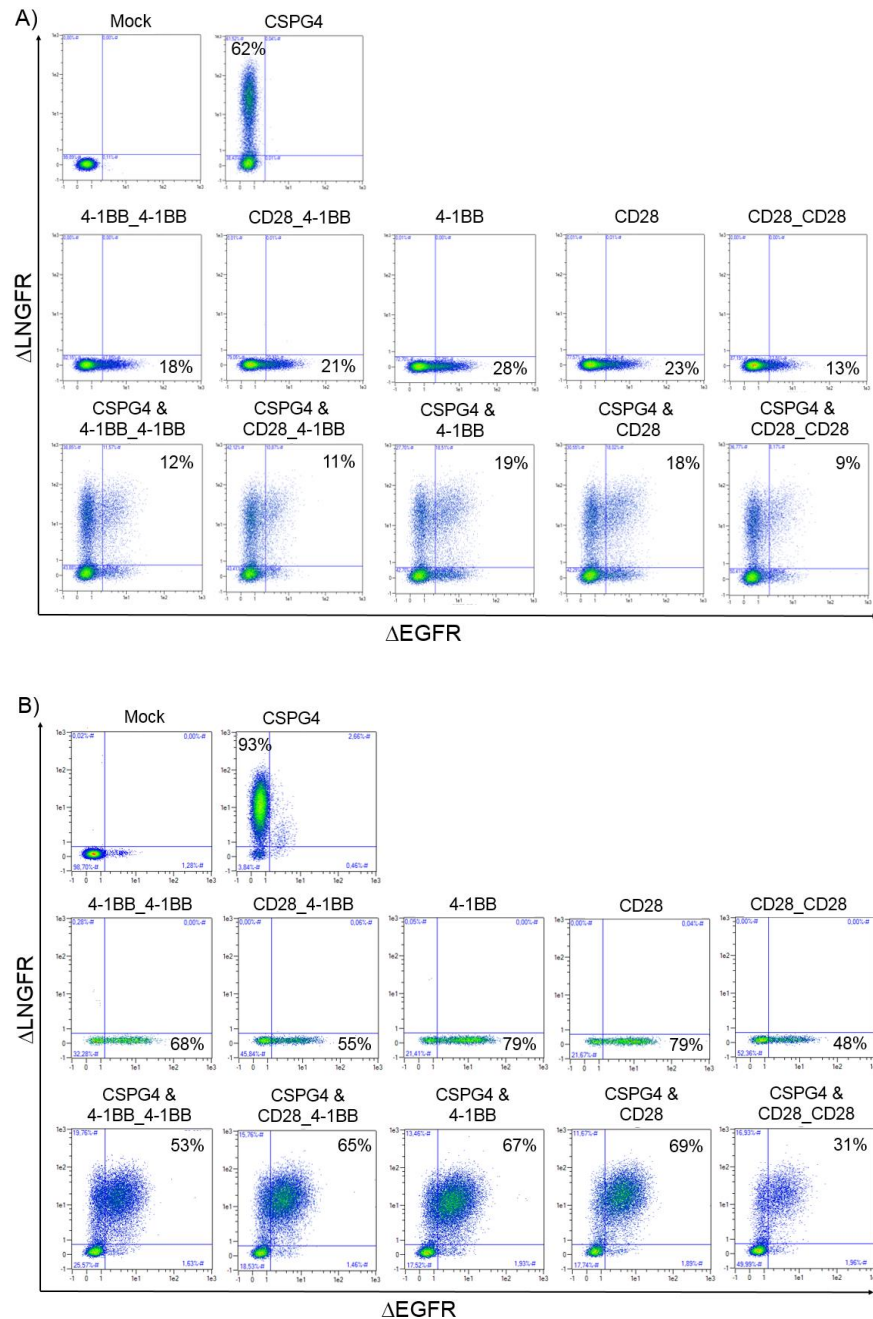
Fig. 37 **Frequency of CAR and CCR co-expressing T cells could be enhanced using a double-enrichment strategy.** Transgenic ΔLNGFR and ΔEGFR co-expression was analyzed by flow cytometry using anti-LNGFR-APC and anti-EGFR-PE antibodies (A) pre- and (B) post enrichment.
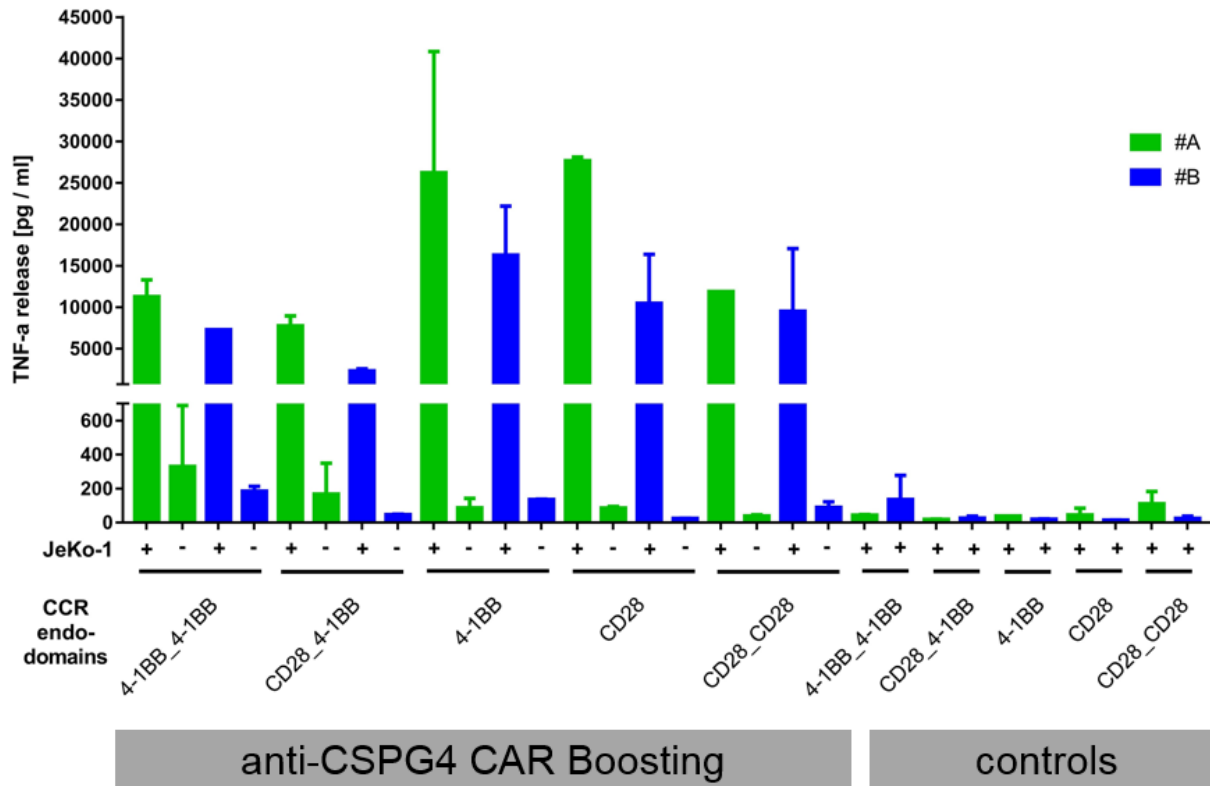
Fig. 38 **Only simultaneous activation of CAR and CCR resulted in a boosted TNF-α release.** Engineered T cells were co-cultured on Mel526 cells in the presence or absence of JeKo-1 cells revealing a boosting potential for all tested CCRs. #A and #B represent different donors.

Analyzing the release of additional proinflammatory cytokines like IFN-γ, IL-2 and IL-6 further proved the boosting potential of 4-1BB and CD28 endodomains equipped CCRs (Fig. 39). As a result, it was not possible to define any decisive advantage for a given CCR endodomain in the used *in vitro* trans-experiment since the cytokine release pattern was approximately identical. Minor differences most likely resulted from varying transduction efficiencies of the engineered T cells.
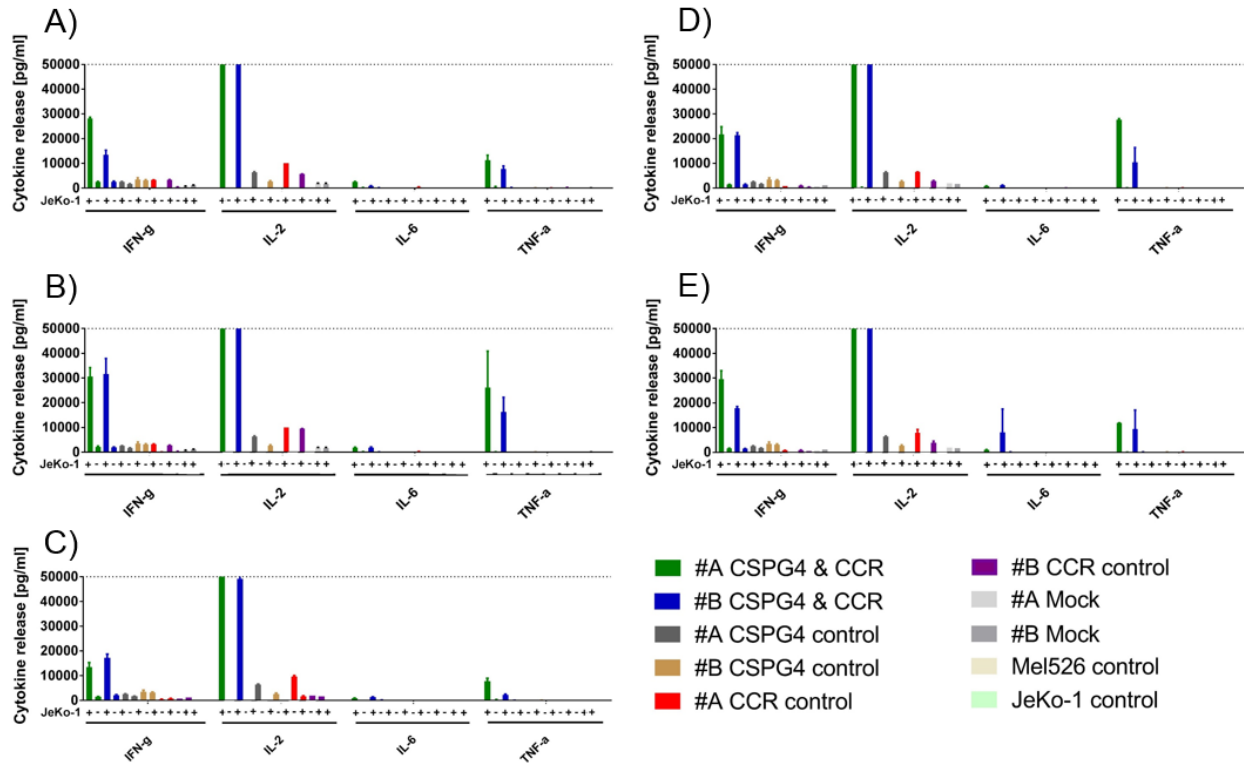
Fig. 39 **CCRs equipped with 4-1BB and/or CD28 endodomains equally boost the cytokine release**
in vitro. (A) 4-1BB_4-1BB, (B) 4-1BB, (C) CD28_4-1BB, (D) CD28 or (E) CD28_CD28 endowed CCRs
induced the release of comparable amounts of cytokines. Hence, it was not possible to define a most
favorable construct in this experiment. #A and #B represent different donors. (50000 pg/ml was the detection
limit)

The cytokine release experiment in cis was performed analogue to the trans experiment
(Cap. 2.5.3). 2E4 Mel^{CD20_FFluc_eGFP} cells were co-cultured with 1E5 either Mock, controls
or transgenic CAR T cells expressing CAR and CCR for 24 h. Measuring the expressed
cytokine amounts demonstrated both: first, although CD28_4-1BB equipped CCRs
seemed to induce the weakest boost, all combinations increased the release of
proinflammatory cytokines of the anti-CSPG4 CAR for donor A and B with a factor of at
least 3.8 and 2.4, respectively (Fig. 40). Second, the results confirmed the findings of the
trans-experiment. Due to the fact that no benefits for a specific CCR construct became
apparent in this experiment, *in vivo* experiments are indispensable to assess the suitability
and advantageous of a defined CCR structure.
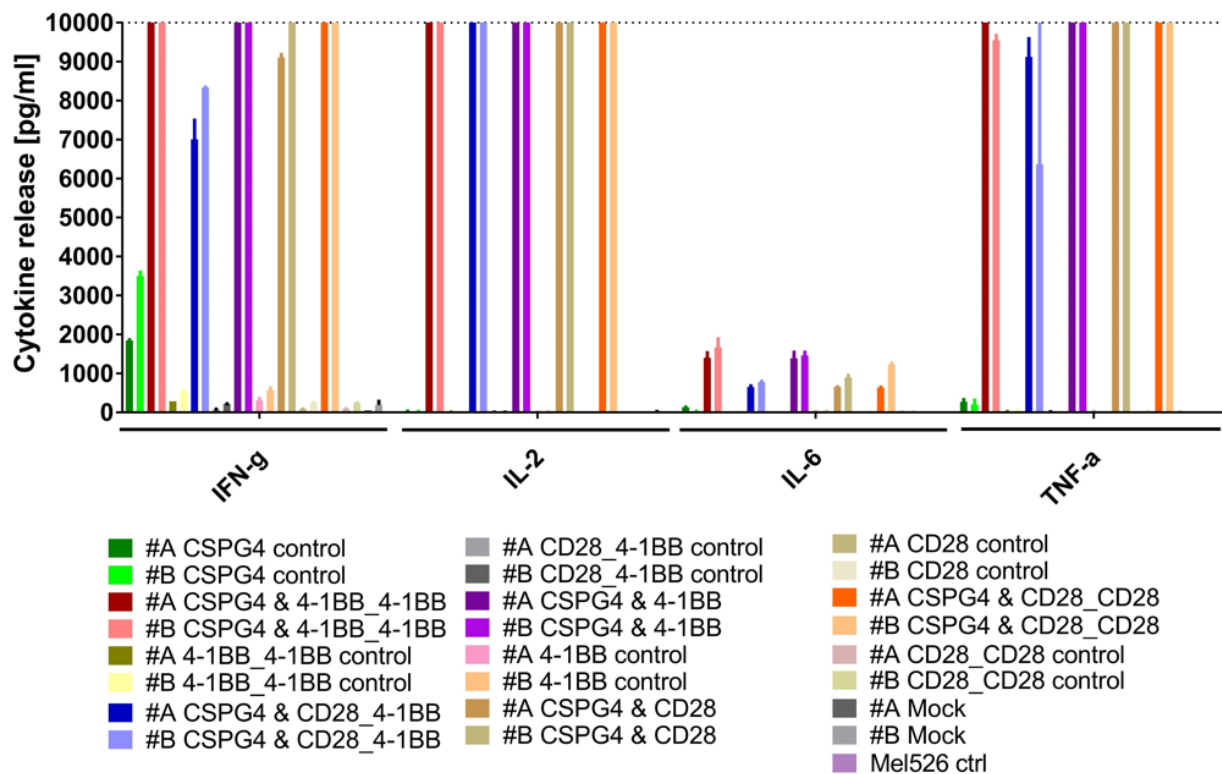
Fig. 40 **Comparison of CCRs endowed with 4-1BB and/or CD28 endodomains in cis using transgenic CD20-positive Mel526 cells.** Co-culture assays using CD20-positve Mel526 cells and effector cells revealed that CAR T cells that additionally express a CCR sequence induced a boosted release of IFN-γ, IL-2, IL-6 and TNF-α without any noticeable difference between the different CCRs. #A and #B represent different donors. The indication CSPG4 means that the T cells in this group were CAR transduced. The indication after the `&´ (e.g. 4-1BB_4-1BB) stands for the endodomains of the CCR directed against CD20. (10000 pg/ml was the detection limit)

2E4 Mel526$^{CD20\_FFluc\_eGFP}$ cells were co-cultured with controls or CAR/CCR-positive T cells in different E:T ratios for 18 h to measure target cell killing via a bioluminescence-based killing assay (Cap.2.5.2). While transgenic CAR and CCR expressing T cells killed in average 43.0 ± 17.1% at a 10:1 E:T ratio, T cells that only expressed the CSPG4 CAR killed in a range of 18.1 ± 12.1% (Fig. 41A). In combination with a CAR CD28_CD28 CCRs showed the highest killing efficiency of 50.0 ± 20.1%, while 4-1BB_4-1BB induced the weakest boost of 35.0 ± 25.8% in this experiment. CCR sequence expressing control T cells did not show any killing at a E:T ratio of 5:1 or lower (Fig. 41B). Only a moderate killing at the highest ratio was observed for 4-1BB equipped CCRs with 12.0 ± 19.1%. T cells modified with LV-CD20_5 (4-1BB_CD3ζ), however, killed even at the lowest E:T ratio 1.25:1 > 40% of the CD20-positive Mel526 cells confirming the susceptibility of this transgenic Mel526 cells to a CD20-directed killing (Fig. 41C). In summary, it could be

shown that the potential of anti-CSPG4 CARs can be significantly enhanced by using a CCR with either 4-1BB_4-1BB or CD28_4-1BB endodomains (Fig. 41D). It was also apparent that 4-1BB_4-1BB endowed CCRs have a significantly higher capacity to increase the TNF-α release than the one equipped with CD28_4-1BB.
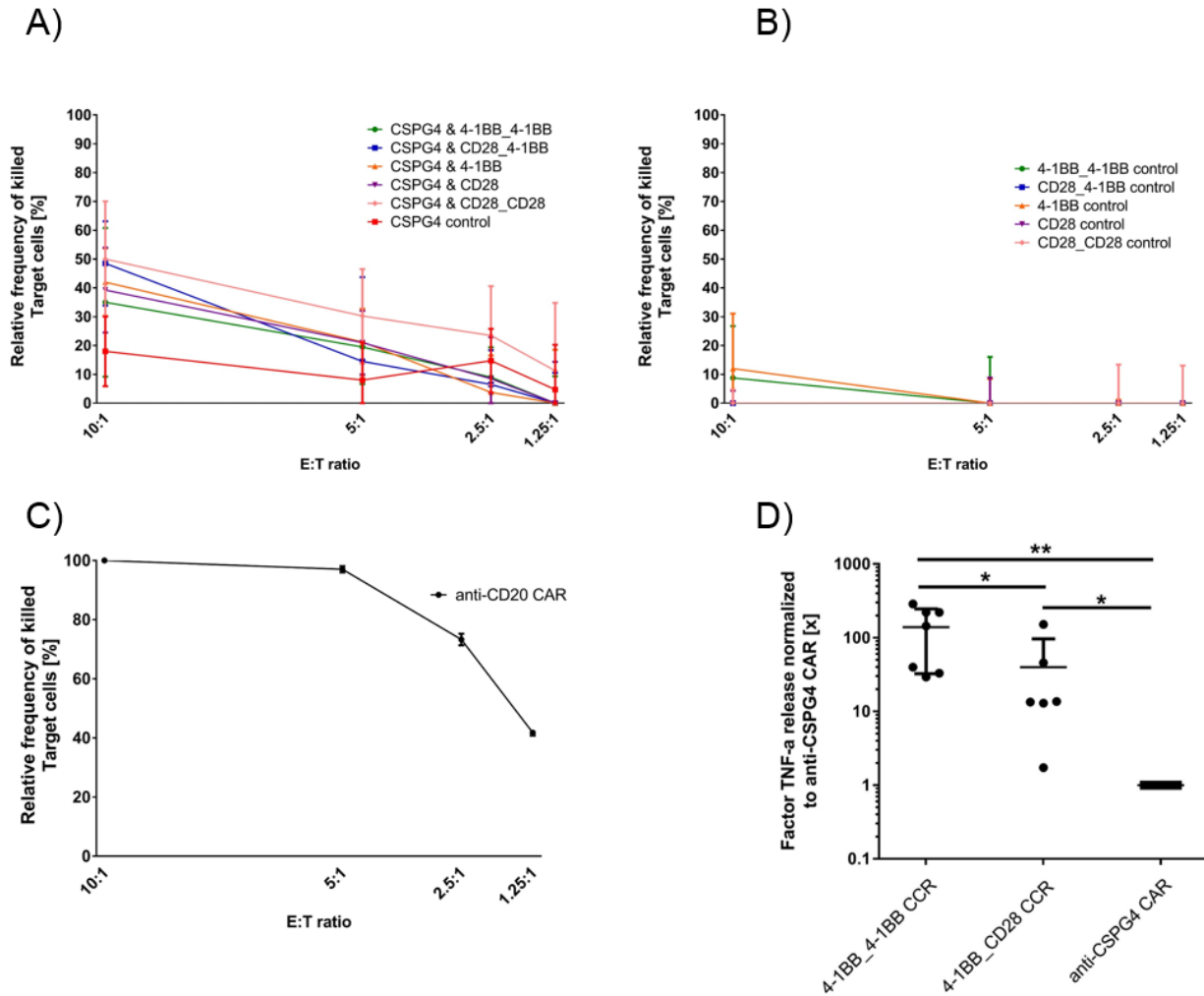
Fig. 41 **Bioluminescence-based killing assays confirmed the potential of CCRs to enhance the anti-CSPG4 CAR T cell response.** Mel526 cells were co-cultured with either Mock, controls or co-transduced T cells in different E:T ratios. Bioluminescence was measured after 18h. (A) CCR supported CAR T cells killed 43.0 ± 17.1% CD20-positive Mel526 cells at a 10:1 E:T ratio while anti-CSPG4 CAR T cells without CCR killed 18.1 ± 12.1%. (B) CCR endowed T cells did not show a comparable killing of Mel526 cells. (Each sample tested in duplicates; n=2). (C) T cells expressing a conventional anti-CD20 sequence efficiently lysed transgenic CD20-positive Mel526 cells. (Tested in duplicates; n=1). (D) Overall, the potential of CCRs with either 4-1BB_4-1BB (n=7) or CD28_4-1BB (n=6) endodomains to boost the anti-CSPG4 CAR T cell response could be confirmed. Thus, CCRs significantly increase the TNF-α release only when both CAR and CCR were activated (Parametric unpaired t-test with 95% and 99% confidence level). The indication CSPG4 means that the T cells in this group were CAR transduced. The indication after the `&´ (e.g. 4-1BB_4-1BB) stands for the endodomains of the CCR directed against CD20.

3.4.4   Improving the experimental boosting set-up

Although the functionality of anti-CD20 CCRs could be confirmed *in vitro*, further construct modifications were indispensable due to two reasons. First, the generated lentiviral constructs encoded the modified IgG1-derived spacer [40] which was eventually responsible for the loss of functionality *in vivo* (Fig. 25). Second, manufacturing of CAR T cells that are transgenic for both CAR and CCR is very complex and labor-intensive. Hence, a lentiviral construct, namely DC_1, was generated that encodes a PGK promoter driven anti-CD20 4-1BB_4-1BB CCR, a P2A element-linked CSPG4-directed CAR followed by a T2A element-linked ∆LNGFR (Fig. 42).

Initially, a human CD8 spacer derived from MB_004 was cloned into the CCR encoding construct. Subsequently, a synthesized element which encodes a human CD116 leader, a 225.28s-derived scFv with two C-terminally linked cMyc tags, an IgG4 spacer (hinge_CH2_CH3) with 4/2 NQ mutation in the CH2 domain [39] as well as a S→P substitution in the hinge region [42], 4-1BB, CD3ζ and a T2A-element linked ∆LNGFR was subcloned using *Nhe* I and *Sal* I (Cap. 2.2.2).
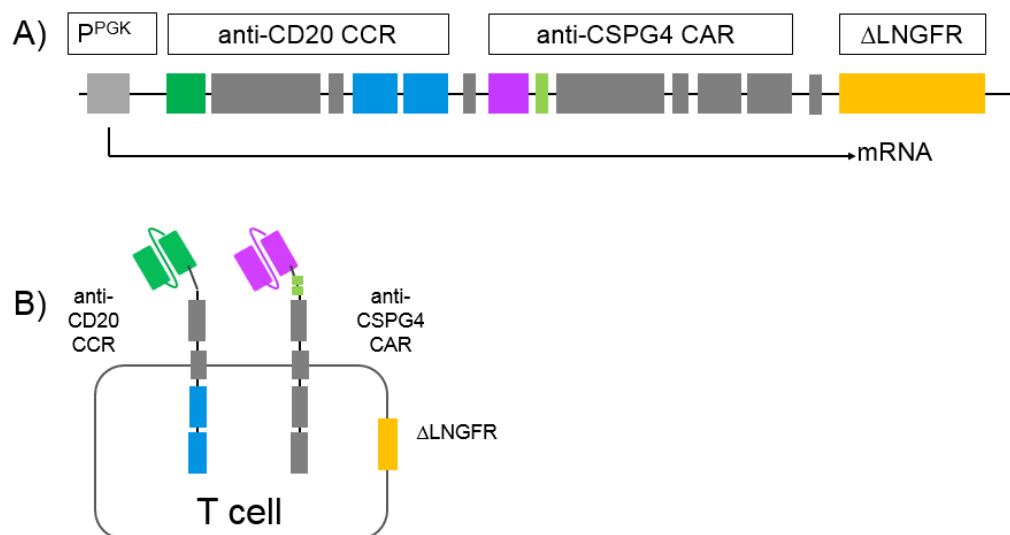
Fig. 42   **Simplified representations of DC_1, an anti-CD20 CCR_anti-CSPG4 CAR encoding lentiviral construct.** The 4-1BB_4-1BB equiped CCR was modified as following: (A) initially the IgG1 spacer was exchanged against a human CD8 spacer and subsequently the ∆EGFR element was replaced with an anti-CSPG4 CAR_T2A_∆LNGFR encoding DNA element. (B) The surface expression of the polycistronic vector genes can be measured separately by using a PE-linked CD20 peptide for the CCR or specific conjugated antibodies for either cMyc (C-terminally linked to the CSPG4-directed scFv) or ∆LNGFR.

Lentiviral particles were produced using the standard protocol (Cap. 2.3.6) before T cells derived from two donors were transduced with LV-DC_1 (Cap. 2.4.1), magnetically selected using ΔLNGFR-directed microbeads (Cap. 2.4.3) and subsequently expanded (Cap. 2.3.2) in TexMACS supplemented with 12.5 ng/ml IL-7, IL-15 and TransAct with a titer of 1:500 for T cell re-activation. On day 19, the transgenic surface co-expression of CCR, CAR and ΔLNGFR was measured and compared using flow cytometry (Cap. 2.3.7) as shown for one representative donor (Fig. 43). This analysis, however, revealed a discrepancy regarding CCR (PE-linked CD20 peptide), CAR (cMyc-directed conjugated antibody) and ΔLNGFR (ΔLNGFR-directed conjugated antibody) staining. Thus, > 60% of the T cells were positive for surface protein ΔLNGFR while only 42% were stainable with the CD20 peptide or rather 23% with the cMyc-directed antibody. Even though the staining protocol has to be optimized, the functionality of the construct was verified enabling to perform *in vitro* experiments to prove whether the change from an IgG1 spacer to CD8 in the CCR as well as the implementation of cMyc tags influenced the boosting potential or functionality of the chimeric receptors.
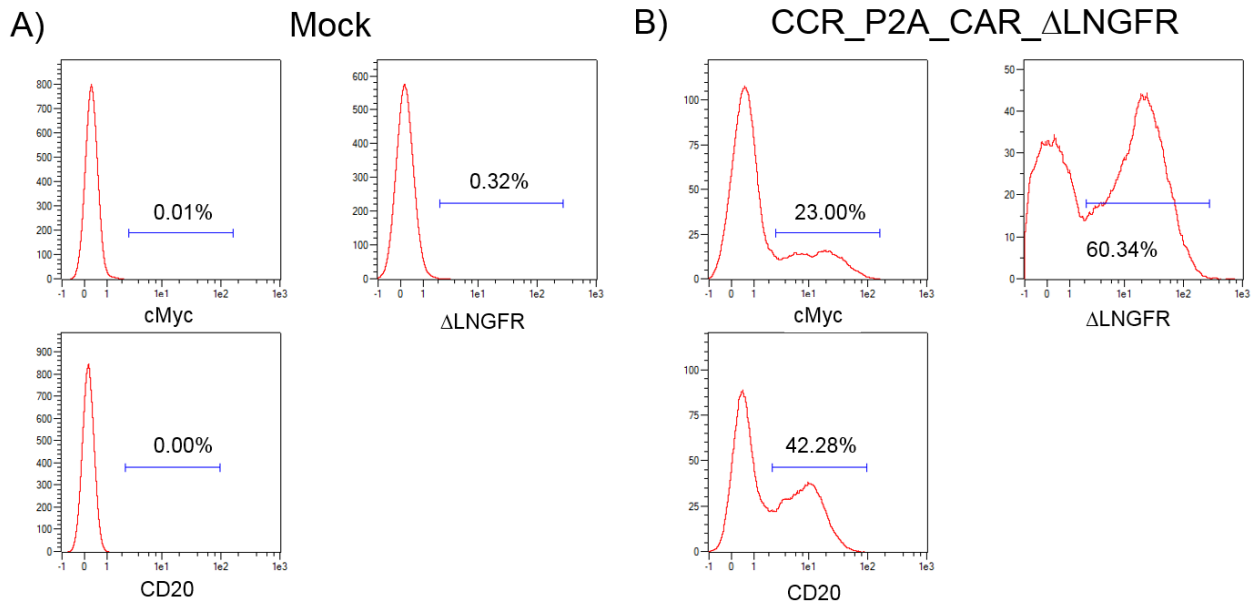
Fig. 43 **T cells co-expressing the transgenes CCR, CAR and ΔLNGFR confirmed the functionality of the polycistronic lentiviral vector DC_1.** Activated T cells were transduced with LV-DC_1, magnetically enriched and expanded. The transgenic expression of either CCR, CAR and ΔLNGFR was analyzed on day 19 using appropriate conjugates and flow cytometry. (A) While Mock T cells were negative for all transgenes (B) transduced T cells expressed all of them simultaneously.

To assess the functionality of both chimeric receptors encoded in one construct, 1E5 CAR and CCR co-expressing T cells were co-cultured with 2E4 Mel526 cells and either 1E5 CD20-positive JeKo-1, CD20-negative JeKo-1 (Cap. 3.1.2) or without any potential CCR activator. Mock as well as conventionally generated CCR- and CAR-positive T cells (Cap. 3.4.3) using the lentiviral constructs CD20_6 with an IgG1 spacer and 4-1BB_4-1BB endodomains as well as CSPG4_2 served as control. After 24 h the TNF-α release was measured in the supernatant (Cap. 2.5.3) showing that the implementation of cMyc tags N-terminally to anti-CSPG4 CAR scFv as well as spacer exchange in the CCR had no effect on functionality or on boosting potential (Fig. 44A). While CSPG4-directed CAR T cells released 1120.8 ± 90.7 pg/ml TNF-α in the presence of JeKo-1 only 384.1 ± 88.6 pg/ml were released in the absence of JeKo-1. Interestingly, the release also increased to 1207.6 ± 165.1 pg/ml when co-culturing anti-CSPG4 CAR T cells with CD20-negative JeKo-1 cells. T cells modified with LV-DC_1, however, showed a > 5 fold increase in the TNF-α release compared to the anti-CSPG4 CAR control which only occurred when JeKo-1 cells were present. Co-culturing this effector cells with CD20-negative JeKo-1 cells led to the release of 474.1 ± 212.1 pg/ml TNF-α, a factor of at least 14 lower. Similar results were observed for T cells modified with the two independent constructs CD20_6 and CSPG4_2. Mock and cell line controls including JeKo-1, JeKo-1 CD20 ko and Mel526 did not release TNF-α. Analyzing the release of IFN-γ and IL-2 further confirmed those findings (Fig. 44B). Thus, the CSPG4-directed CAR was functional, however, its immune response was boosted only when the CD20 specific CCR was activated.
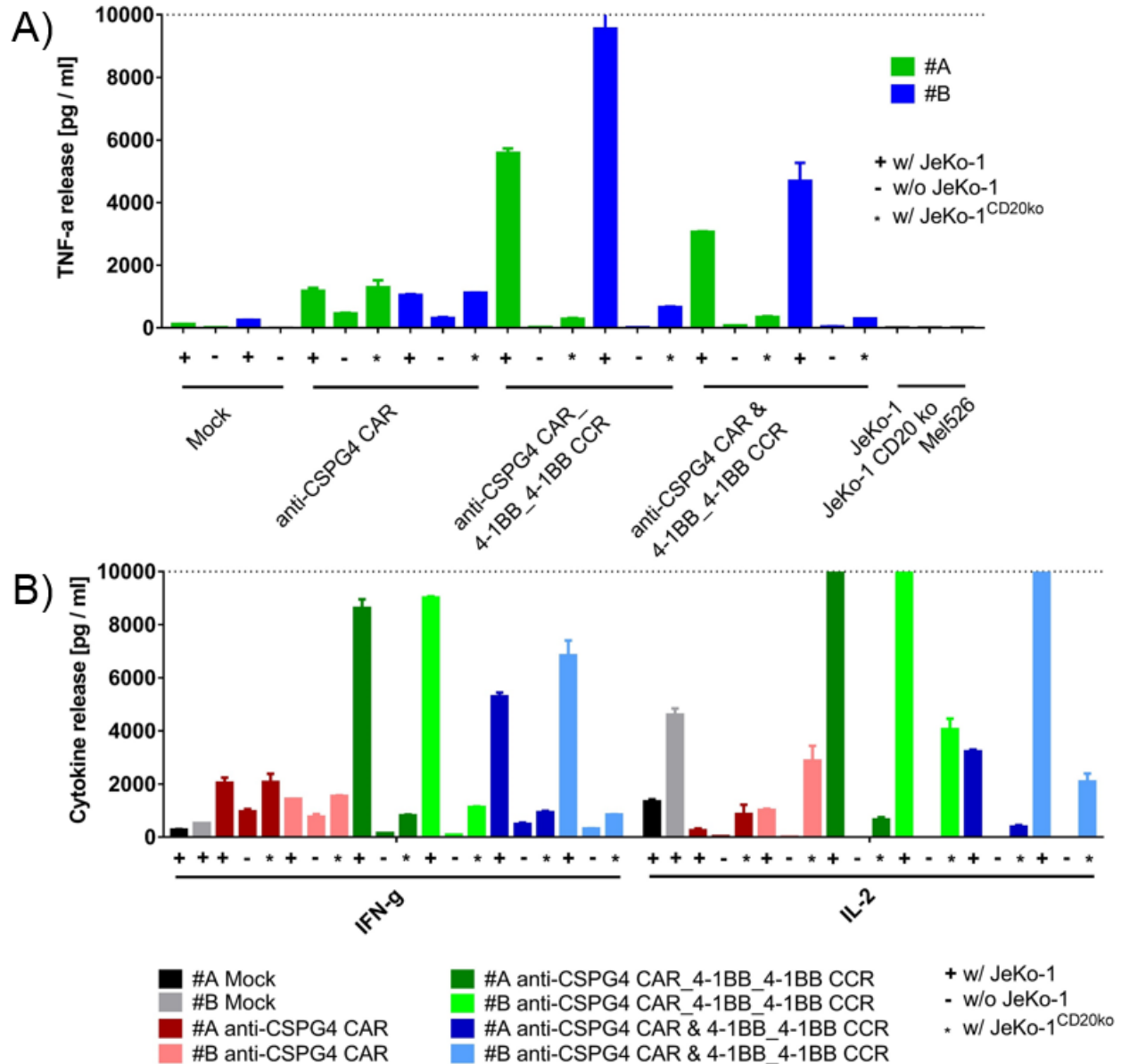
Fig. 44 **T cells engineered with a polycistronic lentiviral construct encoding an anti-CD20 CCR and a CSPG4-directed CAR induce a boosted immune response only when both targets were present.** Mel526 cells were co-cultured with Mock, anti-CSPG4 CAR controls or CCR/CAR-positive T cells in the presence of either CD20-positive or CD20-negative JeKo-1 cells or without any JeKo-1 cells. After 24 h (A) TNF-α, (B) IFN-γ and IL-2 were measured confirming the functionality of both chimeric receptors; the CCR with a shorter CD8 spacer instead of the long IgG1 spacer and the CAR with implemented cMyc tags. Hence, an increased release of proinflammatory cytokines was only detectable when both CCR as wells as CAR were activated. #A and #B represent different donors.

Finally, the killing effiency of DC_1 modified T cells (Cap. 2.4.1) was assessed. For this purpose, 2E4 CD20-positve Mel526$^{FFluc\_eGFP}$ were co-cultured with 2.5E4 CAR/CCR co-expressing T cells for 72h using an IncuCyte device (Cap. 2.5.4) (Fig. 45). Mock as well as anti-CSPG4 CAR T cells served as control. During the first 24 h the GFP-positive target cells showed comparable growth kinetics, independent of the co-cultured effector cells. Afterwards, however, only T cells expressing both CAR and CCR were able to efficiently eradicate Mel526 cells and thus outperformed anti-CSPG4 CAR T cells. Nevertheless, tumor cell growth kinetic decelerated in the presence of CSPG4-directed CAR T cells compared to Mock and thus further confirmed the previously determined moderate potency of this CAR.
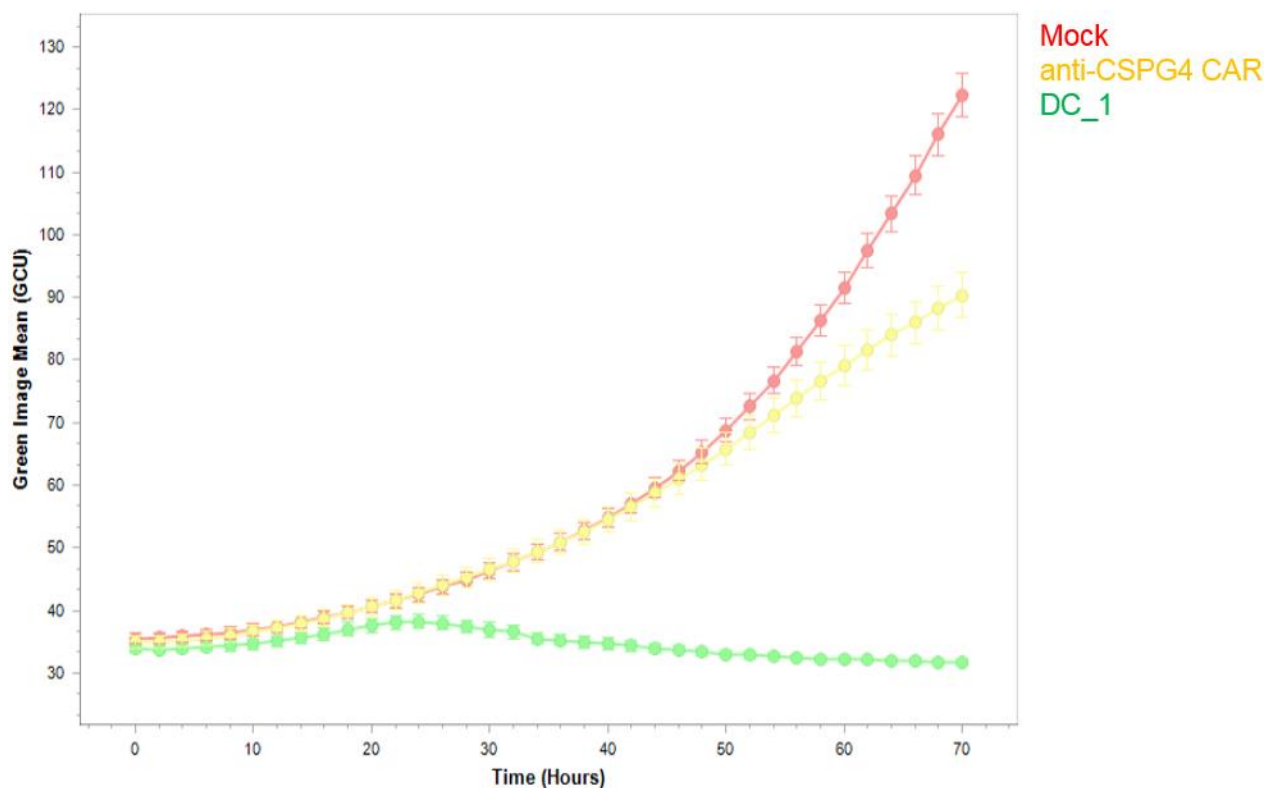
Fig. 45 **T cells expressing both chimeric receptors CAR and CCR outperformed T cells without any additional co-stimulatory ligands in killing assays.** CD20-positive Mel526 cells were co-cultured with either Mock, anti-CSPG4 expressing CAR T cells or CAR/CCR-positive T cells at an E:T ratio of 1.25 : 1 for 72h. Killing efficiency was measured using an IncuCyte device revealing a superior lysis of target cells by T cells equipped with an anti-CSPG4 CAR and a CD20-directed CCR compared to T cells bearing only the CAR. Mock cells did not show any anti-tumorigenic potential. (Tested in duplicates; n=1)

4   Discussion

Genetically engineered T cells not only represent a promising tool for the treatment of patients with cancer or infectious diseases but also a great challenge for scientists and physicians. Thus, especially the CD19-directed CAR manifested a "paradigm" for the treatment of B cell malignancies [106]. Its clinical success, however, cannot be generalized. Accordingly, there is still a high demand on technologies with the potential to improve the safety of CAR-based therapies to prevent potential severe side effects. Furthermore, the effectiveness of CARs, for instance, in a solid cancer setting has yet to be validated [107] and it is likely that novel strategies and therapies are required to ameliorate T cell function in such settings. In addition, a cost-effective and efficient manufacturing process as well as technologies are of utmost importance to further promote the emerging field of ACT [108].

4.1   Establishment of preclinical protocols, tools and technologies

More and more pharmaceutical and biotechnology companies are growing in the field of ACT and the "race to the finish line" as Carl June recently published [109] is in full swing. Although all must fulfil the same preclinical requirements for their living drugs, cost-effectiveness and pace are of utmost importance for the entire product development and production process. Accordingly, a continuous development of tools, protocols and cell lines is not only advantageous to evaluate the potential of different CAR formats but also required to assess novel CAR technologies.

In this study, a highly efficient, cheap and universally usable molecular biological platform was established allowing to generate lentiviral constructs with reduced workload compared to conventional technologies. The used Type IIS enzyme enabled cloning

without implementation of cloning sites that might encode matrix metalloproteinase recognition sites leading to a post-translational protein degradation [110, 111].

Since nearly 50 years, the Chromium release assay has been widely used, especially to determine the cytotoxicity of T cells *in vitro* and can still be designated as "gold standard" [112, 113]. However, due to nuclear radiation of ^{51}Cr, the laborious radioactivity measurement, the time-consuming target cell labeling time and the low signal-to-noise ratio the flow-based as well as bioluminescence-based cytotoxicity assay established in this work offer several advantages [114]. Thus, labeled target cells cannot only be distinguished from effector cells but also PI, 7-AAD or Annexin V could be used to further differentiate between living and dying cells applying flow cytometric analysis [113]. Due to the intracellular ATP-dependent luciferase reaction [115] the bioluminescence assay was highly specific and robust compared to the Chromium release assay where membrane-associated Chromium [116] might underrate the actual cytotoxic potential of CAR T cells. By transducing different target cell lines with a lentiviral construct encoding FFluc in combination with GFP, different killing assays including flow-based, bioluminescence-based as well as IncuCyte-based were established enabling to perform highly sensitive and high-throughput analysis of cytotoxicity without any additional labeling steps. In addition, the generated JeKo-1 knockout clones (Fig. 12) also represent an additional valuable tool enabling a comprehensive evaluation of CAR engineered T cells not only regarding functionality but also specificity. Especially in the context of the development and testing of novel CAR technologies including AND or NOT logic gates those JeKo-1 clones were the basis of several *in vitro* and *in vivo* experiments. The established knockout system for both CD19 and CD20 could be further used for the modification of additional cell lines expanding the available tool box for additional CAR T cell evaluations.

Concerns regarding the validity by using genetically modified target cells in preclinical studies to assess the cytolytic potential of effector cells are legitimate, however, pose no problem particularly for the pursued short-term *in vitro* assays. The suitability to use this transgenic cell lines *in vivo* was furthermore proved in this study. Thus, a JeKo-1- as well as a Raji-derived lymphoma xenograft model was successfully established which was verified by IVIS, weight loss and an autopsy revealing a massive expansion of tumorigenic cells in combination with an observed splenomegaly [117] (Fig. 15 and Fig. 16).

To reduce the discrepancy between preclinical data and clinical outcome [118-120], extended systemic approaches are required, however, was beyond the scope of this thesis. Overall, this work laid the foundations for a profound preclinical evaluation of CAR T cells *in vitro* as well as *in vivo*.

4.2   Anti-CD20 CAR development and testing

Anti-CD19 CAR expressing T cells have demonstrated a remarkable clinical success in several clinical trials including ALL [26, 27, 29], CLL [30, 31] and non-Hodgkin lymphoma [28]. Maude *et al.* [54] recently reported complete remissions in 27 out of 30 (90%) patients with relapsed and refractory ALL for up to two years after treating them with CD19-directed autologous T cells. Nevertheless, some patients relapsed during the CAR T cell therapy due to the deficient CD19 expression which was observed in 60% of this patients [55]. Such a loss is generally associated with disease relapse for the patients [57]. An explanation for losing this surface protein was provided by Sotillo *et al.* [56]. They confirmed that combinatorial molecular biological mechanisms including frameshifts and missense mutations as well as alternative splicing of CD19 led at best to the expression of N-terminally truncated CD19 isoforms which the CAR does not recognize anymore.

CD20 as therapeutic target, however, gains more and more attention. First, CD20 is not only expressed on a majority of malignant B cells [44, 121, 122] but also on a minor subset of cancer-initiating melanoma cells [60, 61]. Secondly, in contrast to CD19, CD20 is not reported to become generally internalized upon antibody binding [44, 58, 59]. The expression level of CD20 in B cell malignancies is strongly dependent on type and differentiation status of the lymphocytic B cells with relatively low expression in patients suffering from CLL or ALL but comparatively high expression in patients with DLBCL as well as HCL [121-124]. In summary, CD20 represents an important target which defines the basis for the CAR development described in this thesis.

Based on a gamma-retroviral construct which was kindly provided by H. Abken (ZMMK Cologne), in this work, a lentiviral anti-CD20 CAR encoding vector was generated

enabling genetic modifications of T cells under state-of-the-art conditions. For safety reasons, the lentiviral pRRL used contained a chimeric RSV-HIV 5´ LTR as well as 3´ LTR with SIN modification which allowed to produce replication-deficient SIN vectors at high titers [102, 103, 125]. In addition to a higher cargo-capacity and the ability to also transduce non-dividing cells, lentiviral vectors have not been associated with an increased risk of target cell malignant transformation. In contrast retroviruses have been reported to show biased genome integration towards proto-oncogenic or tumor suppressive genetic loci [126-129]. While retroviral transductions require higher technical efforts including spin transduction protocols and cationic polymer-pretreated culture plates [130, 131], lentiviral modification of T cells does not necessitate these steps which represent also a considerable advantage towards automating the manufacturing process.

In this thesis, all viral particles were pseudotyped with vesicular stomatitis virus glycoprotein (VSV-G) due to the following advantages: I) extensive tropism with the low density lipoprotein receptor (LDLR) as entry port, II) high transduction efficiencies and III) the possibility to concentrate viral particles due to an outstanding stability [132-134]. A very promising alternative to VSV-G pseudotyping, however, would be the use of measles virus (MV)-derived glycoproteins H and F changing the tropism specific for CD46 and signaling lymphocyte-activation molecule (SLAM). Thus, a cell cycle independent transduction would be possible as demonstrated by Frecha *et al.* [135] allowing to transduce even resting T cells which is not possible with the VSG-G pseudotyped lentiviral vector due to missing expression of LDLR on unstimulated lymphocytes [136]. Linking an scFv to the H protein might modify MV tropism, potentially enabling specific lymphocyte subset transduction. Such an approach can contribute to systemic *in vivo* gene therapy strategies with the potential to change the perspective of cellular therapies [137-139]. However, hurdles like low titer production need to be overcome.

The generated anti-CD20 CAR encoding lentiviral construct CD20_1 contained the original retroviral CAR nucleotide sequence to initially test the protocols for the generation of lentiviral particles, establishing assays and protocols to assess the cytolytic potential of CD20-directed CAR T cells and to finally compare the potential of retrovirally and lentivirally modified T cells. Accordingly, a three plasmid system (Fig. 18) was used to produce lentiviral particles [140]. Viral titer was determined by transducing Jurkat cells

revealing a titer of 1.1E9 LV-particles/ml. Although some labs prefer non-functional titration methods including real-time qPCR or ELISA protocols [141, 142] to measure their titer, in this work, the transgene expression following a limiting dilution was analyzed by flow cytometry allowing to quantify functional vectors. Consequently, in contrast to non-functional methods, more predictable and precise titers could be determined [143] which allowed virus-batch independent comparisons of transduced, CAR engineered T cells.

In a next step, the cell-mediated cytotoxicity of LV-CD20_1 modified T cells was analyzed using co-culture assays with autologous B cells as targets to measure both target cell lysis as well as effector cell function. The cytokine release assay confirmed that only CD20-directed CAR T cells, in contrast to untransduced Mock T cells, induced the release of proinflammatory cytokines including IFN-γ, IL-2 and TNF-α (Fig. 23). In addition to the applied degranulation assay, a flow based killing assay further confirmed anti-target reactivity (Fig. 22). Overall, it could not only be shown that high titers of lentiviral particles could be produced but also the functionality of the originally transferred anti-CD20 CAR was verified. Interestingly, lentivirally modified T cells did not significantly differ from retrovirally transduced T cells regarding CD4/CD8 ratio or CAR expression (Fig. 21). Nonetheless, the latter induced T cells to release significantly higher amounts of cytokines upon encountering their target and in addition killed better at the highest E:T ratio with 10:1 (Fig. 23B) which was rather unexpected. At E:T ratios lower 5:1, however, the observed differences disappear and even changed at the lowest E:T ratio of 1:1 to a higher cytotoxicity of lentivirally engineered T cells for two out of three donors tested. As this comparison of differently transduced T cells was not only aiming to assess the functionality but as well considered the laborious production of retroviral particles, the expensive RetroNectin-assisted spin transduction and the high risk of insertional oncogenesis by using retroviral particles, especially with regard to an automated manufacturing process for engineered T cells and their subsequent use in the clinic, the advantages for lentivirally engineered T cells are obvious. Not least, the suitability of the used protocols and functionality assays to analyze the potential of gene modified T cells was used for the following experiments.

4.3   Anti-CD20 CAR construct optimizations

Essential characteristics of a CAR include intracellular T cell derived activation domains as well as a spacer linked antigen binding domain [106]. The latter is predominantly a scFv which comprises a heavy and a light chain, connected by a short linker. Ideally, this binding moiety is derived from a clinically approved or even tumor specific antibody to preferably prevent off-target toxicity as for instance reported by Morgen *et al.* [41].

CD20_1 originally encoded a murine Leu-16 scFv in a vh/vl orientation as published by Müller *et al.* [144] and used by Schmidt *et al.* [61]. Nevertheless, Till *et al.* [44] assessed both safety and potential of a first generation CAR with a Leu-16 scFv in a vl/vh orientation in a proof-of-concept clinical trial (ClinicalTrials.gov Identifier NCT00012207) for the treatment of patients with relapsed or refractory NHL or MCL. Even though they observed only modest clinical efficacy, Till *et al.* showed the safety of their anti-CD20 CAR T cells and thus defined an important basis for this work. Consequently, the scFv was adapted to CD20_2. The construct was further refined by deleting non-assignable sequences including a *Not* I site encoding a potential matrix metalloproteinase recognition site 3´ prime of the scFv and several mutations throughout the anti-CD20 CAR encoding sequence. Furthermore, the murine kappa chain leader sequence was replaced against a human CD8 leader sequence. Accordingly, the Leu-16 scFv was the only non-human element and therefore is still potentially immunogenic [145]. To prevent HAMA responses limiting T cell persistency as well as anaphylactic reactions after repeated injections in the patient the use of an entirely humanized CAR would be advantageous [146, 147] but was not available.

While CD20_2 was still driven by the internal human PGK promoter, in the further modified version CD20_3 an EF-1α promoter was used instead. However, both PGK as well as EF-1α induced stable transgenic expression in T cells that was slightly higher in the latter case as demonstrated by Milone *et al.* [148, 149]. Given the fact that neither PGK nor EF-1α was hampering the production of lentiviral particles due to promoter competition as described by Schambach *et al.* [125] and confirmed in this work (data not shown), both promoters were suited to drive the CAR sequence transcription. Nevertheless,

considering the circumstance that the clinical approved anti-CD19 CAR was also driven by the EF-1α promoter [149], this promoter was selected for this study as well.

Comparing the different constructs in T cells revealed that all of them were functional, however, the revised versions with the human CD8 leader sequence, reversed scFv orientation and eliminated cloning sites showed a higher cytolytic potential than the initially generated construct CD20_1 (Fig. 24). Furthermore, it could be shown that the EF-1α promoter driven construct lysed more JeKo-1 cells (mean 56.7 ± 19.5%) than the pendant with the PGK promoter (mean 43.8 ± 11.4%). Consequently, these findings confirmed not only the decision for EF-1α but also the need to amend the primary construct. In a next step, thus, the extracellular domains including spacer as well as scFv were further modified leading to the lentiviral constructs CD20_4 and CD20_5. Both encoded a human CD8 spacer instead of the IgG1-derived spacer and in addition the scFv orientation in CD20_5 was changed back to vh/vl.

The important role of the spacer domain in a CAR context has been demonstrated in many publications revealing that several aspects are crucial for an optimal CAR T cell functionality. Defined spatial biological circumstances between T cell and target cell have to be considered and interactions empirically adjusted by varying the extracellular spacer length as shown by Hudecek *et al.* [39]. Nevertheless, in addition, the distance between CAR T cell and target cell is decisive as well, enabling the formation of the immunological synapse and thus excluding, for instance, CD45 or CD148, phosphatases with large ectodomains (> 15 nm) [150]. An ideal point of reference is defined by the fixed distance of T cell receptor and major histocompatibility complex (MHC)-peptide complex of approximately 13 – 15 nm [150, 151]. In accordance with this hypothesis, CAR T cells targeting membrane-proximal antigens are more susceptible to exploit their full cytolytic potential compared to those targeting membrane-distal targets [150, 152, 153].

Hudecek *et al.* [39] furthermore proved the discrepancy between *in vitro* and *in vivo* testing of CAR T cells and thus, in accordance with others, confirmed that FcγR binding to the spacer is associated with AICD and therefore CAR T cells neither persist nor induce a tumor regression *in vivo* [39, 40, 154, 155]. Consequently, an IgG1 spacer featured with a PELLGG➜PPVAG and ISR➜IAR mutation was used in this study replacing FcγR

binding sites against the corresponding sequence derived from IgG2 [40, 156, 157]. While all CAR T cells equipped with those spacers showed a high cytolytic potential *in vitro*, it was rather unexpected that the same T cells did not show any anti-tumor reactivity in xenograft models (Fig. 25). Indeed, Hombach *et al.* [40] verified that their IgG1 mutations do not interact with FcγR expressed on monocytes or NK cells, however, they only focused on FcγRI (CD64), a high-affinity IgG1 binder in humans (K_A approximately 6.5E7 M^{-1}), as well as FcγRII (CD32), a low affinity IgG1 binding family member (K_A approximately 2E5 M^{-1}) [158], in their *in vitro* experiments and thus not considering alternative FcγRs that may bind to the spacer *in vivo*. A 4/2 NQ modified IgG4 spacer which demonstrated both functionality and persistency in xenograft experiments [39] represented a promising alternative and was accordingly used for the CAR library, established in this study.

In summary, not only the spatial distance but also antigen location and FcγR binding are factors that greatly influence the potential of CAR T cells; accurate clinical predictions, though, are not possible at present and thus empirical studies including *in vitro* and *in vivo* testing are still of utmost importance [39].

It could also be shown that the CD20-directed CAR constructs CD20_4 (data not shown) and CD20_5 efficiently lysed tumorigenic cells and rapidly controlled tumor outgrowth (Fig. 25). The fact that the scFv orientation vh/vl demonstrated to a slightly better tumor killing than vl/vh (data not shown) led to the decision to use the first mentioned for two different clinical trials. Nonetheless, due to the clinically unproven scFv orientation, off-target toxicity has to be addressed carefully in this trials in order to make a final safety statement of this anti-CD20 CAR.

Overall, an anti-CD20 CAR was developed in the course of this work which demonstrated potent anti-tumor reactivity *in vitro* as well as *in vivo*.

4.4 Facilitating the manufacture of CAR T cells through automation

The dissemination of CAR T cell therapies to a wider number of patients is still hampered by the complexity of the manufacturing process requiring both extensively trained operators as well as a dedicated infrastructure [66]. Moreover, the multistep procedure leaves a wide room for errors that might be associated with fatal consequences during the clinical treatment. Hence, the development in this work, of a cGMP-compliant, fully-closed and automated TCT Process on the CliniMACS Prodigy platform for the generation of engineered T cells was evaluated. The possibility to use this device for the manufacturing of CAR T cells at clinical scale was recently demonstrated by collaborators Mock *et al.* and Priesner *et al.* [70, 71]. Starting from leukapheresis from healthy donors, T cells were isolated, activated, transduced, enriched and finally formulated. Not considering minor differences regarding selection, cytokine support or lentiviral vector used for the transduction, Mock *et al.* [70] as well as Priesner *et al.* [71] successfully expanded gene-modified lymphocytes (5.4 – 28.4 fold; 28 – 42 fold, respectively). Functionality was further addressed by Mock *et al.* [70] verifying the cytolytic potential of CD19-directed CAR T cells *in vitro* as well as *in vivo*. With this work, several additional aspects were addressed to answer the following questions: I) Is it possible to expand engineered T cells starting from heavily pre-treated PM? II) Can cryopreserved starting material be used? III) Is it possible to develop a robust automated manufacturing process despite the use of different devices on different days controlled by varying operators?

Analyzing expansion, cellular composition, phenotypical characteristics as well as functional response (cytolytic potential and cytokine secretion) of either HD- or PM-derived starting material not only confirmed robustness and reproducibility of the TCT Process but also showed that differences regarding the cellular composition of the incoming product did not negatively influence quality of the manufactured clinical product and that therapeutic doses could be obtained in all cases. Expansion rates were comparable and varied from 43 ± 14 fold for HD and from 65 ± 36 fold for PM (Fig. 27G). In addition, despite high variances regarding the cellular composition of the incoming

product, after twelve days under the established culture conditions favoring a T cell outgrowth, the frequency of T cells was nearly identical with 91.3 ± 5.0% for HD and 88.3 ± 7.1% for PM (Fig. 28B). The remaining autologous NKT cells (5.1 ± 2.2% for HD and 8.0 ± 4.3% for PM), initially designated as `contaminating´ cells (Cap. 3.3.2), might represent an additional clinical relevant source of cells for ACT [159]. For instance, they have an inherent potential to kill tumors expressing CD1d [160-163]. Consequently, autologous NKT cells, even though engineered to express a CAR, most likely do not pose a health risk by injecting them back into the patient and could potentially be advantageous. However, conclusive evidence is still missing and has to be delivered on the role of gene-modified NKT cells.

Albeit the viability of cryopreserved and fresh cells slightly differed during the cultivation process, in total no significant differences were observed among HD- and PM-derived samples in the final product (90.4 ± 4.3% for HD; 88.4 ± 7.4% for PM; Fig. 27F). As a result, either LP, BC or WB, cryopreserved as well as fresh, were qualified as starting material for the TCT Process. Interestingly, the procedure allowed to get therapeutic doses from limited starting patient material (starting with a fifth of the 1E8 enriched cells generally used) (Tab. 9). However, limits of the system using lowest and highest starting cell numbers and cells from different stages of patient treatments for various indications must be further tested to enable optimal recommendations and meet the reality of clinical diversity.

While Mock *et al.* [70] cultured their T cells in TexMACS supplemented with human recombinant IL-2, Priesner *et al.* [71] as well as this study used human recombinant IL-7 and IL-15 supplemented medium. Cieri *et al.* [75] recently reported about the correlation of cytokines used for the T cell culture with specific functional features of the generated T cell subset. Indeed, they report that the combination of IL-7 and IL-15 led to the generation of T_{SCM} that, due to their inherent stemness-associated potential to self-renewal and ability to differentiate into potent effector T cells, represent a clinically relevant "weapon in adoptive T cell therapy against cancer". Moreover, they demonstrated that in addition to CD3/CD28 stimulation IL-7 is required for the differentiation and maintenance of T_{SCM} while IL-15 or, with a reduced extend, IL-2 are suitable and required to induce expansion of particularly T_{SCM}. Interestingly, comparing the phenotypical characteristics

of HD- and PM-derived final products revealed significant differences in this work. Despite using identical culture conditions, T_{SCM} were underrepresented in the PM runs with 8.9% compared to 45.0% for HD runs (Fig. 28D). A marked difference between HD and PM was the strongly reduced presence of T_N in the starting material of PM. Although not proven by this work, presence of T_N in the starting material seems to be essential in order to obtain T_{SCM} in the final product on day twelve. PM came from heavily pre-treated patients having undergone several rounds of chemotherapy that can explain a different cellular composition and reduced T_N compared to HD. If T_{SCM} turn out to be the most effective T cell carrier for clinical effectiveness, it may become essential to use starting material from PM prior to heavy pre-treatments and possibly move T cell therapy up in the line of treatment (before chemotherapy). On the other hand, Robbins *et al.* [164] proved in their studies for the treatment of metastatic melanoma that the persistence of transferred cells correlates with the therapeutic efficacy. In line with these findings, Wang *et al.* [77] investigated the engraftment potential of defined T cell subsets and their long-term anti-tumor activity in a mouse model and figured out that T_{CM}-derived effector cells outperform T_{EM}-derived effector cells. Those results were in accordance with Berger *et al.* [76] who showed in macaques that only T_{CM} persisted long-term, preserved a memory T cell pool and therefore maintained T cell immunity. Since the cumulative frequency of memory T cells in expanded products of HD and PM were comparable in this study (45.0% T_{SCM} and 34.0% T_{CM} for HD; 8.9% T_{SCM} and 64.7% T_{CM} for PM) (Fig. 28D) it is possible to assume that CAR T cells generated from patient material will be clinically effective. The proof will be obtained during clinical applications of the results of this work in the coming years.

A further difference in the manufacturing protocol between Priesner *et al.* [71] and this work was the isolation of CD62L-positive cells in contrast to CD4/CD8 selection. Thus, Priesner and his colleagues achieved frequencies > 95% CD62L-positive cells comprising mainly T_N (>75%) and smaller populations of T_{CM}. However, due to the following three reasons CD62L enrichment was not considered in the present study: I) this marker gets downregulated upon cryopreservation [71] and thus would hamper the initial selection step. II) CD62L is widely expressed on hematopoetic cells including monocytes, NK cells, granulocytes and B cells [165-168] and especially the co-enrichment of monocytes is

associated with a reduced transduction efficiency and an impaired expansion of T cells as reported by Stroncek *et al.* [169] in accordance with own findings (data not shown). III) The selection of CD62L-positive malignant B cells, their subsequent genetic modification during the transduction and the even low possibility to reinfuse those cells back into the patient would be an undeniable safety risk for ACT.

Finally, the cytolytic potential of automatically manufactured CAR T cells was assessed and compared *in vitro* revealing that both HD- and PM-derived effector cells efficiently lysed CD20-positive target cells (Fig. 29C & D). Thus, at an E:T ratio of 1:1 the mean killing frequency for HD was 44.2 ± 19.3% and only slightly higher than the frequency of PM with 39.3 ± 21.3% but not significantly different. Although the generated CAR T cells showed cytotoxic function *in vitro,* their full function was better demonstrated *in vivo* using a challenging model of a seven day established lymphoma xenograft model, demonstrating that only CD20-directed CAR T cells, not Mock T cells, were able to control tumor outgrowth (Fig. 30). Even though similar results are expected for PM-derived engineered T cells, the experimental proof is still missing and has to be assessed.

Alternatives for the production of engineered T cells were, *inter alia*, published by Ramanayake *et al.*, Tumaini *et al.* or Lu *et al.* [67-69]. In contrast to the last two publications, Ramanayake *et al.* used gas-permeable G-Rex10 flasks (Wilson Wolf Manufacturing) to expand piggyBac pre-transfected T cells that were either stimulated with irradiated PBMC or NALM-6 cells. After 23 days, their protocol yielded in up to 765 fold expansion for HD-derived samples (72% median CAR expression) and 180 fold expansion when PM (81% median CAR expression) was used as starting material. Tumaini *et al.* as well as Lu *et al.* transduced and expanded their T cells in PermaLife bags (OriGen Biomedical). Within eleven days, Tumaini and colleagues achieved a 10.6 fold expansion with a viability of 70.4% and a frequency of 68.4% CAR-positive T cells. With the protocol defined by Lu *et al.* expansion rates ranging from 4.5 – 16 fold were attained within six days (viability was not determined; transduction efficiency: 43.6 ± 8.3%). Even though all protocols provided a possibility for the manufacturing of engineered T cells, there are several disadvantages compared to the CliniMACS Prodigy based TCT Process. Especially multiple open handling steps that were required, for instance, for sample preparations, transfection or RetroNectin-coating and subsequent washing of their

expansion bags greatly increase the risks of contaminations. In addition, not enriching T cells in the beginning of the process also increases the probability to genetically modify malignant B cells and to subsequently administer those cells back into the patient. Finally, the biodegradable MACS GMP T Cell TransAct for the polyclonal T cell activation was used instead of anti-CD3/anti-CD28 Dynabeads (Invitrogen). Accordingly, a bead-removal step was not required in the TCT Process.

Last but not least, there are regulatory requirements for the clinical manufacture of ATMPs that are requesting class A/B (GMP EU) cleanrooms (2003/94/EC of 8 October 2003) to "minimize the risk of error and to permit effective cleaning and maintenance in order to avoid contamination, cross contamination and, in general, any adverse effect on the quality of the product". Those cleanrooms are a significant investment on basis of the infrastructure required, while one CliniMACS Prodigy device is not only space-saving but also represents a closed entity meeting relevant standards [66]. Overall, although alternative protocols for the manufacturing of engineered T cells using semi-closed systems were successfully applied [67-69], the fully-closed TCT process offers many benefits including a lower contamination risk, high robustness and in addition an improved cost efficiency especially regarding facility and personal expenses.

In conclusion, this study proved that the TCT Process yields, independent of operator or device, a clinically relevant dose of potent engineered T cells. Furthermore, it was demonstrated that a large variety of starting cell products can be used. Consequently, the fully-closed, automated cGMP-compliant process is suited to manufacture gene-modified T cells under state-of-the-art conditions and thus might promote a further distribution of CAR-based and/or other individualized therapies towards patients benefits. Although this work on automation defines a huge step in this direction, further work is required to develop additional technological advances to allow the manufacturing of patient specific cell therapies as simple as an off-the-shelf drug.

4.5   Boosting CAR T cell responses

Recently, Zhao *et al.* [50] designated CD19-directed CAR T cells as "poster child for CAR therapies" as complete remission rates > 88% have been repeatedly reported using this artificial receptor [52-54]. However, headlines in the context of solid tumor treatment using CAR T cells are less promising. Notwithstanding the toxicity originating from CAR T cells especially in those settings, the clinical responses are sobering. The best data reported so far was generated in a clinical trial with a GD2-directed CAR for the treatment of neuroblastoma (ClinicalTrials.gov Identifier NCT00085930) in which 3 out of 11 patients achieved complete remission [170].

Reasons for the limited success of CAR engineered T cells for the treatment of solid tumors are not fully understood yet, but surely associated with tumor-associated histopathological features which impedes tumor infiltration and creates a highly immunosuppressive tumor-microenvironment including intrinsic factors such as hypoxia, low pH or nutritional depletion [78, 81, 171] as well as mechanisms preventing T cell activation or maintenance of an activated status. The tumor-induced recruitment of immune suppressor cells such as T_{reg}, MDSC or immature dendritic cells and the upregulated expression of inhibitory receptors are further aggravating factors [49, 79].

Approaches that support a strong activation of T cells by for instance suppressing the breaks of the immune response (e.g. anti-PD-1, anti-CTLA-4 blockade) have shown that T cells can overcome such hurdles and deliver anti-tumor responses even in settings of established solid tumors [16-18]. Melero *et al.* [88, 89] also demonstrated that an artificial co-stimulation led to an increased T cell immunity circumventing the challenges that are associated with the inhospitable tumor-microenvironment. Thus, they not only demonstrated that 4-1BB-directed monoclonal agonist antibodies can be systemically administered which induced a strong T cell-mediated anti-tumor immunity but they also showed that engineered P815 tumor cells expressing 4-1BBL (CD137L) strongly increased the potential of tumor-reactive T cells. Even though their findings confirmed the possibility to boost the T cell immunity, both technologies are associated with risks as well

as limitations including, amongst others, a non-specific T cell activation and poor clinical success [172-174].

Nevertheless, inspired by these findings, Stephan *et al.* [90] proved that genetically engineered T cells expressing CD80 and 4-1BBL can provide both auto-co-stimulation as well as trans-co-stimulation and thus strengthens T cell immunity *in vitro* as well as *in vivo*. They compared additional combinations of co-stimulatory ligands including OX40L, CD70 or CD30L and demonstrated that CD80 and 4-1BBL led to the highest T cell boost. The T cell associated cis- as well as trans-stimulation has two decisive advantages compared to the technologies mentioned above: I) the T cell boost is locally restricted and thus does not compromise safety by a general T cell activation. II) Tumor engineering is not required for the approach to be highly effective.

It was a striking finding that CAR T cells that additionally express a 4-1BBL outperformed CAR T cells without any extra stimulation *in vivo* [50]. This approach demonstrated the importance of constitutively expressed co-stimulatory ligands as tools to ameliorate the CAR T cell immunity. The present work, however, used CCRs based on a modular design instead of naturally occurring ligands to induce a T cell boost and thus additionally addressed specificity and adjustability. Based on a melanoma setting with CSPG4-directed CAR T cells and a CCR specific for CD20 first proof-of-principle experiments were conducted. One advantage was that appropriate scFvs used in CAR formats were already published, however, potency of those anti-CSPG4 CARs can in the best case only be regarded as moderate [61, 84, 175]. Though, such scFvs were preferred in order to better assess and compare the potential benefit of different CCRs. A 225.28s-derived scFv with a long IgG4 spacer outperformed all other constructs (Fig. 31) in *in vitro* functionality assays (data not shown) and thus was used to evaluate the CCR related boosting concept. CCRs had to be designed in a way that they only enhance an already existing T cell response and were not allowed to induce lysis or T cell proliferation on their own. Initial CCRs comprised different combinations of 4-1BB, CD28 and CD3ε. While 4-1BB and CD28 represent the conventional `signal 2´ for T cell activation, the latter was experimentally chosen particularly with regard to the single immunoreceptor tyrosine-based activation motif (ITAM) [176] and a superior functionality in an alternative setting with genetically engineered T cells (A. Kaiser, Miltenyi Biotec, unpublished data).

Initial *in vitro* experiments revealed the potential of defined CCRs to enhance the CAR T cell immunity in trans. Here we demonstrate, to our knowledge for the first time, that CCRs equipped with either 4-1BB_4-1BB or CD28_4-1BB strongly increase the release of proinflammatory cytokines only upon a simultaneous activation of both CAR and CCR (Fig. 34 and Fig. 35). While for this first experiments autologous B cells were used to activate the CCR in trans, in following experiments CD20-positive JeKo-1 cells were used. This was mainly due to the experimental range requiring high quantities of CD20-positive cells which could not be provided for all donors. Initial concerns with regard to a different co-stimulation potential of cell lines and autologous primary cells were dismissed after demonstrating comparable results in terms of T cell boost function in the cis experiments (Fig. 35). In a next step, the relevance of 4-1BB and CD28 co-stimulation was further investigated especially with regard to signaling domains and resulting boost. For this purpose, additional constructs with other combinations of 4-1BB and CD28 were generated (Fig. 36) and tested in trans as well as in cis. Surprisingly, all novel CCRs enhanced the release of TNF-α with a factor > 50 (Fig. 38). A direct comparison was difficult and due to the varying frequency of CAR and CCR co-expressing T cells (31 – 69%) not possible (Fig. 37B), but also not compulsory since this experiment aimed to exclude candidates for following *in vivo* experiments in which the different formats will be finally assessed. This study not only showed that the implementation of CCRs led to an increased release of cytokines (Fig. 39 & Fig. 40) but also that more tumor cells were eradicated by T cells expressing CAR and CCR compared to CAR T cells without any additional co-stimulation (Fig. 41).

Even though this study proved protocols for the generation of CAR and CCR expressing T cells and furthermore confirmed the functionality of different CCRs *in vitro*, upcoming *in vivo* experiments necessitated further improvements. The IgG1-derived CCR spacer, which was most likely responsible for the loss of functionality of the CD20 CAR *in vivo* (Fig. 25) was deemed suboptimal and had to be exchanged against the CD8 spacer which was already shown to be effective in xenograft models. Furthermore, a polycistronic lentiviral vector encoding for CAR as well as CCR was cloned into a single vector (Fig. 42) which facilitated the complex and labor-intensive generation of this genetically engineered T cells. To confirm the expression of every single element after a transduction

with LV-DC_1, the anti-CSPG4 CAR was further modified with two cMyc tags, implemented 3´ of the scFv sequence. Thus, the CCR was stainable with the PE-labeled CD20 peptide, CAR and ΔLNGFR could be measured using anti-cMyc and anti-ΔLNGFR antibodies, respectively. Discrepancies regarding CAR, CCR and ΔLNGFR measurement (Fig. 43) were rather unexpected since the transgenic expression was based on a single mRNA from a polycistronic DNA element, driven by a single promoter. The challenge of using different labeling reagents with different affinities for their ligand may in part be responsible for the differences in frequencies observed. This is, however, unlikely to explain the extent of the differences and other factors such as steric hindrances or physical CAR/CCR internalization must be considered. Further dedicated studies are required to understand why each of the three proteins were not systematically co-expressed. It will be interesting to study the persistence of T cells infused *in vivo* and their pattern of CAR and CCR expression (for e.g. potential preferential persistence of double positive T cells).

Finally, the functionality of the tri-cistronic LV-DC_1 engineered T cells was shown for cytokine release as well as killing experiments (Fig. 44 and Fig. 45). Accordingly, neither the CCR spacer exchange nor the implementation of cMyc tags negatively influenced functionality of both chimeric receptors. Nevertheless, *in vivo* experiments have to be conducted to evaluate different CCRs and their impact with regard to T cell persistence, anti-tumor efficacy and safety. Schneider *et al.* [177] recently pointed to the narrow ridge between functionality and toxicity of CAR T cells *in vivo*. They demonstrated that T cells co-expressing two highly effective CARs which were supposed to kill Raji cells in a xenograft model, although being very efficacious, were associated with a massive death of mice. The authors thus hypothesized that the large release of proinflammatory cytokines, as already detected *in vitro*, and the subsequent resulting cytokine storm were mainly responsible for the acute toxicity observed in the animal model. Considering the fact that mice, in contrast to human patients, do not receive any complementary therapy including corticosteroids or specific cytokine antagonists as an acute toxicity treatment [178-180] no conclusions regarding the CCRs established during this work should be neglectfully drawn especially with regard to the fact that the combination of CAR and CCR may be safer than the use of two CARs. In addition, it should be noted that Schneider *et*

al. [177] used a leukemia xenograft model with a high tumor burden and consequently induced a systemic toxicity. Locally triggered effects, for instance, by treating solid tumors, though, would most likely be associated with a more moderate cytokine release syndrome in the same animal model. Should it become apparent that CD20-directed CCRs, in combination with a CAR, induce the release of high amounts of proinflammatory cytokines upon a simultaneous activation and thus are toxic, alternative approaches including artificial CCR targets could be an ideal solution. Accordingly, CCR activation could not only be precisely induced but also controlled in terms of intensity. Furthermore, it is expected that an exclusive CCR activation will, due to a strong co-stimulation, ensure survival and persistency of CAR T cells. In this context, findings from Long *et al.* [38] suggest that especially 4-1BB, but not CD28, prevents an early T cell exhaustion and consequently improve persistence. They supported these claims with gene expression profiles of CAR T cells equipped either with 4-1BB or CD28 co-stimulation domains. Thus, the analysis of 4-1BB equipped CARs revealed an upregulation of transcription factors that were, amongst others, associated with memory differentiation (*KLF6*, *JUN* and *JUNB4*) [181] and anti-apoptotic pathways, instead of a stronger expression of inhibitory or exhaustion-regulating factors (*TBX21*, *EOMES*, *Blimp-1* and *IKZF2*, *LAG3*, *TIM-3*, *CTLA4*, *BTLA* and *CD244*) [72, 182-185] as detected for the CD28 counterpart [38]. Even though those CAR findings cannot be directly transposed to CCRs without a CD3ζ stimulation motif that also influences the fate of T cells, other publications are also underlining the importance of 4-1BB signaling in CAR-independent settings [186, 187].

Chmielewski *et al.* [188] refer to the beneficial effects of a locally induced release of proinflammatory cytokines that alter the tumor microenvironment and trigger immune effector cells. For this purpose, Chmielewski and co-workers generated `T cells redirected for universal cytokine killing´ (TRUCKs) and proved that a CAR activation that additionally resulted in a specific release of IL-12 led to an improved tumor eradication. The combination of TRUCKs, the so-called fourth generation of CAR T cells [189] with CCRs may open up increased therapeutic windows [190-192]. The possibility, however, to harness the immune system is what makes CAR T cell therapies so attractive but potentially increasing T cell function will inevitably lead to increased risks of inducing toxicities. A challenge that the field is likely to address in the next years.

Particularly combinations of CARs with low affinity scFvs that spare low level target antigen expression in basal tissues and CCRs as tools to boost their limited anti-tumorigenic potential opens up a wide range of clinical therapies as shown in this work. However, further work is required to assess the potential of CCRs also in combinations with high affinity scFvs which might further increase the scope of this tool.

Overall, next experimental steps will include *in vivo* studies to basically analyze CCR activation kinetics, compare CCRs equipped with different co-stimulatory domains with regard to persistency and potential to boost various CARs and finally widen the potential clinical applications from melanoma to additional tumors including triple negative breast cancer and acute myeloid leukemia.

4.6   Conclusions and outlook

Primary objectives of the work presented here were to design CAR T cells for clinical applications, improve their manufacturing and further development of CAR technologies to potentially improve the treatment outcome. In this respect, the development and manufacturing of CD20-directed CAR T cells was investigated towards the use in two independent clinical trials. Starting from a retroviral vector, a lentiviral anti-CD20 CAR encoding construct was generated, further optimized and thoroughly analyzed in hereby established *in vitro* as well as *in vivo* experiments. In addition, this work proved the robustness of the cGMP-compliant TCT Process and thus demonstrated that potent engineered T cells, independently of starting material, can be automatically manufactured which might facilitate the dissemination of ACT.

In future, the use of fully humanized CARs must be preferred to prevent HAMA responses and anaphylactic reactions (Cap. 4.3). Accordingly, a screening for human scFvs targeting CD20 is currently in the focus of our efforts. The same applies to possibilities to prevent long-term side-effects like B cell aplasia caused by CARs for the treatment of B cell malignancies [193]. In this context, the implementation of clinically approved suicide genes like *Herpes simplex*-derived thymidine kinase (TK) [194] or an artificial inducible caspase 9 [195] would be a first step, however, potential improvements for both systems are required [196, 197]. Thus, particularly combinations of molecular biological approaches and epitope based CAR T cell elimination mechanisms such as RQR8 [198] offer promising opportunities for ACT. Switchable-CAR [199, 200] or Split-CAR [85, 201] approaches represent alternative technologies that address both safety as well as preventing tumor escape. Treatment can be controlled by administration defined concentrations of one or several antibodies.

T cell engineering will additionally be a key aspect of following investigations. In this respect, we want to address both alternative CAR delivery systems and targeted integrations. While most CAR T cells are generated using retroviral and lentiviral vectors, Monjezi *et al.* [202] recently demonstrated the advantages of non-virally modified T cells using a *Sleeping Beauty* system in combination with minicircle encoded CARs. Using

Transposases to modify T cells instead of viral constructs has several advantages including higher cargo-capacity, better safety profile, a superior efficiency as well as an improved cost efficiency [202-204]. Additionally, in this context, further amendments could be realized by combining the *Sleeping Beauty* system or other transposon systems with the CRISPR/Cas9 technology which would not only allow a knock-out of the endogenous T cell receptor which could open the door for allogenic therapies but also enable adjustable CAR expression after a targeted integration of a gene-trap construct that has been shown to improve CAR T cell functionality [205].

The treatment of solid tumors still poses a particular challenge. Hence, the identification of tumor associated antigens and the highly immunosuppressive tumor microenvironment have to be specifically addressed. Even though, this study proved the use of CCRs to potentiate CAR T cell function *in vitro*, subsequent studies have to focus on *in vivo* experiments to, firstly, investigate the functionality of our boosting approach and, secondly, assess and compare the different CCRs as well as their activation kinetics. Finally, the combination of CCRs is conceivable with alternative approaches including transcriptionally controlled CCR expression to specifically induce a boost or enhancing naturally occurring immune effector cells like TILs.

Despite the major clinical achievements and the resulting increased significance of CAR T cells for the treatment of cancer and infectious diseases, a retrospective analysis of scientific and medical reports highlights the challenges that must be addressed to improve CAR designs. Thus, an optimal CAR treatment will avoid tumor escape, will be highly efficacious, includes off-switch possibilities for better control, shows no adverse events and no off-target toxicity in order to be safe. Even though multidisciplinary collaborations are required to meet all demands, translational research has a particular responsibility and is already providing some solutions. Consequently, relapses due to the downregulation of targeted antigens could be virtually prevented by the use of dual-CAR, Tan-CAR or tandem-CAR approaches [55, 177, 206, 207]. Generally, the focus from mono-therapies has to shift towards versatile treatments including not only conventional clinical approaches such as chemotherapy and monoclonal antibodies but also checkpoint-inhibitors, cancer vaccination and other immune effectors like B cells, TILs, NK cells, NKT cells or cytokine-induced killer (CIK) cells.

5   References

1.   Siegel, R.L., Miller, K.D., and Jemal, A., *Cancer Statistics, 2017.* CA Cancer J Clin, 2017. 67(1): p. 7-30.

2.   Kaatsch, P., Spix, C., Katalinic, A., et al., *Krebs in Deutschland 2011/2012.* Robert Koch-Institut, 2015. 10. Ausgabe (ISBN 978-3-89606-228-4).

3.   Palucka, A.K. and Coussens, L.M., *The Basis of Oncoimmunology.* Cell, 2016. 164(6): p. 1233-47.

4.   Plenderleith, I.H., *Treating the treatment: toxicity of cancer chemotherapy.* Can Fam Physician, 1990. 36: p. 1827-30.

5.   Slamon, D.J., Leyland-Jones, B., Shak, S., et al., *Use of chemotherapy plus a monoclonal antibody against HER2 for metastatic breast cancer that overexpresses HER2.* N Engl J Med, 2001. 344(11): p. 783-92.

6.   Van Cutsem, E., Kohne, C.H., Hitre, E., et al., *Cetuximab and chemotherapy as initial treatment for metastatic colorectal cancer.* N Engl J Med, 2009. 360(14): p. 1408-17.

7.   Held, G., Poschel, V., and Pfreundschuh, M., *Rituximab for the treatment of diffuse large B-cell lymphomas.* Expert Rev Anticancer Ther, 2006. 6(8): p. 1175-86.

8.   Plosker, G.L. and Figgitt, D.P., *Rituximab: a review of its use in non-Hodgkin's lymphoma and chronic lymphocytic leukaemia.* Drugs, 2003. 63(8): p. 803-43.

9.   Jagannath, S., Barlogie, B., Berenson, J., et al., *A phase 2 study of two doses of bortezomib in relapsed or refractory myeloma.* Br J Haematol, 2004. 127(2): p. 165-72.

10.   Field-Smith, A., Morgan, G.J., and Davies, F.E., *Bortezomib (Velcadetrade mark) in the Treatment of Multiple Myeloma.* Ther Clin Risk Manag, 2006. 2(3): p. 271-9.

11.   Davies, H., Bignell, G.R., Cox, C., et al., *Mutations of the BRAF gene in human cancer.* Nature, 2002. 417(6892): p. 949-54.

12.   Wheler, J., Yelensky, R., Falchook, G., et al., *Next generation sequencing of exceptional responders with BRAF-mutant melanoma: implications for sensitivity and resistance.* BMC Cancer, 2015. 15: p. 61.

13.   Sosman, J.A., Kim, K.B., Schuchter, L., et al., *Survival in BRAF V600-mutant advanced melanoma treated with vemurafenib.* N Engl J Med, 2012. 366(8): p. 707-14.

14.   Chapman, P.B., Hauschild, A., Robert, C., et al., *Improved survival with vemurafenib in melanoma with BRAF V600E mutation.* N Engl J Med, 2011. 364(26): p. 2507-16.

15.   Couzin-Frankel, J., *Breakthrough of the year 2013. Cancer immunotherapy.* Science, 2013. 342(6165): p. 1432-3.

16.   Weber, J., Thompson, J.A., Hamid, O., et al., *A randomized, double-blind, placebo-controlled, phase II study comparing the tolerability and efficacy of ipilimumab administered with or without prophylactic budesonide in patients with unresectable stage III or IV melanoma.* Clin Cancer Res, 2009. 15(17): p. 5591-8.

17.   Guo, L., Zhang, H., and Chen, B., *Nivolumab as Programmed Death-1 (PD-1) Inhibitor for Targeted Immunotherapy in Tumor.* J Cancer, 2017. 8(3): p. 410-416.

18.   Motzer, R.J., Rini, B.I., McDermott, D.F., et al., *Nivolumab for Metastatic Renal Cell Carcinoma: Results of a Randomized Phase II Trial.* J Clin Oncol, 2015. 33(13): p. 1430-7.

19.   Dudley, M.E., Gross, C.A., Langhan, M.M., et al., *CD8+ enriched "young" tumor infiltrating lymphocytes can mediate regression of metastatic melanoma.* Clin Cancer Res, 2010. 16(24): p. 6122-31.

20.   Rosenberg, S.A., Yannelli, J.R., Yang, J.C., et al., *Treatment of patients with metastatic melanoma with autologous tumor-infiltrating lymphocytes and interleukin 2.* J Natl Cancer Inst, 1994. 86(15): p. 1159-66.

21.   Gross, G., Waks, T., and Eshhar, Z., *Expression of immunoglobulin-T-cell receptor chimeric molecules as functional receptors with antibody-type specificity.* Proc Natl Acad Sci U S A, 1989. 86(24): p. 10024-8.

22.   Barrett, D.M., Grupp, S.A., and June, C.H., *Chimeric Antigen Receptor- and TCR-Modified T Cells Enter Main Street and Wall Street.* J Immunol, 2015. 195(3): p. 755-61.

23.   Eshhar, Z., Waks, T., Gross, G., et al., *Specific activation and targeting of cytotoxic lymphocytes through chimeric single chains consisting of antibody-binding domains and the gamma or zeta subunits of the immunoglobulin and T-cell receptors.* Proc Natl Acad Sci U S A, 1993. 90(2): p. 720-4.

24.   Savoldo, B., Ramos, C.A., Liu, E., et al., *CD28 costimulation improves expansion and persistence of chimeric antigen receptor-modified T cells in lymphoma patients.* J Clin Invest, 2011. 121(5): p. 1822-6.

25.   Kershaw, M.H., Westwood, J.A., Parker, L.L., et al., *A phase I study on adoptive immunotherapy using gene-modified T cells for ovarian cancer.* Clin Cancer Res, 2006. 12(20 Pt 1): p. 6106-15.

26.   Brentjens, R.J., Davila, M.L., Riviere, I., et al., *CD19-targeted T cells rapidly induce molecular remissions in adults with chemotherapy-refractory acute lymphoblastic leukemia.* Sci Transl Med, 2013. 5(177): p. 177ra38.

27.   Grupp, S.A., Kalos, M., Barrett, D., et al., *Chimeric antigen receptor-modified T cells for acute lymphoid leukemia.* N Engl J Med, 2013. 368(16): p. 1509-18.

28.   Kochenderfer, J.N., Dudley, M.E., Kassim, S.H., et al., *Chemotherapy-refractory diffuse large B-cell lymphoma and indolent B-cell malignancies can be effectively treated with autologous T cells expressing an anti-CD19 chimeric antigen receptor.* J Clin Oncol, 2015. 33(6): p. 540-9.

29.   Lee, D.W., Kochenderfer, J.N., Stetler-Stevenson, M., et al., *T cells expressing CD19 chimeric antigen receptors for acute lymphoblastic leukaemia in children and young adults: a phase 1 dose-escalation trial.* Lancet, 2015. 385(9967): p. 517-28.

30.   Porter, D.L., Hwang, W.T., Frey, N.V., et al., *Chimeric antigen receptor T cells persist and induce sustained remissions in relapsed refractory chronic lymphocytic leukemia.* Sci Transl Med, 2015. 7(303): p. 303ra139.

31.   Porter, D.L., Levine, B.L., Kalos, M., et al., *Chimeric antigen receptor-modified T cells in chronic lymphoid leukemia.* N Engl J Med, 2011. 365(8): p. 725-33.

32.   Zhong, X.S., Matsushita, M., Plotkin, J., et al., *Chimeric antigen receptors combining 4-1BB and CD28 signaling domains augment PI3kinase/AKT/Bcl-XL activation and CD8+ T cell-mediated tumor eradication.* Mol Ther, 2010. 18(2): p. 413-20.

33. Hombach, A.A., Chmielewski, M., Rappl, G., et al., *Adoptive immunotherapy with redirected T cells produces CCR7- cells that are trapped in the periphery and benefit from combined CD28-OX40 costimulation.* Hum Gene Ther, 2013. 24(3): p. 259-69.

34. Tang, X.Y., Sun, Y., Zhang, A., et al., *Third-generation CD28/4-1BB chimeric antigen receptor T cells for chemotherapy relapsed or refractory acute lymphoblastic leukaemia: a non-randomised, open-label phase I trial protocol.* BMJ Open, 2016. 6(12): p. e013904.

35. Priceman, S.J., Forman, S.J., and Brown, C.E., *Smart CARs engineered for cancer immunotherapy.* Curr Opin Oncol, 2015. 27(6): p. 466-74.

36. Hombach, A.A., Rappl, G., and Abken, H., *Arming cytokine-induced killer cells with chimeric antigen receptors: CD28 outperforms combined CD28-OX40 "super-stimulation".* Mol Ther, 2013. 21(12): p. 2268-77.

37. Kawalekar, O.U., O'Connor, R.S., Fraietta, J.A., et al., *Distinct Signaling of Coreceptors Regulates Specific Metabolism Pathways and Impacts Memory Development in CAR T Cells.* Immunity, 2016. 44(2): p. 380-90.

38. Long, A.H., Haso, W.M., Shern, J.F., et al., *4-1BB costimulation ameliorates T cell exhaustion induced by tonic signaling of chimeric antigen receptors.* Nat Med, 2015. 21(6): p. 581-90.

39. Hudecek, M., Sommermeyer, D., Kosasih, P.L., et al., *The nonsignaling extracellular spacer domain of chimeric antigen receptors is decisive for in vivo antitumor activity.* Cancer Immunol Res, 2015. 3(2): p. 125-35.

40. Hombach, A., Hombach, A.A., and Abken, H., *Adoptive immunotherapy with genetically engineered T cells: modification of the IgG1 Fc 'spacer' domain in the extracellular moiety of chimeric antigen receptors avoids 'off-target' activation and unintended initiation of an innate immune response.* Gene Ther, 2010. 17(10): p. 1206-13.

41. Morgan, R.A., Yang, J.C., Kitano, M., et al., *Case report of a serious adverse event following the administration of T cells transduced with a chimeric antigen receptor recognizing ERBB2.* Mol Ther, 2010. 18(4): p. 843-51.

42. Hudecek, M., Lupo-Stanghellini, M.T., Kosasih, P.L., et al., *Receptor affinity and extracellular domain modifications affect tumor recognition by ROR1-specific chimeric antigen receptor T cells.* Clin Cancer Res, 2013. 19(12): p. 3153-64.

43. Nicholson, I.C., Lenton, K.A., Little, D.J., et al., *Construction and characterisation of a functional CD19 specific single chain Fv fragment for immunotherapy of B lineage leukaemia and lymphoma.* Mol Immunol, 1997. 34(16-17): p. 1157-65.

44. Till, B.G., Jensen, M.C., Wang, J., et al., *Adoptive immunotherapy for indolent non-Hodgkin lymphoma and mantle cell lymphoma using genetically modified autologous CD20-specific T cells.* Blood, 2008. 112(6): p. 2261-71.

45. Shawler, D.L., Bartholomew, R.M., Smith, L.M., et al., *Human immune response to multiple injections of murine monoclonal IgG.* J Immunol, 1985. 135(2): p. 1530-5.

46. Horneff, G., Winkler, T., Kalden, J.R., et al., *Human anti-mouse antibody response induced by anti-CD4 monoclonal antibody therapy in patients with rheumatoid arthritis.* Clin Immunol Immunopathol, 1991. 59(1): p. 89-103.

47. Kandalaft, L.E., Powell, D.J., Jr., and Coukos, G., *A phase I clinical trial of adoptive transfer of folate receptor-alpha redirected autologous T cells for recurrent ovarian cancer.* J Transl Med, 2012. 10: p. 157.

48. Pule, M.A., Savoldo, B., Myers, G.D., et al., *Virus-specific T cells engineered to coexpress tumor-specific receptors: persistence and antitumor activity in individuals with neuroblastoma.* Nat Med, 2008. 14(11): p. 1264-70.

49. Zhang, H., Ye, Z.L., Yuan, Z.G., et al., *New Strategies for the Treatment of Solid Tumors with CAR-T Cells.* Int J Biol Sci, 2016. 12(6): p. 718-29.

50. Zhao, Z., Condomines, M., van der Stegen, S.J., et al., *Structural Design of Engineered Costimulation Determines Tumor Rejection Kinetics and Persistence of CAR T Cells.* Cancer Cell, 2015. 28(4): p. 415-28.

51. Scheuermann, R.H. and Racila, E., *CD19 antigen in leukemia and lymphoma diagnosis and immunotherapy.* Leuk Lymphoma, 1995. 18(5-6): p. 385-97.

52. Davila, M.L., Riviere, I., Wang, X., et al., *Efficacy and toxicity management of 19-28z CAR T cell therapy in B cell acute lymphoblastic leukemia.* Sci Transl Med, 2014. 6(224): p. 224ra25.

53. Turtle, C.J., Hanafi, L.A., Berger, C., et al., *CD19 CAR-T cells of defined CD4+:CD8+ composition in adult B cell ALL patients.* J Clin Invest, 2016. 126(6): p. 2123-38.

54. Maude, S.L., Frey, N., Shaw, P.A., et al., *Chimeric antigen receptor T cells for sustained remissions in leukemia.* N Engl J Med, 2014. 371(16): p. 1507-17.

55. Ruella, M., Barrett, D.M., Kenderian, S.S., et al., *Dual CD19 and CD123 targeting prevents antigen-loss relapses after CD19-directed immunotherapies.* J Clin Invest, 2016. 126(10): p. 3814-3826.

56. Sotillo, E., Barrett, D.M., Black, K.L., et al., *Convergence of Acquired Mutations and Alternative Splicing of CD19 Enables Resistance to CART-19 Immunotherapy.* Cancer Discov, 2015. 5(12): p. 1282-95.

57. Ruella, M. and Maus, M.V., *Catch me if you can: Leukemia Escape after CD19-Directed T Cell Immunotherapies.* Comput Struct Biotechnol J, 2016. 14: p. 357-362.

58. Sapra, P. and Allen, T.M., *Internalizing antibodies are necessary for improved therapeutic efficacy of antibody-targeted liposomal drugs.* Cancer Res, 2002. 62(24): p. 7190-4.

59. Klein, C., Lammens, A., Schafer, W., et al., *Epitope interactions of monoclonal antibodies targeting CD20 and their relationship to functional properties.* MAbs, 2013. 5(1): p. 22-33.

60. Fang, D., Nguyen, T.K., Leishear, K., et al., *A tumorigenic subpopulation with stem cell properties in melanomas.* Cancer Res, 2005. 65(20): p. 9328-37.

61. Schmidt, P., Kopecky, C., Hombach, A., et al., *Eradication of melanomas by targeted elimination of a minor subset of tumor cells.* Proc Natl Acad Sci U S A, 2011. 108(6): p. 2474-9.

62. Hiddemann, W., Kneba, M., Dreyling, M., et al., *Frontline therapy with rituximab added to the combination of cyclophosphamide, doxorubicin, vincristine, and prednisone (CHOP) significantly improves the outcome for patients with advanced-stage follicular lymphoma compared with therapy with CHOP alone: results of a prospective randomized study of the German Low-Grade Lymphoma Study Group.* Blood, 2005. 106(12): p. 3725-32.

63. Pfreundschuh, M., Trumper, L., Osterborg, A., et al., *CHOP-like chemotherapy plus rituximab versus CHOP-like chemotherapy alone in young patients with good-*

prognosis diffuse large-B-cell lymphoma: a randomised controlled trial by the MabThera International Trial (MInT) Group. Lancet Oncol, 2006. 7(5): p. 379-91.

64. Pinc, A., Somasundaram, R., Wagner, C., et al., *Targeting CD20 in melanoma patients at high risk of disease recurrence.* Mol Ther, 2012. 20(5): p. 1056-62.

65. Schlaak, M., Schmidt, P., Bangard, C., et al., *Regression of metastatic melanoma in a patient by antibody targeting of cancer stem cells.* Oncotarget, 2012. 3(1): p. 22-30.

66. Kaiser, A.D., Assenmacher, M., Schroder, B., et al., *Towards a commercial process for the manufacture of genetically modified T cells for therapy.* Cancer Gene Ther, 2015. 22(2): p. 72-8.

67. Lu, T.L., Pugach, O., Somerville, R., et al., *A Rapid Cell Expansion Process for Production of Engineered Autologous CAR-T Cell Therapies.* Hum Gene Ther Methods, 2016. 27(6): p. 209-218.

68. Ramanayake, S., Bilmon, I., Bishop, D., et al., *Low-cost generation of Good Manufacturing Practice-grade CD19-specific chimeric antigen receptor-expressing T cells using piggyBac gene transfer and patient-derived materials.* Cytotherapy, 2015. 17(9): p. 1251-67.

69. Tumaini, B., Lee, D.W., Lin, T., et al., *Simplified process for the production of anti-CD19-CAR-engineered T cells.* Cytotherapy, 2013. 15(11): p. 1406-15.

70. Mock, U., Nickolay, L., Philip, B., et al., *Automated manufacturing of chimeric antigen receptor T cells for adoptive immunotherapy using CliniMACS prodigy.* Cytotherapy, 2016. 18(8): p. 1002-11.

71. Priesner, C., Aleksandrova, K., Esser, R., et al., *Automated enrichment, transduction and expansion of clinical-scale CD62L+ T cells for manufacturing of GTMPs.* Hum Gene Ther, 2016.

72. Blackburn, S.D., Shin, H., Haining, W.N., et al., *Coregulation of CD8+ T cell exhaustion by multiple inhibitory receptors during chronic viral infection.* Nat Immunol, 2009. 10(1): p. 29-37.

73. Kahan, S.M., Wherry, E.J., and Zajac, A.J., *T cell exhaustion during persistent viral infections.* Virology, 2015. 479-480: p. 180-93.

74. Mumprecht, S., Schurch, C., Schwaller, J., et al., *Programmed death 1 signaling on chronic myeloid leukemia-specific T cells results in T-cell exhaustion and disease progression.* Blood, 2009. 114(8): p. 1528-36.

75. Cieri, N., Camisa, B., Cocchiarella, F., et al., *IL-7 and IL-15 instruct the generation of human memory stem T cells from naive precursors.* Blood, 2013. 121(4): p. 573-84.

76. Berger, C., Jensen, M.C., Lansdorp, P.M., et al., *Adoptive transfer of effector CD8+ T cells derived from central memory cells establishes persistent T cell memory in primates.* J Clin Invest, 2008. 118(1): p. 294-305.

77. Wang, X., Berger, C., Wong, C.W., et al., *Engraftment of human central memory-derived effector CD8+ T cells in immunodeficient mice.* Blood, 2011. 117(6): p. 1888-98.

78. Kim, Y., Lin, Q., Glazer, P.M., et al., *Hypoxic tumor microenvironment and cancer cell differentiation.* Curr Mol Med, 2009. 9(4): p. 425-34.

79. Gajewski, T.F., Meng, Y., Blank, C., et al., *Immune resistance orchestrated by the tumor microenvironment.* Immunol Rev, 2006. 213: p. 131-45.

80. Moon, E.K., Wang, L.C., Dolfi, D.V., et al., *Multifactorial T-cell hypofunction that is reversible can limit the efficacy of chimeric antigen receptor-transduced human T cells in solid tumors.* Clin Cancer Res, 2014. 20(16): p. 4262-73.

81. Newick, K., O'Brien, S., Moon, E., et al., *CAR T Cell Therapy for Solid Tumors.* Annu Rev Med, 2017. 68: p. 139-152.

82. Navid, F., Santana, V.M., and Barfield, R.C., *Anti-GD2 antibody therapy for GD2-expressing tumors.* Curr Cancer Drug Targets, 2010. 10(2): p. 200-9.

83. English, D.P., Roque, D.M., and Santin, A.D., *HER2 expression beyond breast cancer: therapeutic implications for gynecologic malignancies.* Mol Diagn Ther, 2013. 17(2): p. 85-99.

84. Geldres, C., Savoldo, B., Hoyos, V., et al., *T lymphocytes redirected against the chondroitin sulfate proteoglycan-4 control the growth of multiple solid tumors both in vitro and in vivo.* Clin Cancer Res, 2014. 20(4): p. 962-71.

85. Lanitis, E., Poussin, M., Klattenhoff, A.W., et al., *Chimeric antigen receptor T Cells with dissociated signaling domains exhibit focused antitumor activity with reduced potential for toxicity in vivo.* Cancer Immunol Res, 2013. 1(1): p. 43-53.

86. Roybal, K.T., Rupp, L.J., Morsut, L., et al., *Precision Tumor Recognition by T Cells With Combinatorial Antigen-Sensing Circuits.* Cell, 2016. 164(4): p. 770-9.

87. Han, X., Bryson, P.D., Zhao, Y., et al., *Masked Chimeric Antigen Receptor for Tumor-Specific Activation.* Mol Ther, 2017. 25(1): p. 274-284.

88. Melero, I., Shuford, W.W., Newby, S.A., et al., *Monoclonal antibodies against the 4-1BB T-cell activation molecule eradicate established tumors.* Nat Med, 1997. 3(6): p. 682-5.

89. Melero, I., Bach, N., Hellstrom, K.E., et al., *Amplification of tumor immunity by gene transfer of the co-stimulatory 4-1BB ligand: synergy with the CD28 co-stimulatory pathway.* Eur J Immunol, 1998. 28(3): p. 1116-21.

90. Stephan, M.T., Ponomarev, V., Brentjens, R.J., et al., *T cell-encoded CD80 and 4-1BBL induce auto- and transcostimulation, resulting in potent tumor rejection.* Nat Med, 2007. 13(12): p. 1440-9.

91. Suntharalingam, G., Perry, M.R., Ward, S., et al., *Cytokine storm in a phase 1 trial of the anti-CD28 monoclonal antibody TGN1412.* N Engl J Med, 2006. 355(10): p. 1018-28.

92. Winkler, U., Jensen, M., Manzke, O., et al., *Cytokine-release syndrome in patients with B-cell chronic lymphocytic leukemia and high lymphocyte counts after treatment with an anti-CD20 monoclonal antibody (rituximab, IDEC-C2B8).* Blood, 1999. 94(7): p. 2217-24.

93. Stebbings, R., Findlay, L., Edwards, C., et al., *"Cytokine storm" in the phase I trial of monoclonal antibody TGN1412: better understanding the causes to improve preclinical testing of immunotherapeutics.* J Immunol, 2007. 179(5): p. 3325-31.

94. Cong, L., Ran, F.A., Cox, D., et al., *Multiplex genome engineering using CRISPR/Cas systems.* Science, 2013. 339(6121): p. 819-23.

95. Soneoka, Y., Cannon, P.M., Ramsdale, E.E., et al., *A transient three-plasmid expression system for the production of high titer retroviral vectors.* Nucleic Acids Res, 1995. 23(4): p. 628-33.

96. Green, M.R. and Sambrook, J., *Molecular cloning - A laboratory manual.* Cold Spring Harbor Laboratory Press, 2012. 1(4th edition): p. ISBN: 1936113422.

97. Pingoud, A., Fuxreiter, M., Pingoud, V., et al., *Type II restriction endonucleases: structure and mechanism.* Cell Mol Life Sci, 2005. 62(6): p. 685-707.

98. Apel, M., Brüning, M., Granzin, M., et al., *Integrated Clinical Scale Manufacturing System for Cellular Products Derived by Magnetic Cell Separation, Centrifugation and Cell Culture.* Chemie Ingenieur Technik, 2013. 85(1–2): p. 103–110.

99. Guest, R.D., Hawkins, R.E., Kirillova, N., et al., *The role of extracellular spacer regions in the optimal design of chimeric immune receptors: evaluation of four different scFvs and antigens.* J Immunother, 2005. 28(3): p. 203-11.

100. Langley, K.E., Villarejo, M.R., Fowler, A.V., et al., *Molecular basis of beta-galactosidase alpha-complementation.* Proc Natl Acad Sci U S A, 1975. 72(4): p. 1254-7.

101. Ruther, U., Koenen, M., Otto, K., et al., *pUR222, a vector for cloning and rapid chemical sequencing of DNA.* Nucleic Acids Res, 1981. 9(16): p. 4087-98.

102. Dull, T., Zufferey, R., Kelly, M., et al., *A third-generation lentivirus vector with a conditional packaging system.* J Virol, 1998. 72(11): p. 8463-71.

103. Zufferey, R., Dull, T., Mandel, R.J., et al., *Self-inactivating lentivirus vector for safe and efficient in vivo gene delivery.* J Virol, 1998. 72(12): p. 9873-80.

104. Zufferey, R., Donello, J.E., Trono, D., et al., *Woodchuck hepatitis virus posttranscriptional regulatory element enhances expression of transgenes delivered by retroviral vectors.* J Virol, 1999. 73(4): p. 2886-92.

105. Kakarla, S. and Gottschalk, S., *CAR T cells for solid tumors: armed and ready to go?* Cancer J, 2014. 20(2): p. 151-5.

106. Sadelain, M., Brentjens, R., and Riviere, I., *The basic principles of chimeric antigen receptor design.* Cancer Discov, 2013. 3(4): p. 388-98.

107. June, C.H., Maus, M.V., Plesa, G., et al., *Engineered T cells for cancer therapy.* Cancer Immunol Immunother, 2014. 63(9): p. 969-75.

108. Anurathapan, U., Leen, A.M., Brenner, M.K., et al., *Engineered T cells for cancer treatment.* Cytotherapy, 2014. 16(6): p. 713-33.

109. June, C.H., Riddell, S.R., and Schumacher, T.N., *Adoptive cellular therapy: a race to the finish line.* Sci Transl Med, 2015. 7(280): p. 280ps7.

110. Jackson, B.C., Nebert, D.W., and Vasiliou, V., *Update of human and mouse matrix metalloproteinase families.* Hum Genomics, 2010. 4(3): p. 194-201.

111. Tallant, C., Marrero, A., and Gomis-Ruth, F.X., *Matrix metalloproteinases: fold and function of their catalytic domains.* Biochim Biophys Acta, 2010. 1803(1): p. 20-8.

112. Brunner, K.T., Mauel, J., Cerottini, J.C., et al., *Quantitative assay of the lytic action of immune lymphoid cells on 51-Cr-labelled allogeneic target cells in vitro; inhibition by isoantibody and by drugs.* Immunology, 1968. 14(2): p. 181-96.

113. Zaritskaya, L., Shurin, M.R., Sayers, T.J., et al., *New flow cytometric assays for monitoring cell-mediated cytotoxicity.* Expert Rev Vaccines, 2010. 9(6): p. 601-16.

114. Karimi, M.A., Lee, E., Bachmann, M.H., et al., *Measuring cytotoxicity by bioluminescence imaging outperforms the standard chromium-51 release assay.* PLoS One, 2014. 9(2): p. e89357.

115. Oba, Y., Ojika, M., and Inouye, S., *Firefly luciferase is a bifunctional enzyme: ATP-dependent monooxygenase and a long chain fatty acyl-CoA synthetase.* FEBS Lett, 2003. 540(1-3): p. 251-4.

116. Das, S.K. and Guha, A.K., *Biosorption of hexavalent chromium by Termitomyces clypeatus biomass: kinetics and transmission electron microscopic study.* J Hazard Mater, 2009. 167(1-3): p. 685-91.

117. Leskov, I., Pallasch, C.P., Drake, A., et al., *Rapid generation of human B-cell lymphomas via combined expression of Myc and Bcl2 and their use as a preclinical model for biological therapies.* Oncogene, 2013. 32(8): p. 1066-72.

118. Cook, N., Jodrell, D.I., and Tuveson, D.A., *Predictive in vivo animal models and translation to clinical trials.* Drug Discov Today, 2012. 17(5-6): p. 253-60.

119. Mak, I.W., Evaniew, N., and Ghert, M., *Lost in translation: animal models and clinical trials in cancer treatment.* Am J Transl Res, 2014. 6(2): p. 114-8.

120. Johnson, J.I., Decker, S., Zaharevitz, D., et al., *Relationships between drug activity in NCI preclinical in vitro and in vivo models and early clinical trials.* Br J Cancer, 2001. 84(10): p. 1424-31.

121. Ginaldi, L., De Martinis, M., Matutes, E., et al., *Levels of expression of CD19 and CD20 in chronic B cell leukaemias.* J Clin Pathol, 1998. 51(5): p. 364-9.

122. Thomas, D.A., O'Brien, S., Jorgensen, J.L., et al., *Prognostic significance of CD20 expression in adults with de novo precursor B-lineage acute lymphoblastic leukemia.* Blood, 2009. 113(25): p. 6330-7.

123. Prevodnik, V.K., Lavrencak, J., Horvat, M., et al., *The predictive significance of CD20 expression in B-cell lymphomas.* Diagn Pathol, 2011. 6: p. 33.

124. Almasri, N.M., Duque, R.E., Iturraspe, J., et al., *Reduced expression of CD20 antigen as a characteristic marker for chronic lymphocytic leukemia.* Am J Hematol, 1992. 40(4): p. 259-63.

125. Schambach, A., Mueller, D., Galla, M., et al., *Overcoming promoter competition in packaging cells improves production of self-inactivating retroviral vectors.* Gene Ther, 2006. 13(21): p. 1524-33.

126. Bushman, F.D., *Retroviral integration and human gene therapy.* J Clin Invest, 2007. 117(8): p. 2083-6.

127. Kalos, M. and June, C.H., *Adoptive T cell transfer for cancer immunotherapy in the era of synthetic biology.* Immunity, 2013. 39(1): p. 49-60.

128. Vannucci, L., Lai, M., Chiuppesi, F., et al., *Viral vectors: a look back and ahead on gene transfer technology.* New Microbiol, 2013. 36(1): p. 1-22.

129. Wang, G.P., Levine, B.L., Binder, G.K., et al., *Analysis of lentiviral vector integration in HIV+ study subjects receiving autologous infusions of gene modified CD4+ T cells.* Mol Ther, 2009. 17(5): p. 844-50.

130. Costello, E., Munoz, M., Buetti, E., et al., *Gene transfer into stimulated and unstimulated T lymphocytes by HIV-1-derived lentiviral vectors.* Gene Ther, 2000. 7(7): p. 596-604.

131. Bunnell, B.A., Muul, L.M., Donahue, R.E., et al., *High-efficiency retroviral-mediated gene transfer into human and nonhuman primate peripheral blood lymphocytes.* Proc Natl Acad Sci U S A, 1995. 92(17): p. 7739-43.

132. Cronin, J., Zhang, X.Y., and Reiser, J., *Altering the tropism of lentiviral vectors through pseudotyping.* Curr Gene Ther, 2005. 5(4): p. 387-98.

133. Finkelshtein, D., Werman, A., Novick, D., et al., *LDL receptor and its family members serve as the cellular receptors for vesicular stomatitis virus.* Proc Natl Acad Sci U S A, 2013. 110(18): p. 7306-11.

134. Burns, J.C., Friedmann, T., Driever, W., et al., *Vesicular stomatitis virus G glycoprotein pseudotyped retroviral vectors: concentration to very high titer and efficient gene transfer into mammalian and nonmammalian cells.* Proc Natl Acad Sci U S A, 1993. 90(17): p. 8033-7.

135. Frecha, C., Costa, C., Negre, D., et al., *Stable transduction of quiescent T cells without induction of cycle progression by a novel lentiviral vector pseudotyped with measles virus glycoproteins.* Blood, 2008. 112(13): p. 4843-52.

136. Amirache, F., Levy, C., Costa, C., et al., *Mystery solved: VSV-G-LVs do not allow efficient gene transfer into unstimulated T cells, B cells, and HSCs because they lack the LDL receptor.* Blood, 2014. 123(9): p. 1422-4.

137. Zhou, Q., Uhlig, K.M., Muth, A., et al., *Exclusive Transduction of Human CD4+ T Cells upon Systemic Delivery of CD4-Targeted Lentiviral Vectors.* J Immunol, 2015. 195(5): p. 2493-501.

138. Zhou, Q. and Buchholz, C.J., *Cell type specific gene delivery by lentiviral vectors: New options in immunotherapy.* Oncoimmunology, 2013. 2(1): p. e22566.

139. Funke, S., Maisner, A., Muhlebach, M.D., et al., *Targeted cell entry of lentiviral vectors.* Mol Ther, 2008. 16(8): p. 1427-36.

140. Sakuma, T., Barry, M.A., and Ikeda, Y., *Lentiviral vectors: basic to translational.* Biochem J, 2012. 443(3): p. 603-18.

141. Scherr, M., Battmer, K., Blomer, U., et al., *Quantitative determination of lentiviral vector particle numbers by real-time PCR.* Biotechniques, 2001. 31(3): p. 520, 522, 524, passim.

142. Gasmi, M., Glynn, J., Jin, M.J., et al., *Requirements for efficient production and transduction of human immunodeficiency virus type 1-based vectors.* J Virol, 1999. 73(3): p. 1828-34.

143. Geraerts, M., Willems, S., Baekelandt, V., et al., *Comparison of lentiviral vector titration methods.* BMC Biotechnol, 2006. 6: p. 34.

144. Muller, T., Uherek, C., Maki, G., et al., *Expression of a CD20-specific chimeric antigen receptor enhances cytotoxic activity of NK cells and overcomes NK-resistance of lymphoma and leukemia cells.* Cancer Immunol Immunother, 2008. 57(3): p. 411-23.

145. Jensen, M.C., Popplewell, L., Cooper, L.J., et al., *Antitransgene rejection responses contribute to attenuated persistence of adoptively transferred CD20/CD19-specific chimeric antigen receptor redirected T cells in humans.* Biol Blood Marrow Transplant, 2010. 16(9): p. 1245-56.

146. Abate-Daga, D. and Davila, M.L., *CAR models: next-generation CAR modifications for enhanced T-cell function.* Mol Ther Oncolytics, 2016. 3: p. 16014.

147. Sommermeyer, D., Hill, T., Shamah, S.M., et al., *Fully human CD19-specific chimeric antigen receptors for T-cell therapy.* Leukemia, 2017.

148. Jones, S., Peng, P.D., Yang, S., et al., *Lentiviral vector design for optimal T cell receptor gene expression in the transduction of peripheral blood lymphocytes and tumor-infiltrating lymphocytes.* Hum Gene Ther, 2009. 20(6): p. 630-40.

149. Milone, M.C., Fish, J.D., Carpenito, C., et al., *Chimeric receptors containing CD137 signal transduction domains mediate enhanced survival of T cells and increased antileukemic efficacy in vivo.* Mol Ther, 2009. 17(8): p. 1453-64.

150. Srivastava, S. and Riddell, S.R., *Engineering CAR-T cells: Design concepts.* Trends Immunol, 2015. 36(8): p. 494-502.

151. Dustin, M.L., *T-cell activation through immunological synapses and kinapses.* Immunol Rev, 2008. 221: p. 77-89.

152. Haso, W., Lee, D.W., Shah, N.N., et al., *Anti-CD22-chimeric antigen receptors targeting B-cell precursor acute lymphoblastic leukemia.* Blood, 2013. 121(7): p. 1165-74.

153. Hombach, A.A., Schildgen, V., Heuser, C., et al., *T cell activation by antibody-like immunoreceptors: the position of the binding epitope within the target molecule determines the efficiency of activation of redirected T cells.* J Immunol, 2007. 178(7): p. 4650-7.

154. Almasbak, H., Walseng, E., Kristian, A., et al., *Inclusion of an IgG1-Fc spacer abrogates efficacy of CD19 CAR T cells in a xenograft mouse model.* Gene Ther, 2015. 22(5): p. 391-403.

155. Jonnalagadda, M., Mardiros, A., Urak, R., et al., *Chimeric antigen receptors with mutated IgG4 Fc spacer avoid fc receptor binding and improve T cell persistence and antitumor efficacy.* Mol Ther, 2015. 23(4): p. 757-68.

156. Armour, K.L., van de Winkel, J.G., Williamson, L.M., et al., *Differential binding to human FcgammaRIIa and FcgammaRIIb receptors by human IgG wildtype and mutant antibodies.* Mol Immunol, 2003. 40(9): p. 585-93.

157. Shields, R.L., Namenuk, A.K., Hong, K., et al., *High resolution mapping of the binding site on human IgG1 for Fc gamma RI, Fc gamma RII, Fc gamma RIII, and FcRn and design of IgG1 variants with improved binding to the Fc gamma R.* J Biol Chem, 2001. 276(9): p. 6591-604.

158. Bruhns, P., Iannascoli, B., England, P., et al., *Specificity and affinity of human Fcgamma receptors and their polymorphic variants for human IgG subclasses.* Blood, 2009. 113(16): p. 3716-25.

159. McEwen-Smith, R.M., Salio, M., and Cerundolo, V., *The regulatory role of invariant NKT cells in tumor immunity.* Cancer Immunol Res, 2015. 3(5): p. 425-35.

160. Fallarini, S., Paoletti, T., Orsi Battaglini, N., et al., *Invariant NKT cells increase drug-induced osteosarcoma cell death.* Br J Pharmacol, 2012. 167(7): p. 1533-49.

161. Metelitsa, L.S., Naidenko, O.V., Kant, A., et al., *Human NKT cells mediate antitumor cytotoxicity directly by recognizing target cell CD1d with bound ligand or indirectly by producing IL-2 to activate NK cells.* J Immunol, 2001. 167(6): p. 3114-22.

162. Wu, D.Y., Segal, N.H., Sidobre, S., et al., *Cross-presentation of disialoganglioside GD3 to natural killer T cells.* J Exp Med, 2003. 198(1): p. 173-81.

163. Hix, L.M., Shi, Y.H., Brutkiewicz, R.R., et al., *CD1d-expressing breast cancer cells modulate NKT cell-mediated antitumor immunity in a murine model of breast cancer metastasis.* PLoS One, 2011. 6(6): p. e20702.

164. Robbins, P.F., Dudley, M.E., Wunderlich, J., et al., *Cutting edge: persistence of transferred lymphocyte clonotypes correlates with cancer regression in patients receiving cell transfer therapy.* J Immunol, 2004. 173(12): p. 7125-30.

165. Xu, H., Manivannan, A., Crane, I., et al., *Critical but divergent roles for CD62L and CD44 in directing blood monocyte trafficking in vivo during inflammation.* Blood, 2008. 112(4): p. 1166-74.

166. Juelke, K., Killig, M., Luetke-Eversloh, M., et al., *CD62L expression identifies a unique subset of polyfunctional CD56dim NK cells.* Blood, 2010. 116(8): p. 1299-307.

167. Sims, G.P., Ettinger, R., Shirota, Y., et al., *Identification and characterization of circulating human transitional B cells.* Blood, 2005. 105(11): p. 4390-8.

168. De Martinis, M., Modesti, M., and Ginaldi, L., *Phenotypic and functional changes of circulating monocytes and polymorphonuclear leucocytes from elderly persons.* Immunol Cell Biol, 2004. 82(4): p. 415-20.

169. Stroncek, D.F., Lee, D.W., Ren, J., et al., *Elutriated lymphocytes for manufacturing chimeric antigen receptor T cells.* J Transl Med, 2017. 15(1): p. 59.

170. Louis, C.U., Savoldo, B., Dotti, G., et al., *Antitumor activity and long-term fate of chimeric antigen receptor-positive T cells in patients with neuroblastoma.* Blood, 2011. 118(23): p. 6050-6.

171. Fischer, K., Hoffmann, P., Voelkl, S., et al., *Inhibitory effect of tumor cell-derived lactic acid on human T cells.* Blood, 2007. 109(9): p. 3812-9.

172. Attarwala, H., *TGN1412: From Discovery to Disaster.* J Young Pharm, 2010. 2(3): p. 332-6.

173. Naldini, L., *Gene therapy returns to centre stage.* Nature, 2015. 526(7573): p. 351-60.

174. Copier, J. and Dalgleish, A., *Overview of tumor cell-based vaccines.* Int Rev Immunol, 2006. 25(5-6): p. 297-319.

175. Beard, R.E., Zheng, Z., Lagisetty, K.H., et al., *Multiple chimeric antigen receptors successfully target chondroitin sulfate proteoglycan 4 in several different cancer histologies and cancer stem cells.* J Immunother Cancer, 2014. 2: p. 25.

176. Sommers, C.L., Dejarnette, J.B., Huang, K., et al., *Function of CD3 epsilon-mediated signals in T cell development.* J Exp Med, 2000. 192(6): p. 913-19.

177. Schneider, D., Xiong, Y., Wu, D., et al., *A tandem CD19/CD20 CAR lentiviral vector drives on-target and off-target antigen modulation in leukemia cell lines.* J Immunother Cancer, 2017. 5: p. 42.

178. Barrett, D.M., Teachey, D.T., and Grupp, S.A., *Toxicity management for patients receiving novel T-cell engaging therapies.* Curr Opin Pediatr, 2014. 26(1): p. 43-9.

179. Lee, D.W., Gardner, R., Porter, D.L., et al., *Current concepts in the diagnosis and management of cytokine release syndrome.* Blood, 2014. 124(2): p. 188-95.

180. Maude, S.L., Barrett, D., Teachey, D.T., et al., *Managing cytokine release syndrome associated with novel T cell-engaging therapies.* Cancer J, 2014. 20(2): p. 119-22.

181. Crawford, A., Angelosanto, J.M., Kao, C., et al., *Molecular and transcriptional basis of CD4(+) T cell dysfunction during chronic infection.* Immunity, 2014. 40(2): p. 289-302.

182. Grosso, J.F., Goldberg, M.V., Getnet, D., et al., *Functionally distinct LAG-3 and PD-1 subsets on activated and chronically stimulated CD8 T cells.* J Immunol, 2009. 182(11): p. 6659-69.

183. Jin, H.T., Anderson, A.C., Tan, W.G., et al., *Cooperation of Tim-3 and PD-1 in CD8 T-cell exhaustion during chronic viral infection.* Proc Natl Acad Sci U S A, 2010. 107(33): p. 14733-8.

184. Kao, C., Oestreich, K.J., Paley, M.A., et al., *Transcription factor T-bet represses expression of the inhibitory receptor PD-1 and sustains virus-specific CD8+ T cell responses during chronic infection.* Nat Immunol, 2011. 12(7): p. 663-71.

185. Shin, H., Blackburn, S.D., Intlekofer, A.M., et al., *A role for the transcriptional repressor Blimp-1 in CD8(+) T cell exhaustion during chronic viral infection.* Immunity, 2009. 31(2): p. 309-20.

186. Vezys, V., Penaloza-MacMaster, P., Barber, D.L., et al., *4-1BB signaling synergizes with programmed death ligand 1 blockade to augment CD8 T cell responses during chronic viral infection.* J Immunol, 2011. 187(4): p. 1634-42.

187. Kudo-Saito, C., Hodge, J.W., Kwak, H., et al., *4-1BB ligand enhances tumor-specific immunity of poxvirus vaccines.* Vaccine, 2006. 24(23): p. 4975-86.

188. Chmielewski, M., Kopecky, C., Hombach, A.A., et al., *IL-12 release by engineered T cells expressing chimeric antigen receptors can effectively Muster an antigen-independent macrophage response on tumor cells that have shut down tumor antigen expression.* Cancer Res, 2011. 71(17): p. 5697-706.

189. Chmielewski, M. and Abken, H., *TRUCKs: the fourth generation of CARs.* Expert Opin Biol Ther, 2015. 15(8): p. 1145-54.

190. Liao, W., Lin, J.X., and Leonard, W.J., *Interleukin-2 at the crossroads of effector responses, tolerance, and immunotherapy.* Immunity, 2013. 38(1): p. 13-25.

191. Tandle, A., Hanna, E., Lorang, D., et al., *Tumor vasculature-targeted delivery of tumor necrosis factor-alpha.* Cancer, 2009. 115(1): p. 128-39.

192. Colombo, N., Peccatori, F., Paganin, C., et al., *Anti-tumor and immunomodulatory activity of intraperitoneal IFN-gamma in ovarian carcinoma patients with minimal residual tumor after chemotherapy.* Int J Cancer, 1992. 51(1): p. 42-6.

193. Maude, S.L., Teachey, D.T., Porter, D.L., et al., *CD19-targeted chimeric antigen receptor T-cell therapy for acute lymphoblastic leukemia.* Blood, 2015. 125(26): p. 4017-23.

194. Lupo-Stanghellini, M.T., Provasi, E., Bondanza, A., et al., *Clinical impact of suicide gene therapy in allogeneic hematopoietic stem cell transplantation.* Hum Gene Ther, 2010. 21(3): p. 241-50.

195. Budde, L.E., Berger, C., Lin, Y., et al., *Combining a CD20 chimeric antigen receptor and an inducible caspase 9 suicide switch to improve the efficacy and safety of T cell adoptive immunotherapy for lymphoma.* PLoS One, 2013. 8(12): p. e82742.

196. Zhou, X., Naik, S., Dakhova, O., et al., *Serial Activation of the Inducible Caspase 9 Safety Switch After Human Stem Cell Transplantation.* Mol Ther, 2016. 24(4): p. 823-31.

197. Traversari, C., Marktel, S., Magnani, Z., et al., *The potential immunogenicity of the TK suicide gene does not prevent full clinical benefit associated with the use of TK-transduced donor lymphocytes in HSCT for hematologic malignancies.* Blood, 2007. 109(11): p. 4708-15.

198. Philip, B., Kokalaki, E., Mekkaoui, L., et al., *A highly compact epitope-based marker/suicide gene for easier and safer T-cell therapy.* Blood, 2014. 124(8): p. 1277-87.

199. Cartellieri, M., Feldmann, A., Koristka, S., et al., *Switching CAR T cells on and off: a novel modular platform for retargeting of T cells to AML blasts.* Blood Cancer J, 2016. 6(8): p. e458.

200. Cao, Y., Rodgers, D.T., Du, J., et al., *Design of Switchable Chimeric Antigen Receptor T Cells Targeting Breast Cancer.* Angew Chem Int Ed Engl, 2016. 55(26): p. 7520-4.

201. Wu, C.Y., Roybal, K.T., Puchner, E.M., et al., *Remote control of therapeutic T cells through a small molecule-gated chimeric receptor.* Science, 2015. 350(6258): p. aab4077.
202. Monjezi, R., Miskey, C., Gogishvili, T., et al., *Enhanced CAR T-cell engineering using non-viral Sleeping Beauty transposition from minicircle vectors.* Leukemia, 2017. 31(1): p. 186-194.
203. Woodard, L.E. and Wilson, M.H., *piggyBac-ing models and new therapeutic strategies.* Trends Biotechnol, 2015. 33(9): p. 525-33.
204. Singh, H., Figliola, M.J., Dawson, M.J., et al., *Manufacture of clinical-grade CD19-specific T cells stably expressing chimeric antigen receptor using Sleeping Beauty system and artificial antigen presenting cells.* PLoS One, 2013. 8(5): p. e64138.
205. Eyquem, J., Mansilla-Soto, J., Giavridis, T., et al., *Targeting a CAR to the TRAC locus with CRISPR/Cas9 enhances tumour rejection.* Nature, 2017. 543(7643): p. 113-117.
206. Hegde, M., Mukherjee, M., Grada, Z., et al., *Tandem CAR T cells targeting HER2 and IL13Ralpha2 mitigate tumor antigen escape.* J Clin Invest, 2016. 126(8): p. 3036-52.
207. Grada, Z., Hegde, M., Byrd, T., et al., *TanCAR: A Novel Bispecific Chimeric Antigen Receptor for Cancer Immunotherapy.* Mol Ther Nucleic Acids, 2013. 2: p. e105.

6 Acknowledgement

I am grateful to…

… Prof. Dr. Peter Lang and Prof. Dr. Hans-Georg Rammensee for their interest in my work and their academic supervision.

… Dr. Andrew Kaiser, not only for his support and guidance during my PhD but also for his motivation, great ideas, exciting discussions and the possibility to implement own ideas. His vision as scientist was always an inspiration.

… Miltenyi Biotec and in particular Dr. Jürgen Schmitz and Dr. Mario Assenmacher for their confidence and the possibility to realize this intriguing project.

… Nadine Mockel-Tenbrinck for sharing her expertise from the very early beginning regarding T cell culture or data analysis and especially for her untold contribution for our joint publication at the end of my dissertation.

… Carola Barth and Daniela Mauer, two real cheerful natures and absolute experts in the lab I really enjoy to work with. Both greatly assisted, *inter alia*, functionality assays, panel stainings and especially the TCT runs.

… Katharina Drechsel, Thomas Schaser, Pierre Abramowski and Jörg Mittelstät for numerous suspenseful discussions as well as promoting proposals.

… Britta Drees, Sandra Dapa and Carolin Kolbe for their excellent help in the lab. It is truly wonderful to have such competent and supportive colleagues.

… Janina Brauner and Wa´el Al Rawashdeh for their support in the animal facility and the practical realization of the *in vivo* studies for the CD20 CAR.

… Bettina Kotter for motivating words in hard times and proofreading this thesis.

… Jan Pietschmann who assisted in the course of his Bachelor thesis to generate the JeKo-1 knock-out clones and in *in vitro* experiments.

… Ian Johnston, Stefan Wild, Stefan Tomiuk, Jutta Kollet, Frank Single, Olaf Hardt as well as a large number of PhD students at Miltenyi Biotec for their continuous support.

7 *Curriculum vitae*

Dominik Peter Lock, M.Sc., born 12.09.1982 in Biberach.

since January 14	**Doctoral studies at Miltenyi Biotec**
	R&D; Dr. Andrew Kaiser, Dr. Mario Assenmacher
	Supervision: apl. Prof. Dr. Lang and Prof. Dr. Rammensee, University of Tübingen
	Title: CAR T cell research for clinical applications
Feb 12 – Nov 13	**Master studies biotechnology, FH Aachen**
	Thesis: "Generierung humaner induziert pluripotenter Stammzell-Reporter-Linien via Rekombinase-vermitteltem Genkassetten Austausch" provided by Miltenyi Biotec
Oct 08 – Jan 12	**Bachelor studies biotechnology, FH Aachen**
	Thesis: "Strategien für den Rekombinase-vermittelten Genkassetten-Austausch in humanen induziert pluripotenten Stammzellen" provided by Miltenyi Biotec
Jul 08 – Oct 08	**Study nurse, University hospital Bon**n
Aug 05 – Jun 08	**Apprenticeship as biological technical assistant, UK Bonn**
Jul 03 – Jun 05	**Military service, German Air Force**
Sep 01 – Jul 03	**Abitur, Gymnasium Aulendorf**

Cologne, October 2017